İSTANBUL TECHNICAL UNIVERSITY ★ INSTITUTE OF SCIENCE AND TECHNOLOGY

NEW POSSIBILITIES IN CURRENT-MODE CIRCUITS USING CURRENT CONTROLLED CONVEYOR (CCCII)

Ph.D. Thesis by

Shahram MINAEI, M.Sc.
(504972014)

Date of submission: 23 May 2001

Date of defence examination: 26 July 2001

Supervisor (Chairman) : Assoc. Prof. Dr. M. Sait TÜRKÖZ (I.T.U)

Member of the Examining Commmitee: Prof.Dr. Hakan KUNTMAN (I.T.U)

Prof.Dr. Avni MORGÜL (B.U)

Assoc. Prof.Dr. Oğuzhan ÇİÇEKOĞLU (B.U)

Assoc. Prof.Dr. Ali ZEKİ (I.T.U)

JULY 2001

İSTANBUL TEKNİK ÜNİVERSİTESİ ★ FEN BİLİMLERİ ENSTİTÜSÜ

KONTROLLU AKIM TAŞIYICI (CCCII) İLE AKIM-MODLU DEVRELERDE YENİ OLANAKLAR

DOKTORA TEZİ

Y.Müh. Shahram MINAEI
(504972014)

Tezin Enstitüye Verildiği Tarih: 23 Mayıs 2001

Tezin Savunulduğu Tarih: 26 Temmuz 2001

Tez Danışmanı: Doç. Dr. M. Sait TÜRKÖZ(İ.T.Ü)

Diğer Jüri Üyeleri: Prof.Dr. Hakan KUNTMAN(İ.T.Ü)

Prof.Dr. Avni MORGÜL(B.Ü)

Doç.Dr. Oğuzhan ÇİÇEKOĞLU(B.Ü)

Doç.Dr. Ali ZEKİ(İ.T.Ü)

TEMMUZ 2001

PREFACE

I would like to express my gratitude to my advisor Associate Prof. Dr. Sait Türköz for his continuous support, encouragement and constructive critiques.

I sincerely thank to Prof. Dr. Hakan Kuntman and Associate Prof. Dr. Oğuzhan Çiçekoğlu for their various contribution.

Finally, special thanks to my parents for continuous supports.

MAY, 2001 Shahram MINAEI

CONTENTS

ABBREVIATIONS

BiCMOS	: Bipolar Complementary metal oxide semiconductor
CC	: Current conveyor
CCI	: First generation current conveyor
CCII	: Second generation current conveyor
CCCII	: Current controlled conveyor
CFOA	: Current feedback operational amplifier
CMOS	: Complementary metal oxide semiconductor
FTFN	: Four terminal floating nullor
IC	: Integrated circuit
OP-AMP	: Operational amplifier
OMA	: Operational mirrored amplifier
OTA	: Operational transconductance amplifier
VLSI	: Very large scale integration

LIST OF TABLES

LIST OF FIGURES

LIST OF SYMBOLS

R_x	: Input resistance at port X of the CCCII
$\alpha(s)$	: Current transfer gain of the CCCII
$\beta(s)$	: Voltage transfer gain of the CCCII
α_o	: The value of current transfer gain of the CCCII at low frequencies
β_o	: The value of voltage transfer gain of the CCCII at low frequencies
ω_α	: Pole of the current transfer gain of the CCCII
ω_β	: Pole of the voltage transfer gain of the CCCII
g_m	: Transconductance
W	: Channel width of the MOS transistor
L	: Channel length of the MOS transistor
μ	: Effective carrier mobility
C_{ox}	: gate oxide capacitance of the MOS transistor per unit area
Z	: Impedans
Y	: Admittance
ω_o	: Resonant angular frequency of actual (non-ideal) bandpass filter
ω_{oi}	: Cutoff angular frequency of ideal lowpass filter
ω_c	: Cutoff angular frequency of actual (non-ideal) lowpass filter
ω_{ci}	: Resonant angular frequency of ideal bandpass filter
Q	: Quality factor of actual (non-ideal) filter
Q_i	: Quality factor of ideal filter
x	: Normalized angular frequency
$\hat{x}_o$	: Normalized resonant angular frequency of the actual bandpass filter
$\hat{x}'_o$	: Normalized resonant angular frequency extracted from the roots of the denominator of the transfer function of the bandpass filter
$\hat{x}_c$	: Normalized cutoff angular frequency of the actual lowpass filter
q	: Normalized quality factor
l	: damping ratio due to the additional roots caused by non-idealities of the CCCII
$\omega_{k\alpha}$	: Normalized pole angular frequencies of the $\alpha(s)$
$\omega_{k\beta}$	: Normalized pole angular frequencies of the $\beta(s)$

NEW POSSIBILITIES IN CURRENT-MODE CIRCUITS USING CURRENT CONTROLLED CONVEYOR (CCCII)

SUMMARY

Current-mode circuits have been received significant attention. This is attributed to their inherent wide bandwidth, greater linearity, wider dynamic range, simple circuitry and low power consumption compared to the voltage-mode circuits. On the other hand, in the recent past, there has been great emphasis on the design and implementation of current-mode circuits using current controlled conveyors (CCCIIs). Using of the CCCII in current-mode circuits provides a wide range of electronic tunability of the circuit parameters and a broad frequency range of operation.

In this thesis, a detail study in non-ideal CCCII is performed. Then to illustrate the usefulness of the CCCII many new CCCII-based applications such as filter, oscillator and inductance simulator are proposed. In order to take the advantages of the BiCMOS technology a new BiCMOS realization for the CCCII is presented.

In the main section of the thesis, an new configuration for realizing second order lowpass and bandpass filters using only one CCCII is presented and the effects of the dominant non-idealities of the CCCII on filter parameters such as resonant angular frequency and quality factor are investigated.

These non-ideality effects are shown in tabular forms and figures. Then simple and accurate formulas for calculating parameters of the filters are extracted. The effects of the non-idealities on the stability and sensitivities of the proposed filters are investigated in details.

Also as an example, a method for modifying the values of passive elements of the filter in order to minimize the deviation of the filter parameters from their ideal values are given.

KONTROLLU AKIM TAŞIYICI (CCCII) İLE AKIM MODLU DEVRELERDE YENİ OLANAKLAR

ÖZET

Son yıllarda akım-modlu devrelere olan ilgi giderek artmaktadır. Bu ilginin nedenleri, akım-modlu devrelerin gerilim-modlu devrelere göre daha büyük bant genişliği, yükselme eğimi, değişim aralığı, daha basit devre yapısı ve düşük güç tüketimi olmasıdır. Diğer yönden yakın zamanda, kontrollu akım taşıyıcılar (CCCII), akım-modlu devrelerin tasarımında çok sık kullanılmaktadır. Kontrollu akım taşıyıcı kullanılarak, akım modlu devrelerin parametreleri ve frekans bölgesi geniş bir değişim aralığında elektronik olarak ayarlanabilmektedir.

Bu tezde ideal olmayan CCCII detaylı olarak incelenmiştir. CCCII'nin hangi devrelerde yararlı olduğunu göstermek amacıyla, çok sayıda CCCII tabanlı filtre, osilator, endüktans simulatörü gibi yeni uygulamalar verilmiştir. BiCMOS teknolojinin avantajını açıklamak amacıyla yeni bir BiCMOS CCCII devresi verilmiştir.

Tezin ana bölümünde, ikinci dereceden alt geçiren, bant geçiren filtreler, sadece bir adet CCCII kullanılarak gerçekleştirme biçimi verilmiş ve CCCII'nin ideal olmamasının filtre frekansı ve değer katsayısı üzerindeki etkileri incelenmiştir.

İdeal olmamanın etkileri, şekil ve tablolarla gösterilmiştir. Filtre parametrelerinin hesaplanacağı basit formüller bulunmuştur. İdeal olmamanın önerilen filtre parametrelerinin duyarlıklarına ve devrenin kararlılığına nasıl etkidiği ayrıntılı olarak incelenmiştir.

Ayrıca, filtre değerlerinin ideal değerlerinden sapmalarınının nasıl minimize etme yöntemi, bir örnek üzerinde açıklanmıştır.

1. INTRODUCTION

Current-mode circuits and related active components such as current conveyor (CC). operational transconductance amplifier (OTA), operational mirrored amplifier (OMA), current feedback operational amplifier (CFOA), four terminal floating nullor (FTFN), have been emerged as an important class of circuits with properties that enable them to rival their voltage-mode counterparts in a wide range of applications. A current-mode circuit may be taken to mean any circuit in which current is used as active variable in preference to voltage, either throughout the whole circuit or only in certain critical areas. A current-mode approach is not just restricted to current processing, but also offers certain important advantages when interfaced to voltage-mode circuits. The use of current rather than voltage as the active parameter can result in higher usable gain, accuracy and bandwidth due to reduced voltage excursion at sensitive nodes [1-2].

Current conveyors, introduced in the early 1970's, are now emerging as an important class of circuits [3]. The first generation current conveyor (CCI) was introduced by Smith and Sedra in 1968 [4]. However CCI had distortion and accuracy limitations due to base current errors and output impedance restrictions [5]. So, in 1970 Sedra and Smith presented a more useful element, which was named second-generation current conveyor (CCII) [6].

Although CCIIs have a great number of applications in the various designs of analog electronics, like amplifiers, filters, impedance converters, gyrators, oscillators or more generally signal processing circuits [7-47], they lack electronic adjustability.

However many applications require electronic adjustability. In particular. sophisticated techniques of signal processing demand the ability to adapt the filter characteristics dynamically [48]. In such cases it is desirable to vary the filter coefficients electronically.

In current-mode circuits, transconductors (OTAs) are used to perform the tuning [49-54]. These are flexible and robust commercial devices, able to provide a transconductance variation over a wide range. However, the non-virtually zero voltage, which exists between the input terminals of the OTAs, is a considerable drawback in filter design [14].

By using the second-generation current controlled conveyor (CCCII) introduced by Fabre *et al* [55-56] current conveyor applications can be extended to the domain of electronically adjustable functions.

At present there is a growing interest in designing current-mode circuits using current controlled conveyors [57-67]. The works based on current controlled conveyors can be summarized as:

1) Kiranon and Kerson [57] proposed a current controlled oscillator using two CCCII+ and two grounded capacitors in 1996. The oscillator circuit has been obtained by using the current-mode bandpass filter proposed in [55] as a resonator of the oscillator and an undamping current amplifier. The oscillation frequency can be varied proportionally to the bias current.

2) By employing one grounded capacitor, two floating resistors and four non-inverting CCII+s as active elements Kiranon and Pawarangkoon [58] in 1997 described a floating inductance simulation circuit. Its inductance may be tuned by means of a single resistance. However the circuit has been modified by using current controlled conveyors in place of some CCIIs, yielding electronically adjustable inductance.

3) In 1998, Fabre *et al* [59] proposed a second order current-mode bandpass filter with high–Q and high frequency response implemented from CCCII. Its application to a mobile communication receiver channel also including voltage/current conversion, current programmable gain amplifier (PGA), and current/voltage conversion circuit has been described. The tuning of the center frequency and Q factor has been obtained by varying DC current sources,

4) A current-mode analog multiplier/divider circuit using two CCCIIs has been outlined by Abuelma'atti and Al-Qahtani in 1998 [60]. The same topology is usable for performing the multiplication and the division. In the same year Abuelma'atti and Tasadduq proposed new current-mode current-controlled filters [61-63]. The

proposed realizations can simultaneously realize lowpass, highpass and bandpass responses. The parameters ω_o and $\frac{\omega_o}{Q}$ can be controlled by adjusting the bias current of CCCIIs.

5) Abuelma'atti and Tasadduq proposed a CCCII-based tunable oscillator in 1998 [64]. In the proposed circuit the frequency of oscillation and the condition of oscillation can be controlled electronically. Also in 1999, the same authors proposed an electronically tunable capacitance multiplier and frequency-dependent negative-resistance (FDNR) simulator using the current controlled conveyor [65]. In the proposed circuits the multiplying factors of the capacitance multipliers and the value of the FDNR are tunable by adjusting the bias current of the CCCII.

6) Minaei and Türköz proposed a new current-mode current controlled universal filter using four single–output current controlled conveyors and two grounded capacitors in 2000 [66]. The proposed filter can simultaneously realize lowpass, bandpass and highpass responses. The circuit provides independent control of the parameters ω_o and $\frac{\omega_o}{Q}$ by adjusting the bias currents of the CCCIIs, without disturbing the gains of the lowpass, bandpass and highpass responses. Also in the same year, a new current-controlled sinusoidal oscillator using three current controlled conveyors has been presented by Türköz and Minaei [67]. The proposed oscillator provides double-bias current-controlled oscillation frequency, fully independent control of oscillation condition and oscillation frequency and suitability for IC implementation due to including only grounded passive elements.

7) In 2000, Khan and Maheshwari, proposed new first order all-pass section using CCCII [68]. In addition the circuit uses two resistors and one capacitor. Although the proposed circuit provides electronic adjustability of the pole frequency, this circuit works in voltage-mode.

8) Minaei and Türköz proposed a new current-mode current controlled universal filter using four single–output current controlled conveyors one current conveyor and three grounded capacitors in 2001 [69]. The proposed filter can simultaneously realize lowpass, bandpass and highpass responses all at high output impedance. The circuit provides independent control of the parameters ω_o and $\frac{\omega_o}{Q}$ by adjusting the

bias currents of the CCCIIs, without disturbing the gains of the lowpass, bandpass and highpass responses. In the same year Minaei *et al* proposed new second-order bandpass, lowpass and highpass filters using only one or two current controlled conveyors [70].

As it can be seen from the mentioned works, there has been great emphasis on the design and implementation of current-mode circuits using CCCIIs, because these circuits provide a wide range of electronic tunability of the circuit parameters and a broad frequency range of operation.

In this thesis, we investigate bipolar implementation of the current controlled conveyor and a detailed study of the non-ideal CCCII. Also using equivalent circuit for non-ideal CCCII suitable for the translinear CCCII, the frequency behavior of the non-ideal CCCII is analyzed in SPICE and its non-ideality elements are calculated in Chapter 2.

On the other hand new applications for the CCCII such as filter, inductance simulation and oscillator configurations are introduced in Chapter 3.

Also, in order to take the advantages of the BiCMOS technology, a new BiCMOS realization of the CCCII is proposed in Chapter 4. The DC transfer characteristic and frequency behavior of the proposed realizations are extracted, which confirm good performance of the circuit.

In Chapter 5, the effects of the current and voltage transfer non-idealities of the CCCII are investigated on a new second order current-mode current controlled filter using only one CCCII proposed by author. The effects of the non-idealities in CCCII are taken into account in the transfer function, resonant angular frequency quality factor of second order current-mode lowpass, and bandpass filters. The stability and sensitivities of the filters are investigated. As an example, the results are used in design of a second order bandpass filter.

2. THE CURRENT CONTROLLED CONVEYOR (CCCII) CONCEPT AND ITS BIPOLAR REALIZATION

In this chapter, at first the definition of the first and second generation current conveyor is given. Then the definition of the ideal current controlled conveyor (CCCII) and its modified implementation are presented. Then the non-ideal CCCII and an equivalent circuit for the translinear implementation of positive or negative CCCII are investigated. This equivalent circuit takes into account various parasitic elements of the conveyor, which includes frequency limitations (gain values, poles of the voltage and current transfers and parasitic impedances). The non-ideality elements of the CCCII are found and the results are given in tabular form.

2.1 Definition of The First and Second Generation Current Conveyor (CCI & CCII)

An ideal first generation current conveyor (CCI), whose circuit symbol is given in Figure 2.1, can be defined by the following matrix equation:

$$\begin{bmatrix} I_y \\ V_x \\ I_z \end{bmatrix} = \begin{bmatrix} 0 & 1 & 0 \\ 1 & 0 & 0 \\ 0 & \pm 1 & 0 \end{bmatrix} \begin{bmatrix} V_y \\ I_x \\ V_z \end{bmatrix} \tag{2.1}$$

where the positive sign refers to positive first generation current conveyor (CCI+) and negative sign refers to negative one (CCI–). From equation (2.1) one can see that the currents at terminals X and Y are equal. Also the voltage of terminal X follows the voltage of terminal Y.

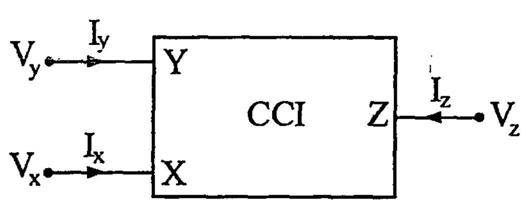

Figure 2.1: Electrical symbol of the CCI

The terminal relations of an ideal second generation current conveyor (CCII) can be given by

$$\begin{bmatrix} I_y \\ V_x \\ I_z \end{bmatrix} = \begin{bmatrix} 0 & 0 & 0 \\ 1 & 0 & 0 \\ 0 & \pm 1 & 0 \end{bmatrix} \begin{bmatrix} V_y \\ I_x \\ V_z \end{bmatrix} \tag{2.2}$$

In this equation, (+) sign denotes a positive second-generation current conveyor (CCII+), whereas (–) sign denotes a negative one (CCII–). Figure 2.2 shows the electrical symbol of the CCII. From equation (2.2), it can be further inferred that terminal impedances at terminals Y and Z must be high, while the impedance at terminal X must be low. The voltage at X follows that applied to Y, thus X exhibits zero input impedance. The current supplied to X is conveyed to the high impedance output terminal Z. The main disadvantage of these elements is lack of electronic adjustability.

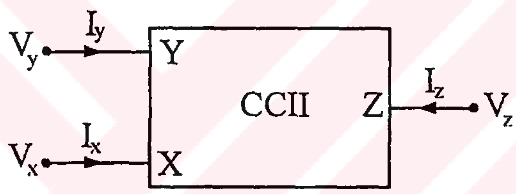

Figure 2.2: Electrical symbol of the CCII

2.2 Definition of The Second Generation Current Controlled Conveyor (CCCII)

The ideal second-generation current controlled conveyor as shown in Figure 2.3, is described by the matrix relationship that exists between voltages and currents of its input-output terminals:

$$\begin{bmatrix} I_y \\ V_x \\ I_z \end{bmatrix} = \begin{bmatrix} 0 & 0 & 0 \\ 1 & R_x & 0 \\ 0 & \pm 1 & 0 \end{bmatrix} \begin{bmatrix} V_y \\ I_x \\ V_z \end{bmatrix} \tag{2.3}$$

In equation (2.3) the positive sign denotes a positive current controlled conveyor (CCCII+) and the negative sign denotes a negative current controlled conveyor (CCCII–).

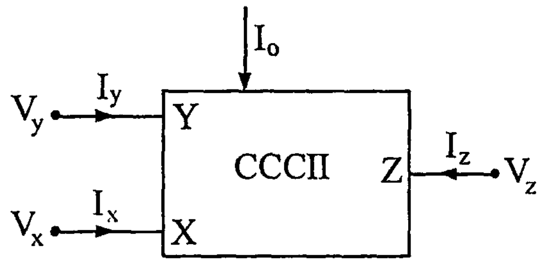

Figure 2.3: Electrical symbol of the CCCII

The input impedances for the ideal CCCII are respectively: infinite at terminal Y and R_x at terminal X. The terminal Z, that is equivalent to a current generator, possesses infinite output impedance. Electronic adjustability of the CCCII is attributed to the dependence of the parasitic resistance at terminal X on the bias current of the current conveyor.

2.3 Bipolar Implementation of The Current Controlled Conveyor

The schematic implementation of the second-generation current controlled conveyor with a positive current transfer from X to Z (CCCII+) is shown in Figure 2.4. It uses the preceding mixed translinear loop (transistors Q_1 to Q_4) as input cell. For each transistor assume that:

(a) The current gain $\beta >> 1$

(b) $V_{BE} > 4V_T$ ($V_T = kT/q \cong 26$mV at 27° C is the thermal voltage)

(c) The collector-base voltage V_{CB} is equal to zero.

The relationship between collector current I_C and base-voltage V_{BE} is

$$I_C = I_s e^{(V_{BE}/V_T)} \tag{2.4}$$

where I_s represents the reverse saturation current of the BE junction. Then the following equation for Figure 2.4 can be written [71]:

$$I_1 I_3 = I_2 I_4 \tag{2.5}$$

Two current mirrors (transistors Q_{11} to Q_{13} and Q_9, Q_{10}) allow the mixed loop to be DC biased by the current I_o ($I_1 = I_3 \cong I_o$). Thus it presents a high impedance input at terminal Y and low impedance at terminal X. Using equation (2.4) the voltage difference between terminals X and Y can be easily found as:

$$V_x - V_y = -V_T \ln \frac{I_2}{I_o} \tag{2.6}$$

Considering $I_1 = I_3 \cong I_o$ and $I_4 = I_2 + I_x$ the currents I_2, I_4 can be derived from (2.5) as:

$$I_2 = \frac{1}{2}(\sqrt{I_x^2 + 4I_o^2} - I_x) \tag{2.7}$$

$$I_4 = \frac{1}{2}(\sqrt{I_x^2 + 4I_o^2} + I_x) \tag{2.8}$$

Therefore by substituting (2.7) into (2.6) and assuming $I_x << 2I_o$, the input resistance at terminal X can be found as:

$$R_x = \frac{V_x - V_y}{I_x} = \frac{V_T}{2I_o} \tag{2.9}$$

So R_x can be controlled by varying the bias current I_o. As a general rule a current controlled conveyor (CCCII) is a CCII to which the possibility of modifying the value of the bias current I_o, will confer electronic adjustability. Output Z, which duplicates the current flowing through terminal X, is realized in a conventional manner, using two complementary mirrors.

The input cell of the CCCII at DC biasing entrance (Q_{12}, Q_{13}, Q_{14}) in Figure 2.4 is slightly modified so that the difference between I_o and the collector currents of transistors Q_1 and Q_3 are decreased with respect to the implementation proposed in [56]. Therefore a larger tuning range for the CCCII is achieved.

A negative current controlled conveyor (CCCII–) can be obtained easily, by only adding two cross-coupled current mirrors [3] in order to reverse the sign of the current I_z. Figure 2.5 shows the implementation of the CCCII–. Figure 2.6 shows the equivalent circuit between terminals Y and X of an ideal CCCII.

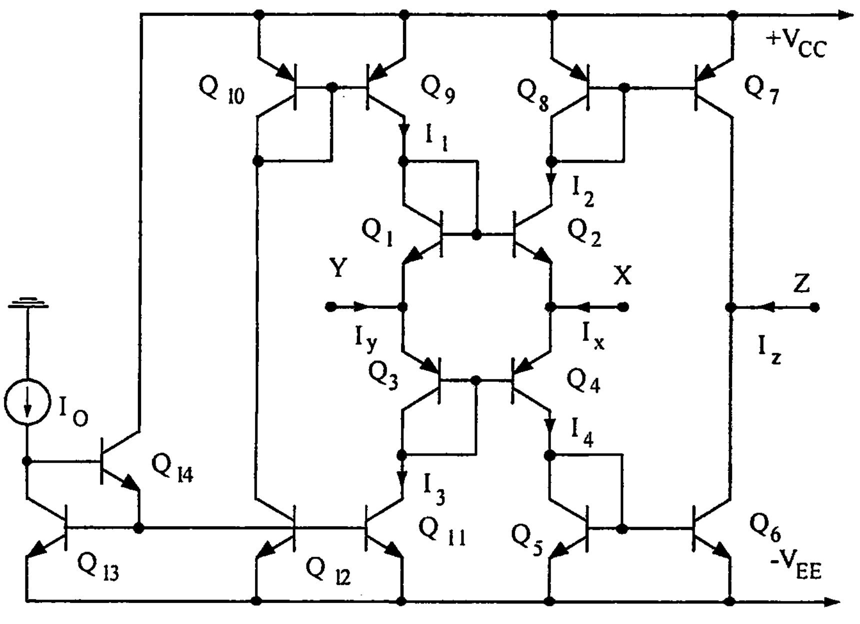

Figure 2.4: Schematic implementation for the CCCII+

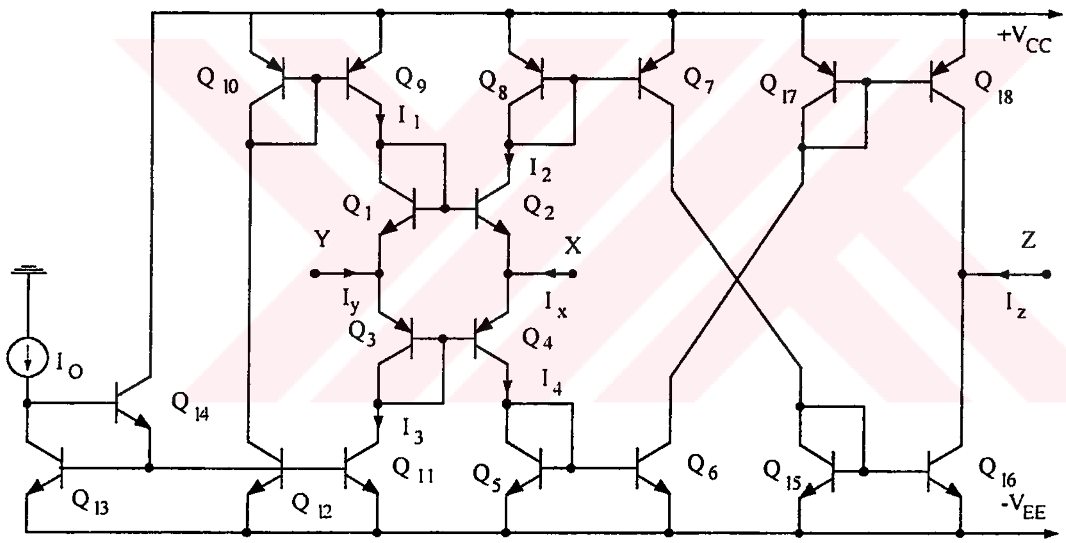

Figure 2.5: Schematic implementation for the CCCII–

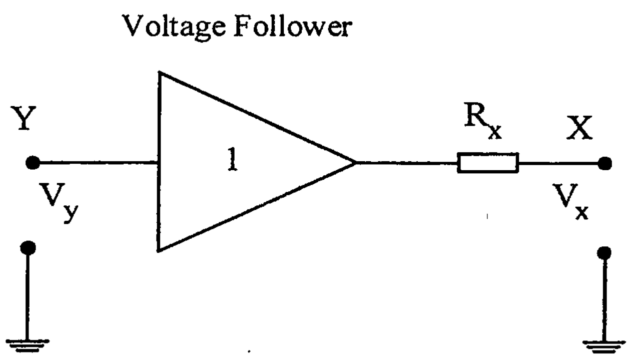

Figure 2.6: Equivalent circuit between terminals Y and X

When the terminal Y of the CCCII+ is grounded and the terminal X constitutes the input of the circuit, the output current $I_z = I_x$ is given by

$$I_z = \frac{2I_o}{V_T}V_x = \frac{1}{R_x}V_x \tag{2.10}$$

Then the output current I_z is controllable by the bias current I_o. The input resistance of this circuit is equal to R_x. When the terminal X of the CCCII+ is grounded, the input of the circuit, on terminal Y, is obtained at high impedance. The output current I_z in this case can be given by

$$I_z = -\frac{2I_o}{V_T}V_y \tag{2.11}$$

Note that when the CCCII+ is replaced by a CCCII–, the respective output currents will be obtained from (2.10) and (2.11) after inversion of the signs. From (2.10) and (2.11) it can be seen that the CCCII can work as a transconductor which its transconductance is $g_m = \frac{2I_o}{V_T}$. Therefore CCCII can be compared to classical OTA implementation. For a conventional bipolar OTA, the value of the transconductance is $g_m = \frac{I_o}{2V_T}$ [72]. It can be observed that for a same value of g_m the bias current I_o of the OTA must be four times greater than the CCCII one. Therefore the use of bipolar OTA as a transconductor leads to a power consumption greater than a current controlled conveyor. Moreover for high values of the DC bias current which is the collector current of the transistors, their maximum operating frequency will decrease considerably because the transition frequency f_T of bipolar transistors falls down quickly for collector currents around a few milliamperes [73]. This indicates that the frequency performances of circuits with controlled conveyors will be much greater than those with OTA implementations.

To demonstrate the accurate representation of the CCCII, the voltage and current DC transfer characteristics and frequency response of current and voltage gains of the CCCII+ are obtained from SPICE simulations, using parameters of the PR100N and NR100N bipolar transistors [74] given in Appendix A. The biasing current is $I_o = 40\mu A$ and the power supply is ±2.5 V.

The voltage transfer characteristic V_x–V_y of the CCCII+, for open circuited terminal X is given in Figure 2.7. The voltage clipping limits at the terminal X were obtained as $V_{x\max} = 2.19$ V and $V_{x\min} = -2.19$ V.

Figure 2.8 shows the DC voltage transfer characteristics V_z–V_y from input terminal Y to the output terminal Z for open circuited terminal Z and short-circuited terminal X. The voltage clipping limits were determined as $V_{z\max} = 2.46$ V and $V_{z\min} = -2.47$ V.

Figure 2.9 shows I_x–V_y characteristics for short-circuited terminal X. The lower and upper boundaries of the current I_x were determined as $I_{x\max} = 3.37$ mA and $I_{x\max} = -2.09$ mA.

The frequency responses of the currents I_x and I_z when terminals X and Z are short-circuited and $I_o = 40\mu A$ are shown in Figure 2.10. Also frequency responses of the voltage gain V_x/V_y (open circuited terminal X and short circuited terminal Z) is shown in Figure 2.11.

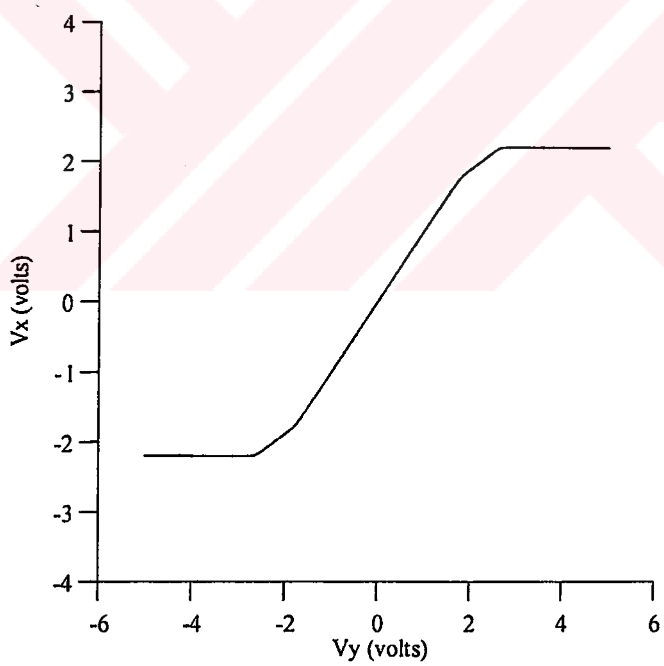

Figure 2.7: V_x-V_y, DC transfer characteristic of the CCCII+

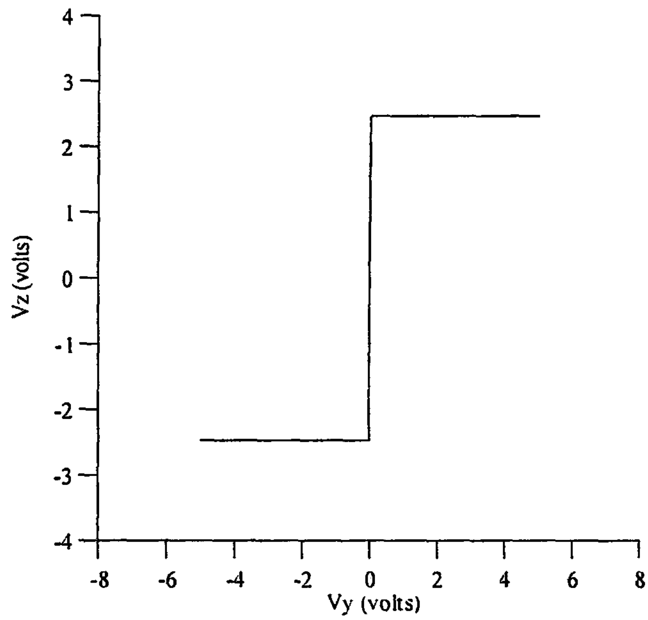

Figure 2.8: V_z–V_y, DC transfer characteristic of the CCCII+

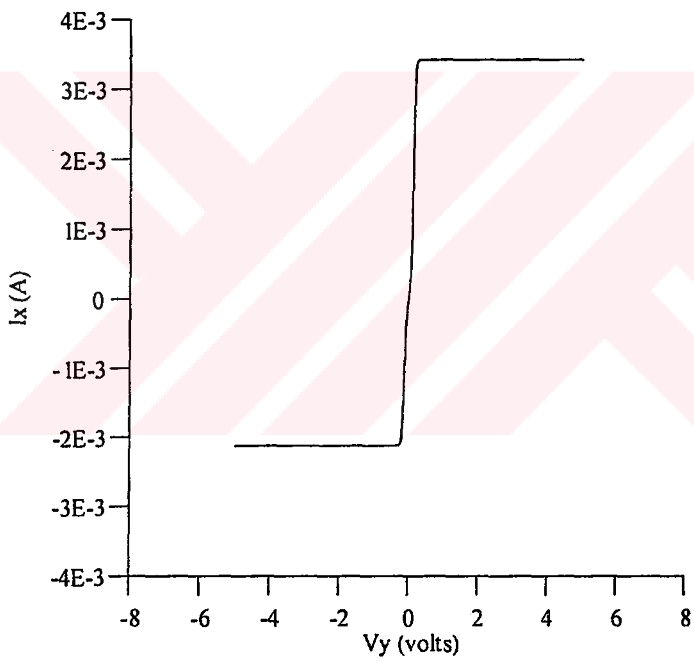

Figure 2.9: I_x–V_y, DC transfer characteristics of the CCCII+

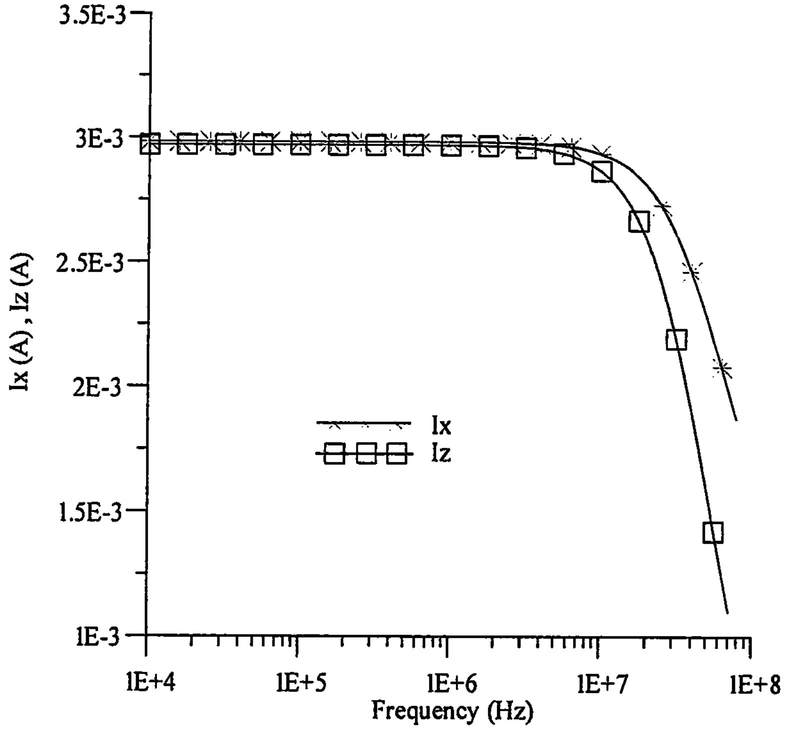

Figure 2.10: Frequency response of currents I_x and I_z

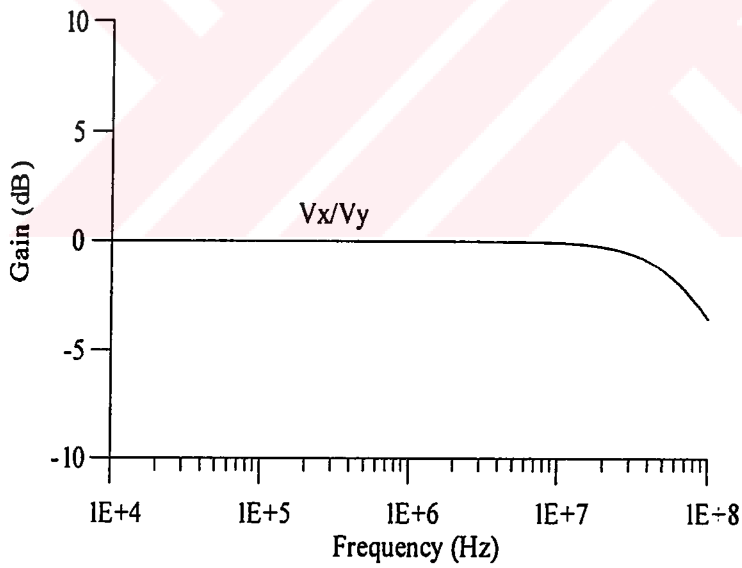

Figure 2.11: Frequency response of the voltage gain

2.4 Non-Idealities In Current Controlled Conveyors

The ideal current controlled conveyor in Figure 2.3, just as the general equation, allows only an approximate analysis of a circuit implemented from CCCIIs. Thus, when the possibilities of an electronic function will have to be determined and notably its performance at frequency above the MHz range, it will be necessary to consider a simplified circuit for the CCCII. But this must be relatively close to the real CCCII. This model will have to include the different parasitic impedances of the circuit as well as the possible variations, according to the frequency of the voltage and current transfers. There are some models for the second-generation current conveyors (CCII), whose input follower cell is realized with an operational amplifier [75-78]. However the values for their parameters are not adapted to the translinear conveyors whose frequential possibilities are much more extended. Here, we investigate equivalent circuit for second-generation current controlled conveyor, which represent the behavior of the real CCCII.

Figure 2.12 shows the non-ideal current controlled conveyor. Between each terminal Y and Z and the ground, the circuit contains a parallel equivalent parasitic impedance, (R_y // C_y) and (R_z // C_z), respectively. Also R_x is the output resistance of the equivalent Thevenin generator seen from terminal X.

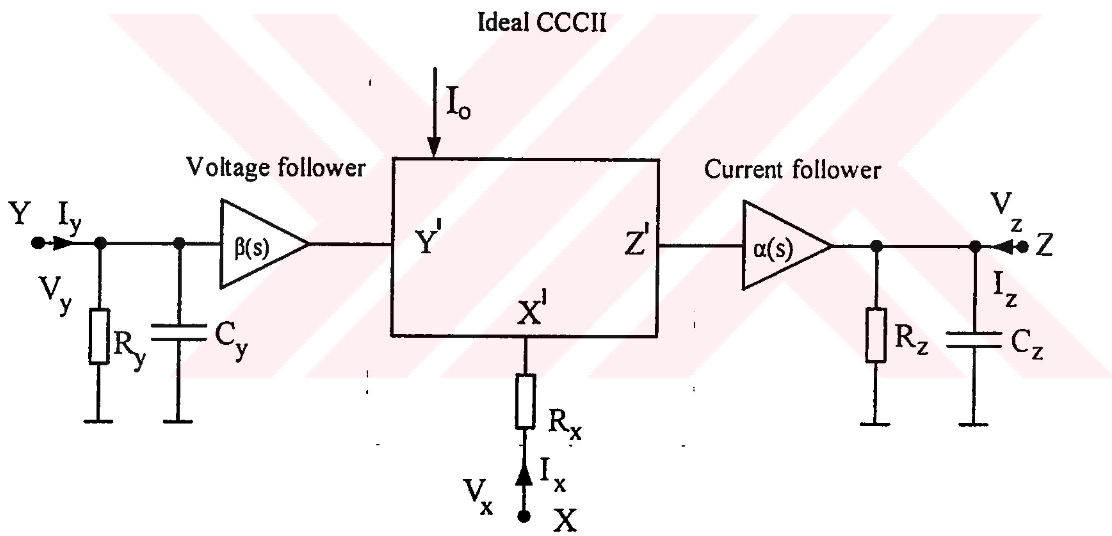

Figure 2.12: The non-ideal CCCII

$\alpha(s)$ and $\beta(s)$ are respectively the current and voltage transfer gains of the conveyor that will generally be described by the following first order functions [79]:

$$\beta(s) = \frac{\beta_o}{1 + \frac{s}{\omega_\beta}} \tag{2.12}$$

$$\alpha(s) = \frac{\alpha_o}{1 + \frac{s}{\omega_\alpha}} \tag{2.13}$$

where β_o and α_o are the values of these transfers at low frequencies. These values are very close to unity. ω_α and ω_β are the poles of the current and voltage transfer gains, respectively. Then, the circuit in Figure 2.12 allows us to complete the matrix equation (2.3) relative to the ideal CCCII, in order to describe correctly the real CCCII as:

$$\begin{bmatrix} I_y \\ V_x \\ I_z \end{bmatrix} = \begin{bmatrix} Y_y(s) & 0 & 0 \\ \beta(s) & R_x & 0 \\ 0 & \pm\alpha(s) & Y_z(s) \end{bmatrix} \begin{bmatrix} V_y \\ I_x \\ V_z \end{bmatrix} \tag{2.14}$$

where

$$Y_y(s) = \frac{1}{R_y} + C_y s \tag{2.15}$$

$$Y_z(s) = \frac{1}{R_z} + C_z s \tag{2.16}$$

SPICE simulation program of ideal and device model of CCCII are given in Appendix A.

2.5 Determination of The Parameters of Non-Ideal CCCII

Using of SPICE simulation is the simplest manner that allows us to determine, by AC analysis, the various elements in Figure 2.12. With a simulator, difficulties linked to physical measurements do not appear by just taking some precautions. NR100N&PR100N bipolar transistors [74], with DC supply voltages ±2.5V and I_o= 40μA are used in simulations.

The values for R_y and C_y must be determined with terminal X loaded by infinite impedance, terminal Z grounded. The input voltage is in this case applied at Y from a generator with zero output resistance. Then the variation according to the frequency of the current I_y that goes into the conveyor allows determining the evolution of the input impedance $Z_y = (R_y // C_y) = V_y / I_y$. R_y is the value of this impedance at low frequencies. The value of C_Y is then deduced from the –3dB cutoff frequency, f_y, of Z_y, $C_y = \frac{1}{2\pi f_y R_y}$. Simulated variation of the impedance Z_y with frequency for CCCII+ is given in Figure 2.13, which results in $R_y = 907\text{k}\Omega$ and $C_y = 4.73\text{pF}$.

The value of R_z and C_z, which constitute the output impedance of the current generator at terminal Z, can be determined for the conveyor driven by an external voltage V_z on Z and with grounded terminals Y and X. Then, the current I_z, which results at terminal Z, allows determining R_z at low frequency: $R_z = V_z / I_z$. The value of C_Z is deduced from the –3dB cutoff frequency, f_Z of this voltage: $C_z = \frac{1}{2\pi f_z R_z}$. Simulated variation of the impedance $Z_z = (R_z // C_z)$ with frequency for CCCII+ is given in Figure 2.14, which results in $R_z = 934\text{k}\Omega$ and $C_z = 2.58\text{pF}$. Note that, In order to obtain accurate values for R_z and C_z, it will often be necessary for this simulation to compensate the offset current existing on Z. The continuous offset current compensation will have to be applied at terminal X.

The value of the R_x at terminal X, is determined with terminal Y and Z grounded. When an input current I_x is applied into terminal X, the resulting voltage V_x and $R_x = V_x / I_x$ allows to determine the input resistance R_x of terminal X. Figure 2.15 represent the variation of the input resistance at terminal X (R_x), as a function of the bias current I_o for CCCII+. It can be seen that the values obtained from SPICE simulation are in good accordance with theoretical ones calculated from equation (2.9).

It can be seen that by using the transistor Q_{14} at together with Q_{12} and Q_{13} in Figure 2.4, a deviation less than 5% is obtained for R_x, in the range of 0.1–500µA for I_o, which is smaller than the conventional one represented in [56] (10% deviation for R_x in the range of 0.1–150µA for I_o). Therefore larger tuning range of the CCCII is achieved.

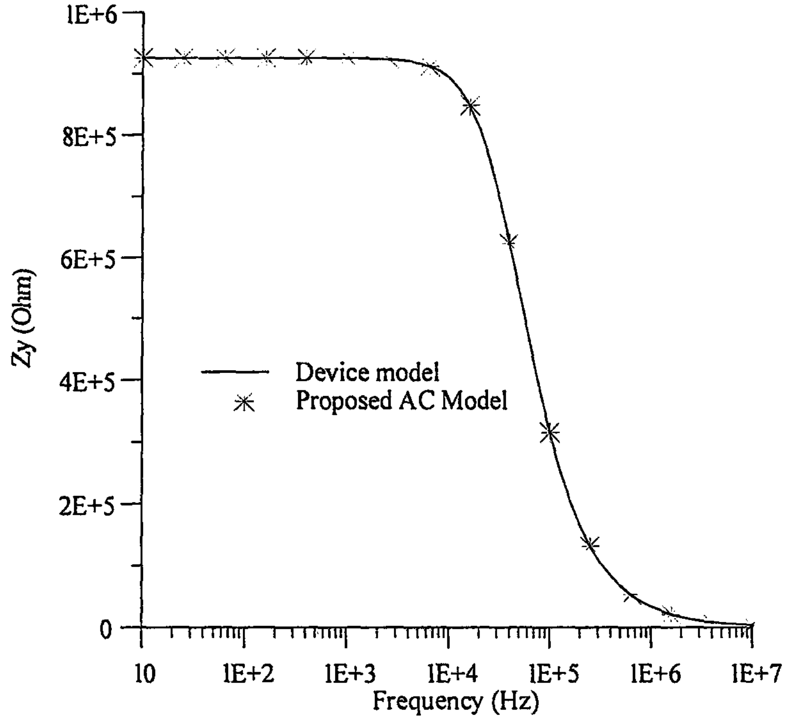

Figure 2.13: Frequency response of Z_y

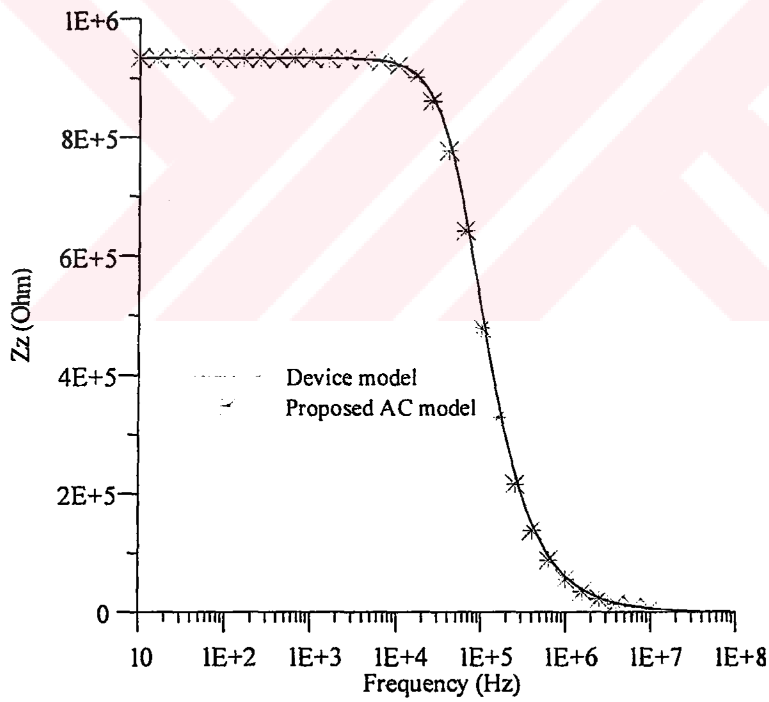

Figure 2.14: Frequency response of Z_z

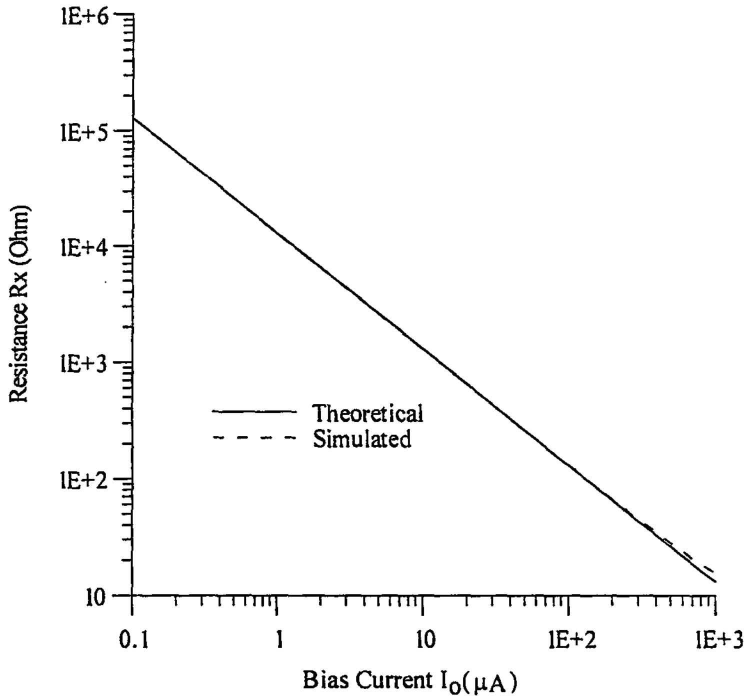

Figure 2.15: Theoretical and simulated values for R_x

The parameter $\beta(s) = V_x/V_y$ is the voltage transfer of the CCCII. It must be determined as a function of the frequency, an infinite load connected at X, output Z grounded and the conveyor being driven at Y by a voltage generator with zero output resistance. Figure 2.16 shows the frequency variation of $\beta(s)$, for both CCCII+ and CCCII– under a biasing current of $I_o = 40\mu A$ and power supply ±2.5 V.

The parameter $\alpha(s) = I_z/I_x$ is the current transfer of the CCCII that will be determined with an input current applied into terminal X. The current I_z is then the current that flows through terminal Z grounded, terminal Y being grounded. Figure 2.17 shows the frequency variation of $\alpha(s)$ for the two conveyors supplied under ±2.5 V and with a bias current I_0 equal to 40μA.

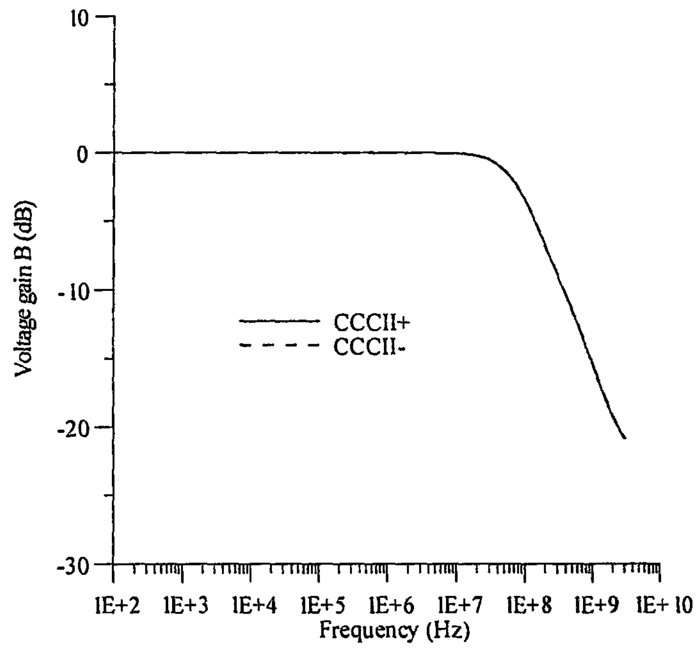

Figure 2.16: Frequency response of the voltage gain β

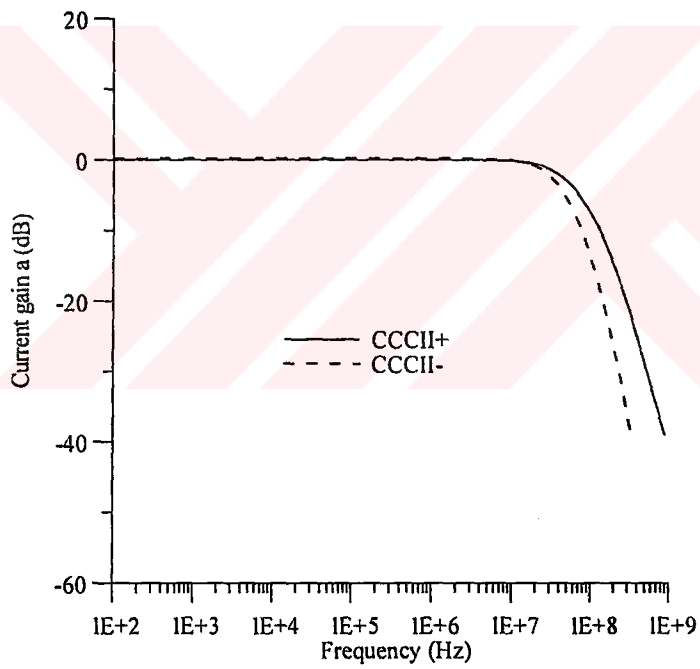

Figure 2.17: Frequency response of the current gain α

Table 2.1 and 2.2 give the values of the DC and AC parameters for the CCCII+ and CCCII– supplied under ±2.5 V and with a bias current I_o equal to 40μA. The DC offsets cannot degrade the frequency response of the circuits using conveyors. They could be compensated if necessary.

The assimilation of $\alpha(s)$ and $\beta(s)$ variations to first order transfer functions for a purpose of simplification, as indicated by equations (2.12) and (2.13) and Tables 2.1 and 2.2, establishes to be often well sufficient.

Table 2.1: Model parameters for the CCCII+; using NR100N&PR100N bipolar arrays, with $V_{CC}=V_{EE}=2.5V$; $I_o= 40\mu A$

Parameter	Value	Parameter	Value
R_y	907kΩ	ω_α	3.12 E+8 r/s
C_y	4.74pF	β_o	0.999
R_z	915kΩ	ω_β	5.68 E+8r/s
C_z	2.6pF	Input offset current at Y (I_{Yoff})	2.27μA
R_x	328Ω	Output offset voltage at X (V_{Xoff})	128μV
α_o	0.996	Output offset current at Z (I_{Zoff})	-1.78μA

Table 2.2: Model parameters for the CCCII−; using NR100N&PR100N bipolar arrays, with $V_{CC}=V_{EE}=2.5V$; $I_o= 40\mu A$

Parameter	Value	Parameter	Value
R_y	907kΩ	ω_α	2.06 E+8
C_y	4.74pF	β_o	0.999
R_z	937kΩ	ω_β	5.57 E+8r/s
C_z	2.44pF	Input offset current at Y (I_{Yoff})	2.27μA
R_x	328Ω	Output offset voltage at X (V_{Xoff})	128μV
α_o	1.02	Output offset current at Z (I_{Zoff})	-1.38μA

2.6 Basic Circuit Implementations with The CCCII

As it mentioned before, the parasitic resistance at terminal X of the CCCII. which can be controlled electronically, opens new applications in addition to those of CCII-based circuits. While tunability can be achieved by combining current conveyors and OTAs, the use of current controlled conveyors allows current conveyor applications to be extended to the domain of electronically tunable functions. Moreover. all the current-mode CCII-based circuits employing one external resistance connected to terminal X can be replaced by CCCII-based circuits by exploiting to advantage the parasitic resistance at terminal X. The basic applications of the CCCII are summarized in Table 2.3. The more complex new applications of the CCCII such as filters and oscillators and floating inductance simulation will be presented in Chapter 3.

Table 2.3: Basic applications of the CCCII

Circuit	Figure	Formulation
Current buffer	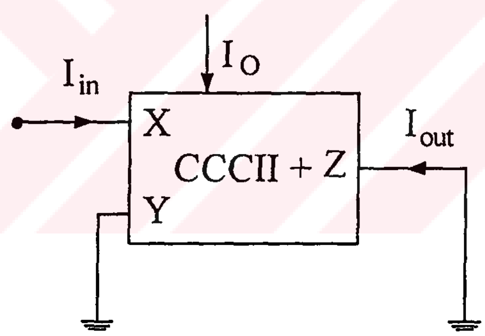	$I_{out} = I_{in}$
Voltage buffer	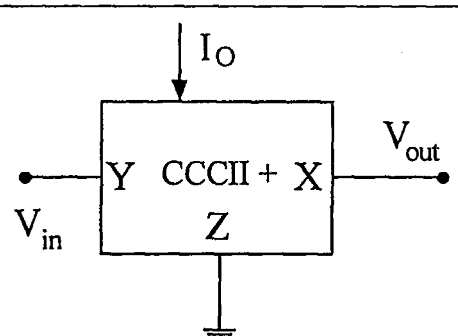	$V_{out} = V_{in}$

Voltage to current converter	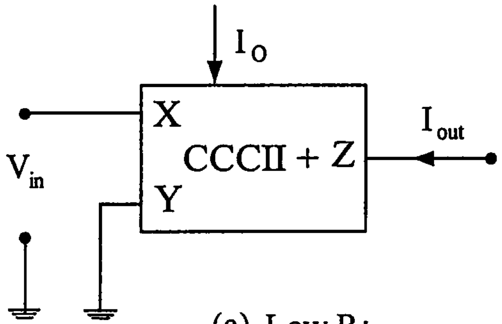 (a). Low R_{in} 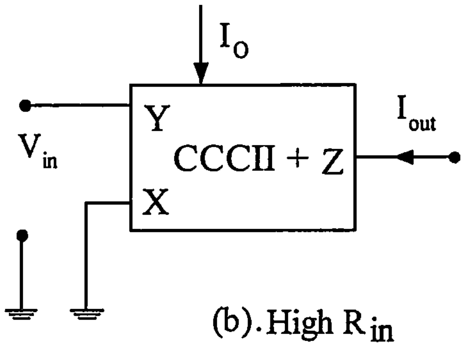 (b). High R_{in}	$I_{out} = \frac{V_{in}}{R_x}$ $I_{out} = -\frac{V_{in}}{R_x}$
Negative resistance	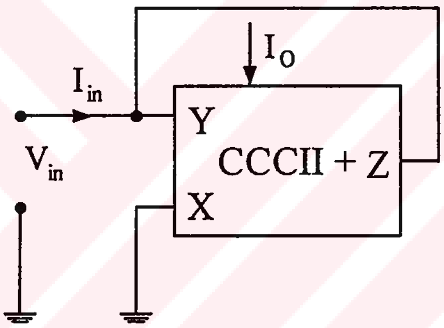	$\frac{V_{in}}{I_{in}} = -R_x$
Current-mode integrator	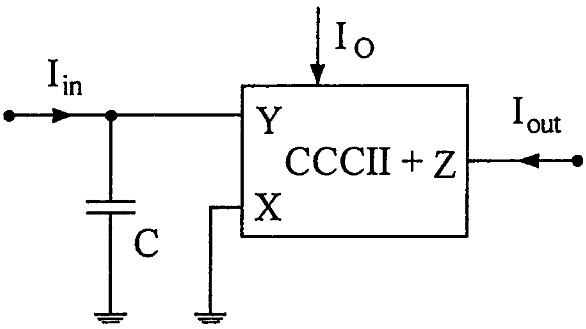	$\frac{I_{out}}{I_{in}} = -\frac{1}{sR_xC}$
Voltage-mode integrator	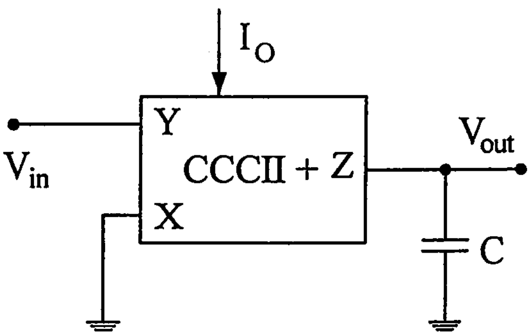	$\frac{V_{out}}{V_{in}} = \frac{1}{sR_xC}$

<table>
<tr><td>Current-mode amplifier</td><td>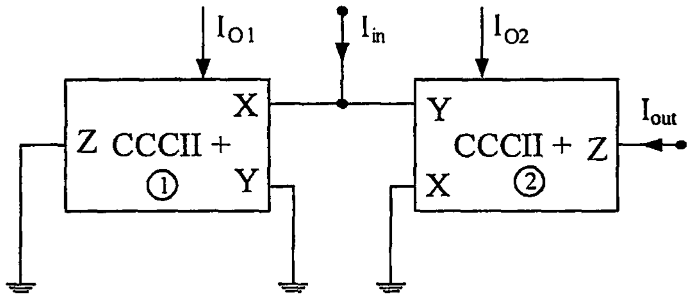
</td><td>$\frac{I_{out}}{I_{in}} = -\frac{R_{x1}}{R_{x2}}$</td></tr>
<tr><td>Voltage-mode amplifier</td><td>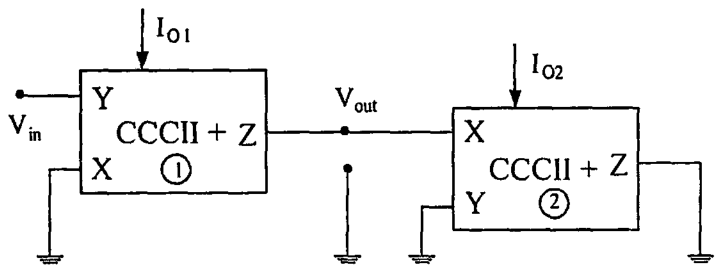
</td><td>$\frac{V_{out}}{V_{in}} = \frac{R_{x2}}{R_{x1}}$</td></tr>
<tr><td>Grounded inductance simulator</td><td>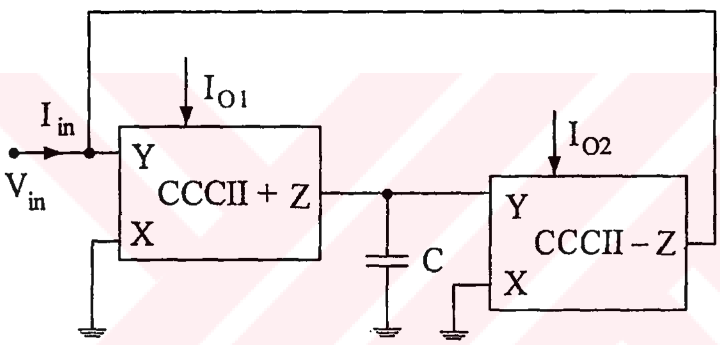
</td><td>$\frac{V_{in}}{I_{in}} = sR_{x1}R_{x2}C$</td></tr>
<tr><td></td><td></td><td></td></tr>
</table>

3. NEW APPLICATIONS OF THE CCCII

The design of different building blocks like oscillators, active filters and inductance simulators require the use of active and passive elements. The operational amplifier played a predominant role in the last two decades. However, the analog circuits employing active elements such as current conveyors have an important role in the IC design in the last decade. A considerable portion of researches in analog circuits today concerns design of current-mode oscillators, active filters and inductance simulators using current conveyors [7-47]. Current-mode techniques offer significant advantages over the respective voltage-mode implementations. They offer high frequency response, compatibility of integration and simplicity of design. In this chapter, new applications of the CCCII such as filters, oscillator and floating inductance simulator are presented.

3.1 Filters

3.1.1 Current-mode universal filters

Over the past few years a number of current-conveyor (CC)-based current-mode universal filters have been presented [9-13]. However these circuits suffer from the lack of electronic adjustability.

Recently, new configurations for realizing current-mode current-controlled universal active filters have been proposed by using the second-generation current controlled conveyors (CCCIIs) [61-63]. Although the CCCII allows current conveyor applications to be extended to the domain of electronically adjustable functions, the filter reported in [61] suffers from the use of six dual-output positive/negative type CCCIIs, which complicates the filter implementation. In the circuit proposed in [62], the parameter ω_o/Q cannot be adjusted electronically without disturbing the gain of the bandpass filter. Also the highpass responses in the circuits proposed in [62-63] are not at high impedance outputs.

Here, we propose a new current-mode current-controlled universal filter using single-output CCCIIs and grounded capacitors [69]. The proposed circuit can simultaneously realize lowpass, bandpass and highpass filters all at high impedance outputs so that this property enables easy cascading in current-mode operation. The realization of allpass and notch functions does not require additional current conveyors in either case as this can simply be achieved by connecting the appropriate nodes. Moreover the circuit provides independent current-control of the parameters ω_o and ω_o/Q without disturbing the gains of the filters.

The proposed circuit is shown in Figure 3.1. The proposed circuit comprises four CCCIIs, one CCII+ and three grounded capacitors. The use of grounded capacitors is particularly attractive for integrated circuit implementation [28]. The CCCIIs 1, 2 and 3 carry out a controlled gyrator, which synthesizes an ideal inductance theoretically.

Routine analysis yields the following transfer functions

$$\frac{I_{LP}}{I_{in}} = \frac{\dfrac{\alpha_1\alpha_3\beta_1\beta_2}{R_{x1}C_1C_2(R_{x2}+R_{x3})}}{D(s)}, \quad \frac{I_{BP}}{I_{in}} = \frac{-\dfrac{\alpha_4}{R_{x4}C_1}s}{D(s)}, \quad \frac{I_{HP}}{I_{in}} = \frac{\dfrac{\alpha\beta C_3}{C_1}s^2}{D(s)} \tag{3.1}$$

Where

$$D(s) = s^2 + \frac{1}{R_{x4}C_1}s + \frac{\alpha_1\alpha_2\beta_1\beta_2}{R_{x1}C_1C_2(R_{x2}+R_{x3})} \tag{3.2}$$

and R_{xi}, $i = 1$–4 is the input resistance at terminal X of the i-th CCCII. Then, the filter simultaneously realizes lowpass, bandpass, and highpass responses. From (3.1) and (3.2) it can be seen that, the gains of the lowpass and bandpass filters are equal to unity ($G_{LP} = \alpha_3/\alpha_2$ and $G_{BP} = -\alpha_4$), while the gain of the highpass filter is equal to $G_{HP} = \dfrac{\alpha\beta C_3}{C_1}$. Note that the coefficient of 's' in (3.2) cannot be equal to zero, so the circuit is always stable. By adding all the current outputs and treating the node thus obtained as the output node, an allpass filter can be obtained, for $C_1 = C_3$. Similarly, by adding the current outputs I_{LP} and I_{HP} one can obtain a regular notch filter, for $C_1 = C_3$. Note that since zero and pole frequencies can take different values, one can also obtain lowpass notch and highpass notch filters for $C_1 > C_3$ and $C_1 < C_3$, respectively.

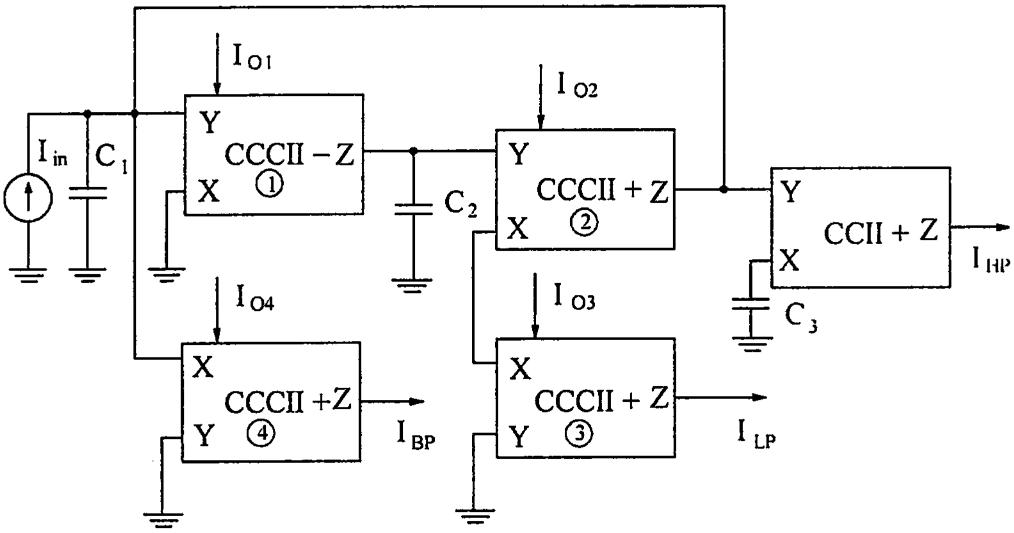

Figure. 3.1: Proposed current-mode current-controlled universal filter

The parameters ω_o, $\frac{\omega_o}{Q}$ and Q can be given as follows:

$$\omega_o = \sqrt{\frac{\alpha_1\alpha_2\beta_1\beta_2}{R_{x1}C_1C_2(R_{x2}+R_{x3})}},\quad \frac{\omega_o}{Q} = \frac{1}{R_{x4}C_1} = \frac{2I_{o4}}{V_T C_1},\quad Q = R_{x4}\sqrt{\frac{\alpha_1\alpha_2\beta_1\beta_2C_1}{R_{x1}C_2(R_{x2}+R_{x3})}} \quad (3.3)$$

It can be seen that the parameter ω_o can be controlled electronically by adjusting the bias current I_{o1} and/or I_{o2} and/or I_{o3} without disturbing the parameter ω_o/Q. Also the parameter ω_o/Q can be controlled by adjusting the bias current I_{o4} without disturbing the parameter ω_o. Furthermore after adjusting ω_o by I_{o1}, I_{o2} and I_{o3}, the quality factor of the filter Q can be controlled by I_{o4} independently of ω_o. The nonzero value of the input resistance at terminal X of actual CCII+ (R_x) limits the performance of the highpass response at high frequencies. The frequency limitation can be easily given by

$$f \langle\langle \frac{1}{2\pi R_x C_3} \quad (3.4)$$

Sensitivity analysis shows that

$$
\left.
\begin{aligned}
& S^{\frac{\omega_o}{Q}}_{R_{x4}} = S^{\frac{\omega_o}{Q}}_{C_1} = -S^{\frac{\omega_o}{Q}}_{I_{o4}} = S^{\frac{\omega_o}{Q}}_{V_T} = S^{\omega_0}_{V_T} = -S^{Q}_{R_{x4}} = -1 \\
& S^{\omega_o}_{\alpha_1} = S^{\omega_o}_{\alpha_2} = S^{\omega_o}_{\beta_1} = S^{\omega_o}_{\beta_2} = -S^{\omega_o}_{R_{x1}} = S^{\omega_o}_{I_{o1}} = -S^{\omega_o}_{C_1} = -S^{\omega_o}_{C_2} = \frac{1}{2} \\
& S^{\omega_o}_{R_{x2}} = -S^{\omega_o}_{I_{o2}} = S^{Q}_{R_{x2}} = -S^{Q}_{I_{o2}} = -\frac{R_{x2}}{2(R_{x2}+R_{x3})} \\
& S^{\omega_o}_{R_{x3}} = -S^{\omega_o}_{I_{o3}} = S^{Q}_{R_{x3}} = -S^{Q}_{I_{o3}} = -\frac{R_{x3}}{2(R_{x2}+R_{x3})} \\
& S^{\omega_o}_{\alpha_3} = S^{\omega_o}_{\alpha_4} = S^{\omega_o}_{R_{x4}} = S^{\omega_0}_{I_{o4}} = S^{\omega_o}_{\alpha} = S^{\omega_0}_{\beta} = S^{\omega_0}_{C_3} = 0 \\
& S^{\frac{\omega_o}{Q}}_{R_{x1}} = S^{\frac{\omega_o}{Q}}_{R_{x2}} = S^{\frac{\omega_o}{Q}}_{R_{x3}} = S^{\frac{\omega_o}{Q}}_{I_{o1}} = S^{\frac{\omega_o}{Q}}_{I_{o2}} = S^{\frac{\omega_o}{Q}}_{I_{o3}} = S^{\frac{\omega_o}{Q}}_{C_2} = S^{\frac{\omega_o}{Q}}_{C_3} \\
& \qquad = S^{\frac{\omega_o}{Q}}_{\alpha_1} = S^{\frac{\omega_o}{Q}}_{\alpha_2} = S^{\frac{\omega_o}{Q}}_{\alpha_3} = S^{\frac{\omega_o}{Q}}_{\alpha_4} = S^{\frac{\omega_o}{Q}}_{\alpha} = S^{\frac{\omega_o}{Q}}_{\beta} = 0 \\
& S^{Q}_{\alpha_1} = S^{Q}_{\alpha_2} = S^{Q}_{\beta_1} = S^{Q}_{\beta_2} = -S^{Q}_{R_{x1}} = S^{Q}_{I_{o1}} = S^{Q}_{C_1} = -S^{Q}_{C_2} = \frac{1}{2}
\end{aligned}
\right\}
\qquad (3.5)
$$

Thus, all of the passive and active sensitivities are low.

To verify the theoretical analysis the circuit proposed in Figure 3.1 has been simulated with SPICE circuit simulation program. The following setting has been selected to obtain the lowpass, bandpass and highpass filters with a pole natural frequency of $f_o = 577.1$ kHz and a pole quality factor of $Q = 0.707$: $I_{o1} = I_{o2} = I_{o3} = I_{o4} = 10\mu$A, $C_1 = C_2 = C_3 = 150pF$. The CCCII+ has been simulated using the schematic implementation proposed in [56] with DC supply voltage $= \pm 2.5$ V. The CCCII– has been simulated by adding cross-coupled current-mirrors to the schematic implementation of CCCII+. The CCII+ has been simulated using the realization proposed in [11]. The PNP and the NPN transistors have been simulated using the parameters of the PR100N and NR100N bipolar transistors [74]. Figure 3.2 shows the simulation results.

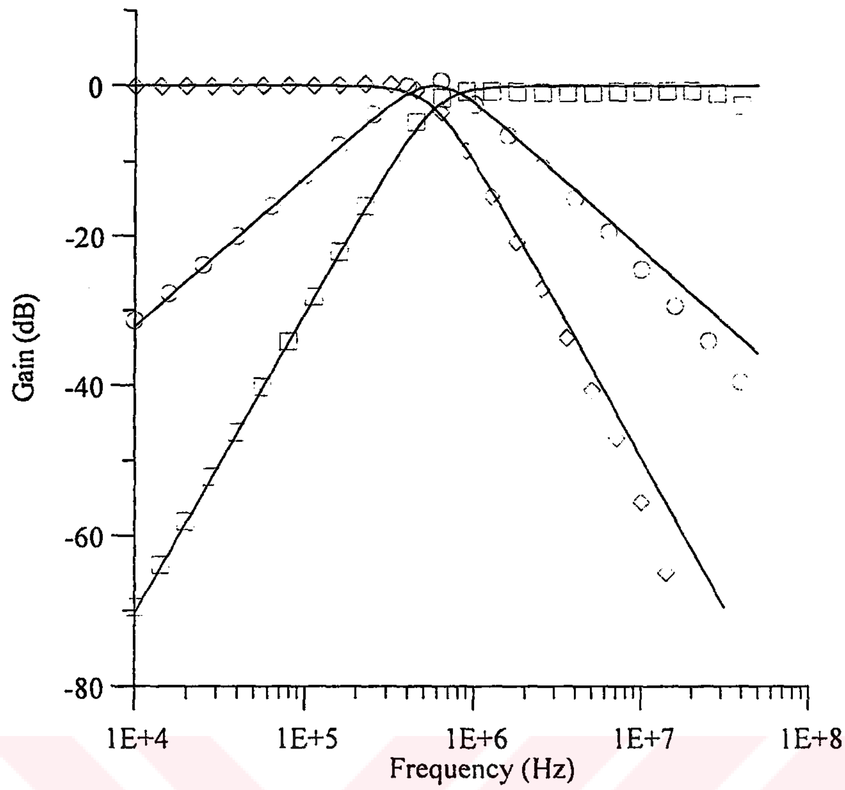

Figure 3.2: SPICE simulation results of the proposed circuit

$I_{o1} = I_{o2} = I_{o3} = I_{o4} = 10\mu\text{A}$, $C_1 = C_2 = C_3 = 150\,\text{pF}$

—— theoretical

◊ simulated lowpass filter response

O simulated bandpass filter response

□ simulated highpass filter response

It appears that the simulation results are in good agreement with the theoretical results. The difference in the high frequency region stems from the parasitic impedances of the current conveyors.

The proposed circuit provides the following advantages:

(i) Simultaneous realization of lowpass, bandpass, and highpass filter functions without changing the circuit topology

(ii) The realization of notch and allpass responses does not require additional active elements.

(iii) Entirely independent current-control of the parameters ω_0 and ω_0/Q without disturbing the gains of the lowpass, bandpass, and highpass filters.

(iv) Use of grounded capacitors, which is attractive for integration.

(v) Low active and passive sensitivities.

3.1.2 Current-mode all-pass filters

First-order all-pass filters are widely used for phase shifting while the amplitude of output signal is constant over the frequency range of interest. Several first order all-pass realizations using current conveyors are available in the literature [28-33, 68]. However, most of these circuits are in voltage-mode [28-31, 68] and suffer from the lack of electronic tunability [28-33].

In this section, two new configurations for realizing first order current-mode all-pass filters, is presented. The proposed configurations use two plus-type current controlled conveyors (CCCII+s) along with three to four passive elements. High output impedance has the advantage that the circuit can be used in cascade without requiring impedance matching device. The first proposed current-mode all-pass filter configuration is shown in Figure 3.3 [80].

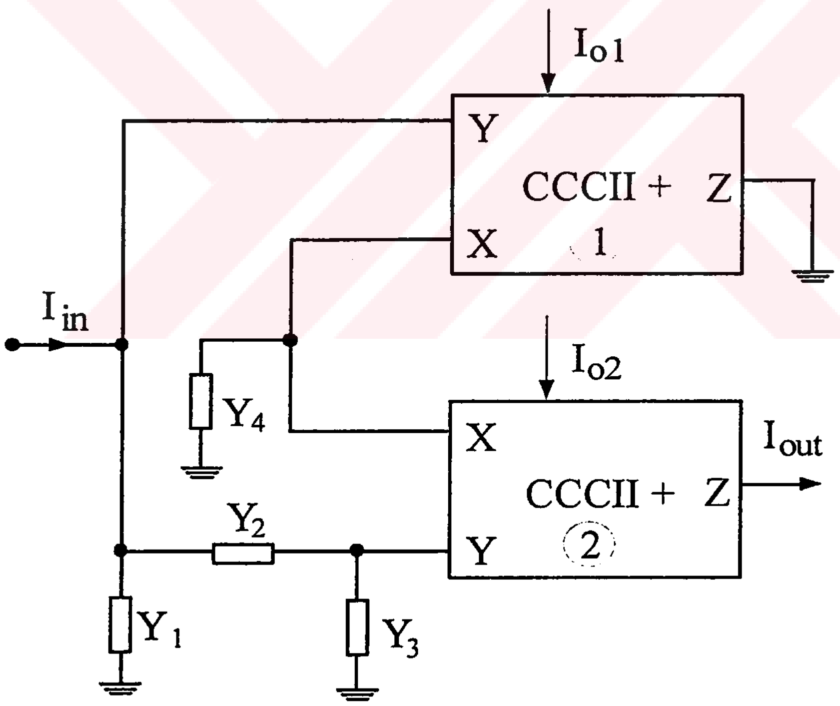

Figure 3.3: The first proposed All-pass configuration

Routine analysis shows that the transfer function of the circuit of Figure 3.3 can be expressed as:

$$\frac{I_{out}}{I_{in}} = \frac{\alpha_2 G_{x2}\left[\beta_2 Y_2 Y_4 - \beta_1 Y_3 G_{x1} + (\beta_2 - \beta_1) G_{x1} Y_2\right]}{(Y_1 Y_2 + Y_2 Y_3 + Y_1 Y_3)(G_{x1} + G_{x2} + Y_4)} \tag{3.6}$$

where α_i and β_i i=1,2 that are current and voltage gain of the i-th CCCII, respectively. In equation (3.6), G_{x1} and G_{x2} are the reciprocal of the input resistance at terminal X of the first and second CCCII+ ($1/R_{x1}$ and $1/R_{x2}$), respectively. For the ideal case of the CCCIIs ($\alpha_i = 1$, $\beta_i = 1$), the transfer function of the filter will be reduced to:

$$\frac{I_{out}}{I_{in}} = \frac{G_{x2}(Y_2Y_4 - Y_3G_{x1})}{(Y_1Y_2 + Y_2Y_3 + Y_1Y_3)(G_{x1} + G_{x2} + Y_4)} \tag{3.7}$$

Selection of different components for Y_1 to Y_4 ideally realizes eight different all-pass filter realizations as given in Table. 3.1. From Table. 3.1 it can be seen that by choosing equal bias current for the first and second CCCII, $I_{o1}=I_{o2}=I_o$ that is $G_{x1}=G_{x2}=G_x$ the matching condition of the realizations 1, 4 and 8 will be independent of the bias currents, therefore the pole angular frequency $\omega_p=1/\tau$ can be controlled by I_o without disturbing the matching condition. Also in realizations 2, 5, 6 and 7, the gain of the filters K, can be controlled with G_{x2} that is I_{x2}, without changing the pole angular frequency and the matching condition.

Table. 3.1: The possible realizations from the first presented configuration

Realization	Y_1	Y_2	Y_3	Y_4	Transfer function I_{out}/I_{in}	Gain, K	Matching condition	Time constant, τ
1	0	G_2	G_3	sC_4	$K\frac{G_{x1}+G_{x2}-sC_4}{G_{x1}+G_{x2}+sC_4}$	$-\frac{G_{x1}G_{x2}}{G_2(G_{x1}+G_{x2})}$	$G_3=\frac{G_2(G_{x1}+G_{x2})}{G_{x1}}$	$\frac{C_4}{G_{x1}+G_{x2}}$
2	0	G_2+sC_2	G_3	G_4	$K\frac{G_3G_{x1}-2sC_2G_4}{G_3G_{x1}+2sC_2G_4}$	$-\frac{G_4G_{x2}}{G_3(G_4+G_{x1}+G_{x2})}$	$G_2=\frac{G_3G_{x1}}{2G_4}$	$\frac{2C_2G_4}{G_3G_{x1}}$
3	0	G_2	G_3+sC_3	G_4	$K\frac{G_3-sC_3}{G_3+sC_3}$	$\frac{G_4G_{x2}}{2G_3(G_4+G_{x1}+G_{x2})}$	$G_2=\frac{2G_3G_{x1}}{G_4}$	$\frac{C_3}{G_3}$
4	0	G_2	G_3	sC_4	$K\frac{G_3G_{x1}-sC_4G_2}{G_3G_{x1}+sC_4G_2}$	$-\frac{(G_3-G_2)G_{x1}}{G_2G_3}$	$G_{x2}=\frac{(G_3-G_2)G_{x1}}{G_2}$	$\frac{C_4G_2}{G_3G_{x1}}$
5	0	G_2+sC_2	G_3	G_4	$K\frac{G_2-sC_2}{G_2+sC_2}$	$-\frac{G_{x1}G_{x2}}{2G_2(G_{x1}+G_{x2})+G_3G_{x1}}$	$G_4=\frac{G_3G_{x1}}{2G_2}$	$\frac{C_2}{G_2}$
6	G_1	sC_2	G_3	G_4	$K\frac{G_1G_3-sC_2(G_1+G_3)}{G_1G_3+sC_2(G_1+G_3)}$	$-\frac{G_{x1}G_{x2}}{G_3G_{x1}+G_1(2G_{x1}+G_{x2})}$	$G_4=\frac{G_{x1}(G_1+G_3)}{G_1}$	$\frac{C_2(G_1+G_3)}{G_1G_3}$
7	G_1	G_2	sC_3	G_4	$K\frac{G_1(G_{x1}-G_4)-sC_3G_{x1}}{G_1(G_{x1}-G_4)+sC_3G_{x1}}$	$\frac{G_4G_{x2}}{G_1(G_4+G_{x1}+G_{x2})}$	$G_2=\frac{G_1(G_{x1}-G_4)}{G_4}$	$\frac{C_3G_{x1}}{G_1(G_{x1}-G_4)}$
8	G_1	G_2	G_3	sC_4	$K\frac{G_3G_{x1}-sC_4G_2}{G_3G_{x1}+sC_4G_2}$	$\frac{G_{x1}(G_2-G_3)}{G_2G_1+G_1(G_2+G_3)}$	$G_{x2}=\frac{(G_3-G_2)G_{x1}}{G_2}$	$\frac{C_4G_2}{G_3G_{x1}}$

The performance of the circuit is demonstrated on a filter design example with realization-4 as shown in Figure. 3.4. The filter is simulated using PSPICE circuit simulation program. The CCCII+s are simulated using the schematic implementation shown in Figure 2.4 with DC supply voltage ±2.5V. The PNP and the NPN transistors in CCCII+ implementation are simulated using the parameters of the NR100N and PR100N bipolar transistors [72]. Selecting $I_{o1}=I_{o2}=I_o$, the matching condition and pole frequency of the filter can be found from Table 3.1 as:

$$\left.\begin{aligned} & R_2 = 2R_3 \quad \text{and} \\ & f_p = \frac{1}{2\pi\tau} = \frac{2I_o}{\pi V_T C_4} \end{aligned}\right\} \tag{3.8}$$

respectively. The passive and active values of the filter were selected as: R_2=1.3kΩ, R_3=650Ω, C_4=5nF and $I_{o1}=I_{o2}=I_o$=20μA, which results in a 90° phase shift at f_p=97.9kHz. The magnitude and phase characteristics of the simulated circuit are shown in Figure 3.5.

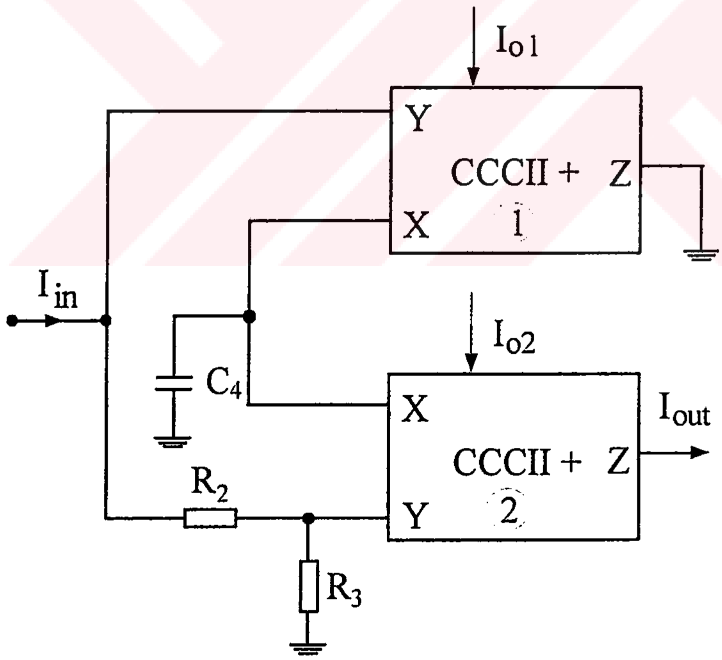

Figure 3.4: Filter design example for simulation

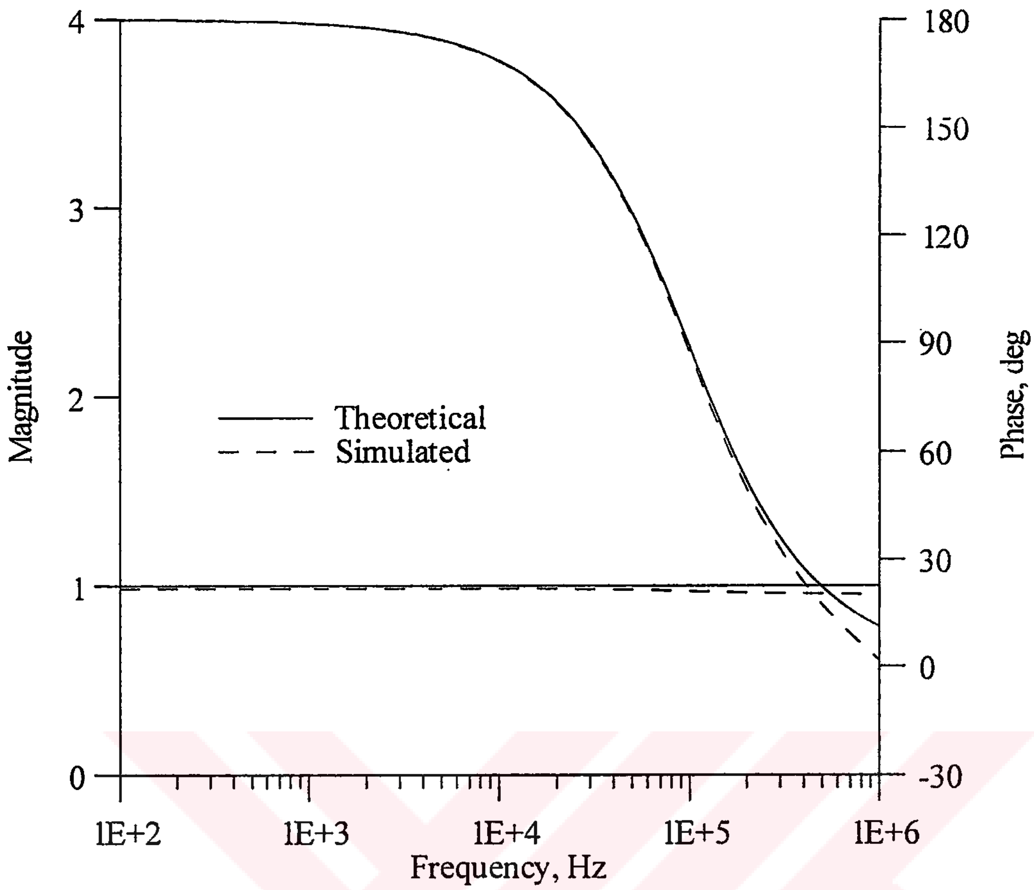

Figure 3.5: Magnitude and phase characteristics of the realization 4 of the first proposed configuration

The second proposed current-mode all-pass filter configuration is shown in Figure 3.6 [81].

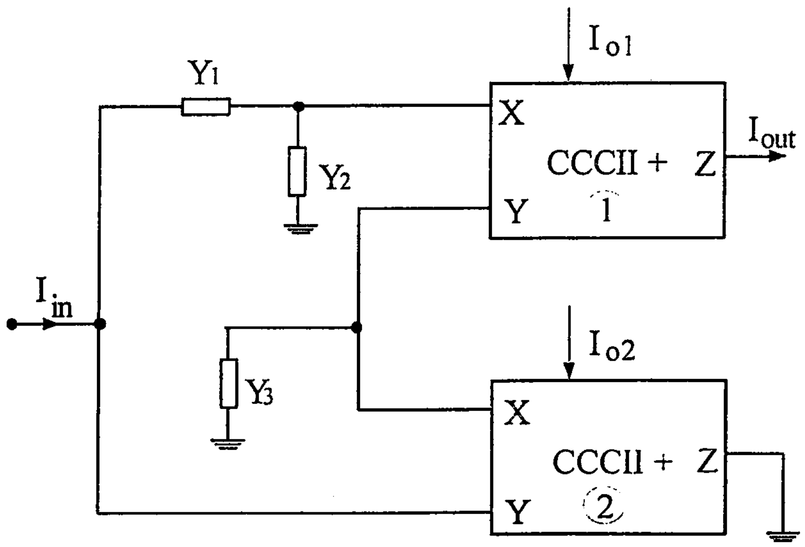

Figure 3.6: The second proposed All-pass configuration

Routine analysis of the circuit shown in Figure 3.6 yields the ideal current transfer function as follows:

$$\frac{I_{out}}{I_{in}} = \frac{G_{x1}(Y_2 G_{x2} - Y_3 Y_1)}{Y_1(Y_3 G_{x1} + Y_2 Y_3 + Y_2 G_{x2})} \tag{3.9}$$

and the non-ideal case as:

$$\frac{I_{out}}{I_{in}} = \frac{\alpha G_{x1}(\beta_1\beta_2 Y_2 G_{x2} + (\beta_1\beta_2 - 1)Y_1 G_{x2} - Y_3 Y_1)}{Y_1\left[(1-\beta_1\beta_2)G_{x1}G_{x2} + Y_3 G_{x1} + Y_2 Y_3 + Y_2 G_{x2})\right]} \tag{3.10}$$

where G_{x1} and G_{x2} are the reciprocal of the input resistance at terminal X of the first and second CCCII+ ($1/R_{x1}$ and $1/R_{x2}$), respectively. Similarly, selection of different components for Y_1 to Y_3 ideally realizes three different all-pass filter realizations as given in Table. 3.2. From Table. 3.2 it can be seen that the realizations 1 and 3 yield a phase shift from 0^o to -180^o while realization 2 yields phase shift from $+180^o$ to 0^o. As the Z-terminal impedance of CCCII Z_z is very high, the circuits have very high output impedances, which enables easy cascadability. The angular pole frequency ω_p of the realization 1 can be controlled by I_{o2} (that is G_{x2}) without disturbing the gain and matching condition of the filter. In realization 3, the gain of the filter can be controlled by I_{o1} (that is G_{x1}) without disturbing ω_p. The gain of the realization 2 is always unity.

As it is clear from the transfer functions of different realizations, the poles of the filters always lie in the left half of the s-plane. Even the requirements of matching conditions for all-pass responses also retain the poles of the transfer functions in the left half of the s-plane. Thus, all of the realizations are unconditionally stable.

Table 3.2: The possible realizations from the second presented configuration

Realization	Y_1	Y_2	Y_3	Transfer function I_{out}/I_{in}	Gain, K	Matching condition	Angular pole frequency, ω_p
1	G_1	G_2	sC_3	$K\dfrac{G_2G_{x2}-sC_3(G_2+G_{x1})}{G_2G_{x2}+sC_3(G_2+G_{x1})}$	$\dfrac{G_{x1}}{G_2+G_{x1}}$	$G_1=G_2+G_{x1}$	$\dfrac{G_2G_{x2}}{C_3(G_2+G_{x1})}$
2	G_1	sC_2	G_3	$K\dfrac{G_1G_3-sC_2G_{x2}}{G_1G_3+sC_2G_{x2}}$	-1	$G_{x1}=\dfrac{G_1(G_3+G_{x2})}{G_{x2}}$	$\dfrac{G_1G_3}{C_2G_{x2}}$
3	G_1+sC_1	G_2	G_3	$K\dfrac{G_2G_{x2}-2sC_1G_3}{G_2G_{x2}+2sC_1G_3}$	$-\dfrac{G_3G_{x1}}{G_3G_{x1}+G_2(G_3+G_{x2})}$	$G_1=\dfrac{G_2G_{x2}}{2G_3}$	$\dfrac{G_2G_{x2}}{2C_1G_3}$

PSPICE simulations were performed using bipolar implementation of the CCCII+ shown in Figure. 2.4. The supply voltages were chosen as V_{CC}=2.5 V and $-V_{EE}$= −2.5 V. The PNP and the NPN transistors in CCCII+ implementation are simulated using the parameters of the NR100N and PR100N bipolar transistors. The values of active and passive elements were selected as: I_{o1}=I_{o2}=52μA, R_1=200Ω, R_2=1kΩ, C_3=1nF, which result in a 90° phase shift at f_o=127.3 kHz. The magnitude and phase characteristics of the simulated circuit are shown in Figure 3.7, which shows close agreement with theory. The variability of the pole frequency with the bias current I_{b2} is shown in Figure 3.8. From Figure 3.8, it can be seen that the circuit exhibits a large tuning range.

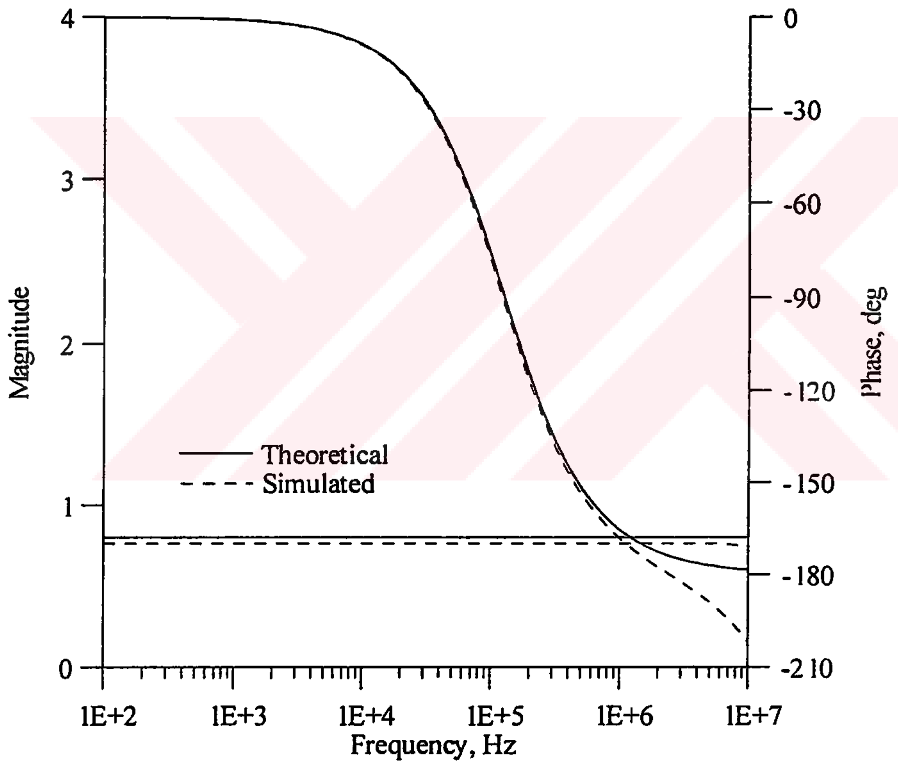

Figure 3.7: Magnitude and phase characteristics of the realization 1 of the Table 3.2

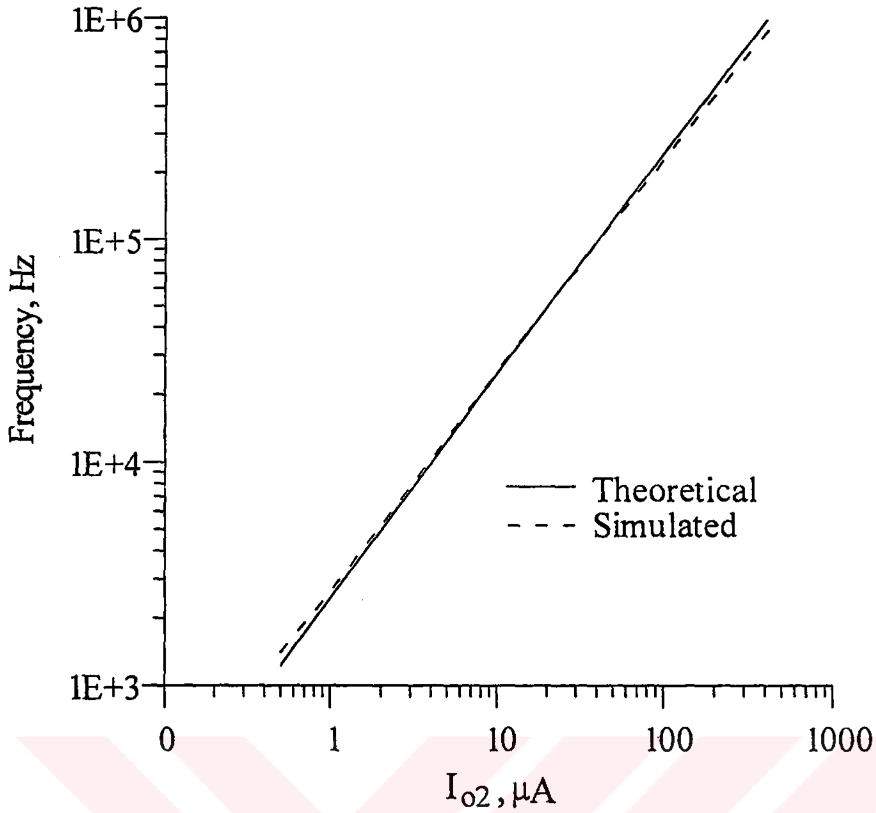

Figure 3.8: Variation of the pole frequency with the bias current I_{o2}

3.2 Inductance Simulator

The applications and advantages in the realization of various filter transfer functions using current conveyors have received considerable attention [1]. Moreover, because of the desire to produce solid-state filters without the use of physical coils, attention soon became focused on the simulation of floating inductor using active elements. A literature survey shows that a large number of circuit realizations for lossy and lossless floating inductors have been reported [34-47, 54, 58]. However it can be seen that most of these circuits suffer from one or more of the following drawbacks:

1. The use of an excessive number of current conveyors (CCII) or operational amplifiers (OP-AMP) [37-42, 47, 58].

2. The use of floating/grounded resistors or capacitors [34-43, 45-47, 58].

3. Active or passive matching condition [37,39,43-44,46].

4. The lack of electronic tunability [34-43, 45-47].

We present a new active only inductance simulation circuit using only one dual output CCCII and one operational amplifier (OP-AMP). The value of the simulated inductance can be controlled by adjusting the bias current of the CCCII over a wide range. The proposed circuit enjoys low active sensitivities and does not require any parameter matching condition. The use of only active elements in the circuit makes it suitable for using in integrated circuits (IC).

The proposed active only floating inductance is shown in Figure 3.9.

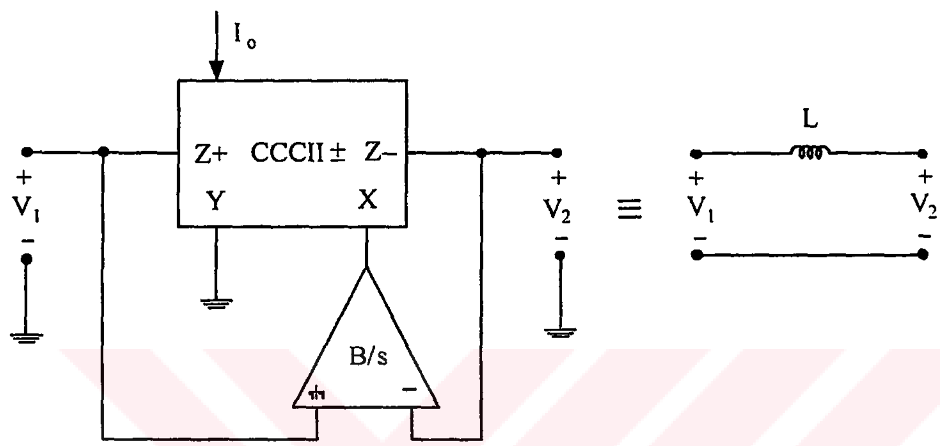

Figure 3.9: Proposed active only floating inductance simulator

It consist of a dual-output translinear bipolar second generation current controlled conveyor (CCCII±) and an operational amplifier (OP-AMP). The dual output translinear bipolar CCCII± can be obtained by modifying the original circuit of the CCCII by adding additional cross-coupled current mirrors to obtain the required minus type output as shown in Figure 3.10.

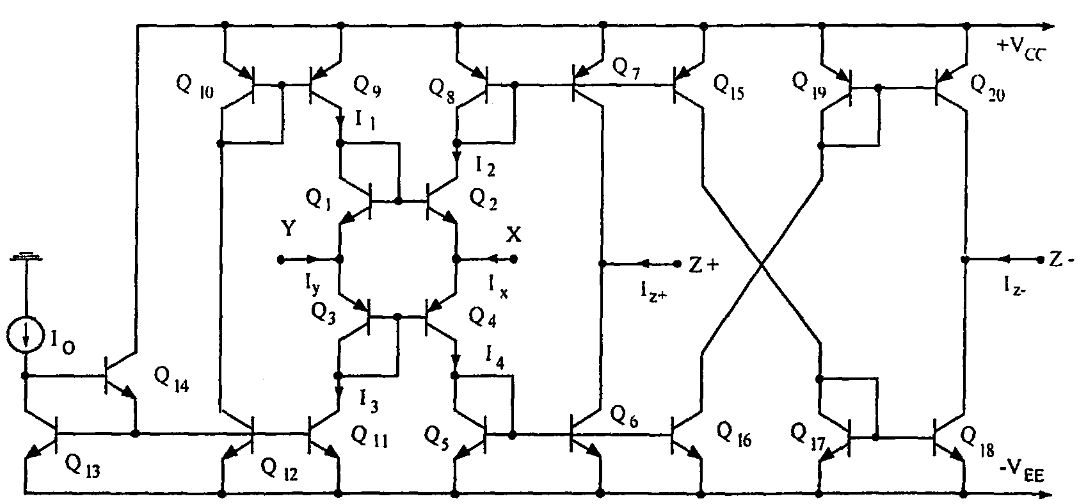

Figure 3.10: Bipolar implementation of the dual output CCCII±

The open-loop gain of a practical operational amplifier (OP-AMP) is represented by the well-known first pole roll-off characteristic [82]

$$A(s) = \frac{A_o \omega_{p1}}{s + \omega_{p1}} = \frac{B}{s + \omega_{p1}} \tag{3.11}$$

where, A_o is open-loop DC gain, ω_{p1} is the first pole frequency and B ($=A_0\omega_{p1}$) is the gain bandwidth product of the operational amplifier. In the frequency range $\omega >> \omega_{p1}$, equation (3.11) is reduced to

$$A(s) \cong \frac{B}{s} \tag{3.12}$$

This integrator model of OP-AMP is valid from a few kilohertz to a few hundred kilohertz range [44].

Routine analysis of the circuit in Figure 3.9 gives the short circuit admittance matrix as

$$\mathbf{Y} = \frac{B}{sR_x}\begin{bmatrix} 1 & -1 \\ -1 & 1 \end{bmatrix} \tag{3.13}$$

Therefore the circuit realizes a lossless floating inductance given by

$$L = \frac{R_x}{B} = \frac{V_T}{2I_o B} \tag{3.14}$$

Equation (3.14) shows that the inductance value (L) can be tuned electronically by varying the bias current (I_o). Sensitivity analysis of the circuit shows that

$$S_{V_T}^{L} = -S_{B}^{L} = -S_{I_o}^{L} = 1 \tag{3.15}$$

which are not more than unity.

3.2.1 Effects of non-idealities in inductance simulator

In this section, we discuss the effects of the non-idealities of the OP-AMP and CCCII± on the admittance matrix of the proposed circuit. Considering the parasitic pole of the OA, the open-loop gain is assumed to be

$$A(s) = \frac{B\omega_{p2}}{s(s+\omega_{p2})} = \frac{B}{s(1+\tau s)} \tag{3.16}$$

where ω_{p2} denotes the second pole of OA, and $\tau = 1/\omega_{p2}$. In the frequency range ($\omega << \omega_{p2}$) of our interest, $A(s)$ is approximated to

$$A(s) \cong \frac{B}{s}(1-\tau s) \tag{3.17}$$

On the other hand, the non-ideal dual output CCCII± can be characterized by $I_{z+} = \alpha_p(s)I_x, I_{z-} = -\alpha_n(s)I_x$, $I_y = 0$, $V_x = I_x R_x + \beta(s)V_y$, where $\alpha_p(s)$, $\alpha_n(s)$ and $\beta(s)$ are the frequency dependent current and voltage transfers of the conveyor, respectively. Reanalysis of the proposed circuit shows that the non-ideal short circuit admittance matrix of the proposed circuit is found to be

$$\hat{\mathbf{Y}} = \frac{B(1-\tau s)}{sR_x}\begin{bmatrix} \alpha_p(s) & -\alpha_p(s) \\ -\alpha_n(s) & \alpha_n(s) \end{bmatrix} \tag{3.18}$$

For matched current mirrors of the dual output CCCII±

$$\alpha_p(s) \cong \alpha_n(s) \cong \alpha(s) = \frac{\alpha_o \omega_\alpha}{s+\omega_\alpha} \tag{3.19}$$

where α_o is the value of this transfer at low frequencies (very close to unity) and ω_α is its corresponding pole and using the fact that $|s| \langle\langle \omega_\alpha$, the equation (3.19) can be simplified as

$$\alpha(s) \cong \alpha_o(1-\tau_\alpha s) \tag{3.20}$$

Considering (3.19) and substituting (3.20) into (3.18) the admittance seen between V_1 and V_2 of Fig. 1 can be expressed as

$$\hat{Y} = \frac{\alpha_o B}{sR_x} - \frac{\alpha_o B(\tau + \tau_\alpha)}{R_x} + \frac{s\alpha_o B\tau\tau_\alpha}{R_x} \tag{3.21}$$

Therefore at high frequencies, the realized floating inductance $L=R_x/\alpha_o B$ is shunted by a negative resistance $R=R_x/\alpha_o B(\tau+\tau_\alpha)$ and a capacitance $C=\alpha_o B\tau\tau_\alpha/R_x$. In this case the effects of the negative resistance can be eliminated by shunting a positive resistance of the same value with the proposed circuit.

The performance of the proposed circuit is verified by SPICE simulation program. The operational amplifier LF356 with the gain-bandwidth product $B=2\pi(6.392)\times10^6$ rad/s and the second pole $\omega_{p2}=2\pi(20.0)\times10^6$ rad/s is used in simulation. The dual output CCCII± is simulated using the implementation shown in Figure 3.10 with the transistor model of PR100N (PNP) and NR100N (NPN) of the bipolar arrays ALA400 from AT&T [74]. The DC voltage supply is ±2.5V. Figure 3.11 shows the simulated and theoretical values of the inductance for different values of the bias current. It can be seen that the inductance value can be tuned by varying the bias current of the CCCII± over a wide range.

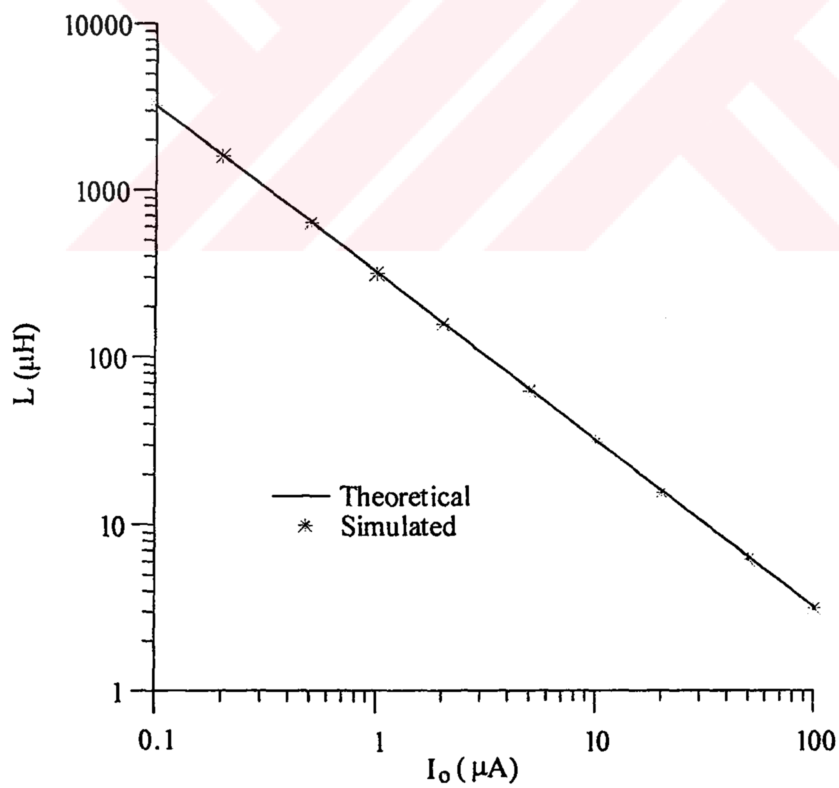

Figure 3.11: Variation of the simulation inductance with the bias current of the CCCII±

As an application the proposed circuit is used to construct a fourth-order elliptic *LC* lowpass filter shown in Figure 3.12 with elements values of L_1=27.4697μH L_2=38.4429μH, C_1=42.0908μF, C_2=3.9940μF, C_3=23.8218μF, R_s=R_L=1Ω [83].

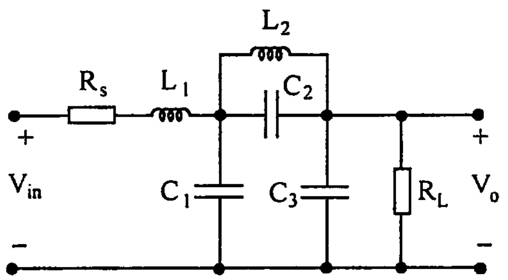

Figure 3.12: Fourth order elliptic lowpass filter

The filter specifications are as follows:

1. 5kHz bandwidth with lower than 0.1dB in-band ripple.
2. Stopband attenuation equal to 40dB at 11kHz.

The corresponding biasing currents of the CCII±s for simulation of inductors L_1 and L_2 are selected as I_{o1}=473.24μA and I_{o2}=338.1μA, respectively. The simulated frequency response of the filter is shown in Figure 3.13. As it can be seen form Figure 3.13, the theoretical and simulation results are in quite good agreement.

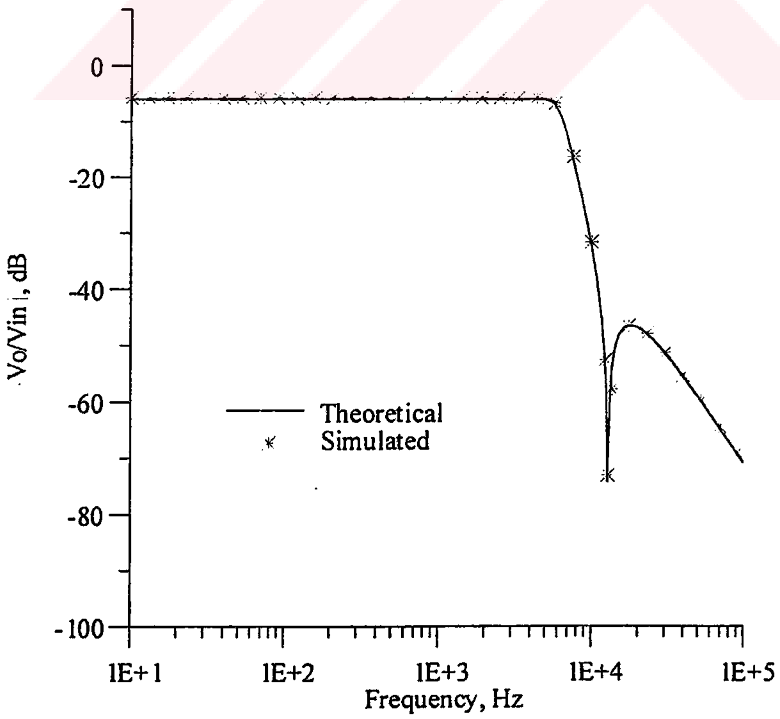

Figure 3.13: Frequency response of the elliptic lowpass filter

3.3 Oscillator

Although several oscillator circuits constructed with current conveyors have been reported in the literature [18–25, 64], most of these oscillator topologies exhibit complex oscillation condition terms and/or at least one parameter is common in equations giving the oscillation condition and the oscillation frequency [18–24, 64]. Furthermore, the oscillator circuits proposed in [18–25] suffer from the lack of electronic tunability.

A new sinusoidal oscillator enabling fully independent control of oscillation condition and oscillation frequency is presented using three single output CCCIIs, two grounded capacitors and one grounded resistor [67].

Consider the proposed oscillator as shown in Figure 3.14; it consists of two positive CCCII, one negative CCCII and three passive components. Its characteristic equation can be derived as

$$s^2 R_{x1} R_{x2} R_{x3} R_1 C_1 C_2 + s R_{x2} R_{x3} C_2 \left(R_{x1} - \alpha_1 \beta_1 R_1 \right) + \alpha_2 \alpha_3 \beta_2 \beta_3 R_1 R_{x1} = 0 \tag{3.22}$$

The oscillation condition and oscillation frequency of the proposed oscillator can be given as

$$R_{x1} = \alpha_1 \beta_1 R_1 \tag{3.23}$$

and

$$\omega_o = \sqrt{\frac{\alpha_2 \alpha_3 \beta_2 \beta_3}{R_{x2} R_{x3} C_1 C_2}} \tag{3.24}$$

where α_i and R_{xi}, $i = 1, 2, 3$ are the current tracking error and the input resistance at terminal X of the *i-th* CCCII, respectively. Using (2.9), (3.23) and (3.24) reduce to

$$I_{o1} = \frac{V_T}{2 \alpha_1 \beta_1 R_1} \tag{3.25}$$

$$\omega_o = \frac{2}{V_T} \sqrt{\frac{\alpha_2 \alpha_3 \beta_2 \beta_3 I_{o2} I_{o3}}{C_1 C_2}} \tag{3.26}$$

As clearly seen from (3.25) and (3.26), oscillation frequency and oscillation condition are completely independent from each other. Also oscillation frequency can be tuned electronically by varying the bias currents I_{o2} and/or I_{o3}. Thus the circuit exhibits a large tuning range.

Sensitivity analysis of this oscillator shows that

$$\left.\begin{array}{l} S_{C_1}^{\omega_o} = S_{C_2}^{\omega_o} = -S_{I_{o2}}^{\omega_o} = -S_{I_{o3}}^{\omega_o} = -S_{\alpha_2}^{\omega_o} = -S_{\alpha_3}^{\omega_o} = -S_{\beta_2}^{\omega_o} = -S_{\beta_3}^{\omega_o} = -\dfrac{1}{2} \\ S_{V_T}^{\omega_o} = -1 \end{array}\right\} \quad (3.27)$$

Thus all passive and active sensitivities are no more than unity.

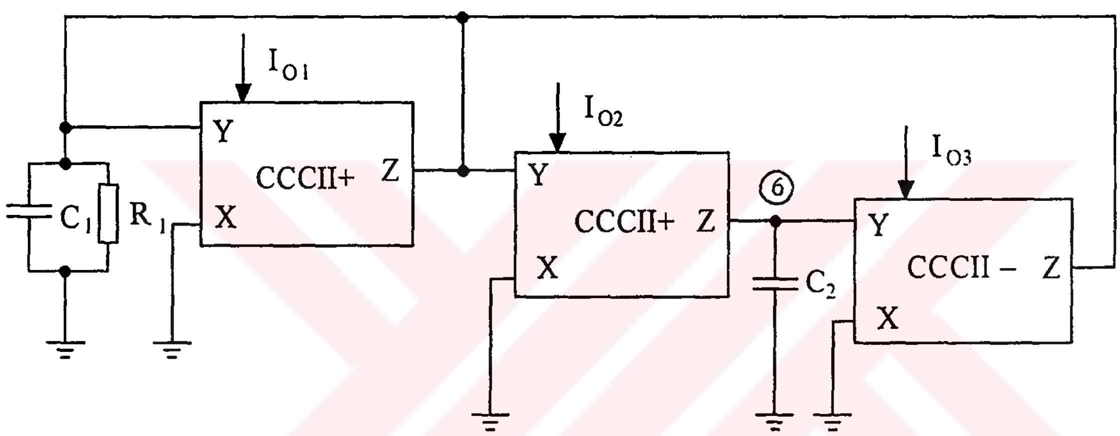

Figure 3.14: Proposed oscillator circuit

Finally to verify the theoretical analysis, the proposed oscillator was simulated using the SPICE simulation program. The CCCIIs were simulated using the schematic implementation proposed in [56] with the typical parameters of the bipolar transistors NR100N and PR100N [74] and DC supply voltage = ± 2.5V. The variability of the oscillation frequency with the bias current $I_{o2}= I_{o3} = I_o$, is shown in Figure 3.15 for different values of $C_1= C_2$. Figure 3.16 shows the simulated oscillation obtained from the circuit of Figure 3.14 with I_{o1}=26μA, I_{o2} = I_{o3}=100μA, R_1= 500Ω and C_1=C_2=2nF. The oscillation frequency is f_o=612kHz. It can be seen that the simulation results confirm the theoretical analysis.

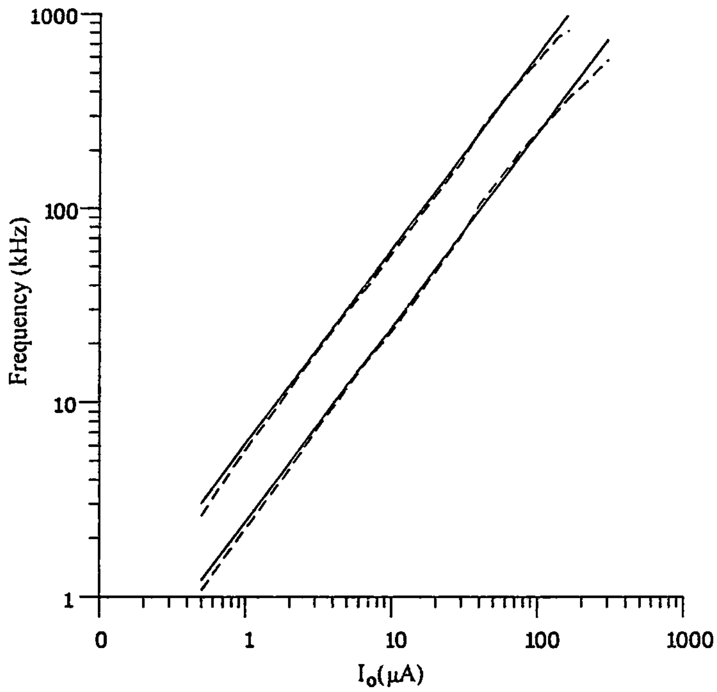

Figure 3.15: Variation of the oscillation frequency with the bias current $I_{o2} = I_{o3} = I_o$

$I_{o1} = 26\mu A$, $R_1 = 500\Omega$

------ Simulation

—— Theory

Lower lines $C_1 = C_2 = 5$ nF

Upper lines $C_1 = C_2 = 2$ nF

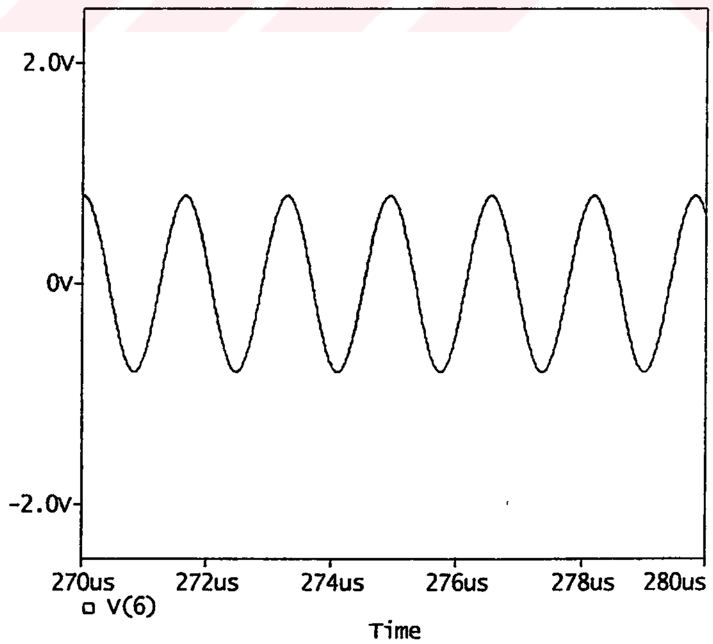

Figure 3.16: Simulated oscillation obtained from the circuit of Figure 3.14 with:

$C_1 = C_2 = 2nF$, $R_1 = 500\Omega$, $I_{o1} = 26\mu A$, $I_{o2} = I_{o3} = 100\mu A$

4. BiCMOS REALIZATION OF THE CURRENT CONTROLLED CONVEYOR

There are two basic technologies for the integrated circuits. The bipolar technology, based on the BJT and CMOS technology, based on NMOS and PMOS transistors. The bipolar transistors have higher transconductance (g_m) over the CMOS transistors at the same DC bias. Also they have superior high frequency performance than their CMOS counterparts. On the other hand the CMOS transistors have high input resistance, low power consumption, and are requiring small silicon area compared to the bipolar transistors.

In this chapter a BiCMOS realization of CCCII is proposed in order to take the advantages of the BiCMOS technology such as requiring small silicon area and high frequency performance together with high input resistance. The resistance at terminal X of the proposed CCCII, which can be controlled electronically by adjusting the bias current of the CCCII, is calculated theoretically. The proposed realization has a wide bandwidth and can be used in high frequency applications. Simulation results, which confirm the performance of the proposed CCCII, are included.

4.1 CMOS Buffer Stage And BiCMOS Realization of The CCCII

The CMOS buffer stage is widely used in the design of current-mode integrated circuits, owing to its simplicity and its high frequency response [84-86]. Consider the buffer stage shown in Figure 4.1. All the transistors used are operating in the saturation region, where the drain current of the MOS transistors operating in that region (neglecting the channel length modulation effect) is given by:

$$I = \frac{K}{2}(V_{GS} - V_T)^2 \tag{4.1}$$

$$K = \mu C_{ox}\left(\frac{W}{L}\right) \tag{4.2}$$

where V_T is threshold voltage, K is the transconductance parameter, μ is the effective carrier mobility, C_{ox} is the gate oxide capacitance per unit area, W is the channel width and L is the channel length.

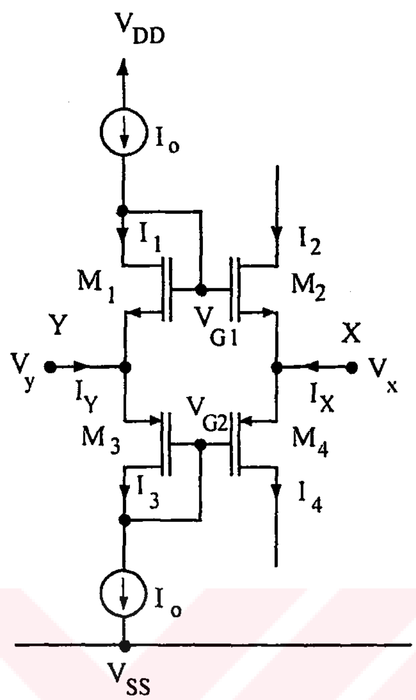

Figure 4.1: CMOS buffer stage

Assuming transistors M_1 and M_2 in Figure 4.1 are perfectly matched ($K_1 = K_2$, $V_{T1} = V_{T2}$) the following equations can be written for these transistors:

$$I_o = \frac{K_1}{2}(V_{G1} - V_Y - V_{T1})^2 \tag{4.3}$$

$$I_2 = \frac{K_1}{2}(V_{G1} - V_X - V_{T1})^2 \tag{4.4}$$

where $K_1 = K_2$ and $V_{T1} = V_{T2}$ are the transconductance parameter and threshold voltage of the transistors M_1 and M_2, respectively. By finding V_{G1} from (4.4) and replacing in (4.3) the current I_2 is found as:

$$I_2 = \frac{K_1}{2}\left(V_y - V_x + \sqrt{\frac{2I_o}{K_1}}\right)^2 \tag{4.5}$$

Similarly, assuming transistors M3 and M4 are perfectly matched ($K_3 = K_4$, $V_{T3} = V_{T4}$) the current I_4 is found as:

$$I_4 = \frac{K_3}{2}\left(V_x - V_y + \sqrt{\frac{2I_o}{K_3}}\right)^2 \tag{4.6}$$

where $K_3 = K_4$ and $V_{T3} = V_{T4}$ are the transconductance parameter and threshold voltage of the transistors M3 and M4, respectively. Combining equations (4.5) and (4.6) the current at terminal X, $I_x = I_4 - I_2$ can be given as:

$$I_x = \frac{1}{2}(K_4 - K_2)(V_x - V_y)^2 + (\sqrt{K_4} + \sqrt{K_2})\sqrt{2I_o}(V_x - V_y) \tag{4.7}$$

From equation (4.7) it can be seen that if the transistors M_1-M_4 are perfectly matched ($K_1 = K_3$) and with no load at terminal X ($I_x = 0$), then $V_x = V_y$ that is no voltage difference will be established between terminals X and Y. However when a load is connected to terminal X ($I_x \neq 0$), there is a voltage difference between terminals X and Y. In this case, the following equation can be found from equation (4.7) as:

$$(V_x - V_y)\frac{\sqrt{K_4} - \sqrt{K_2}}{\sqrt{2I_o}} = -1 + \sqrt{1 + \frac{I_x}{I_o}\frac{\sqrt{K_4} - \sqrt{K_2}}{\sqrt{K_4} + \sqrt{K_2}}} \tag{4.8}$$

Equation (4.8) indicates that the relationship between the voltages established between terminals X and Y and the input current at terminal X is nonlinear. Under small signal conditions with $\frac{I_x}{I_o}\frac{\sqrt{K_4} - \sqrt{K_2}}{\sqrt{K_4} + \sqrt{K_2}} \langle\langle 1$ and using the power series of the form $\sqrt{1+X} \cong 1 + \frac{X}{2} - \ldots$, $-1 \langle X \langle 1$, the resistance at terminal X can be expressed as:

$$R_x = \frac{V_x - V_y}{I_x} = \frac{1}{\sqrt{2I_o}(\sqrt{K_4} + \sqrt{K_2})} \tag{4.9}$$

Therefore under small signal conditions the resistance R_x can be controlled by biasing current I_o.

Using this buffer stage the BiCMOS implementations of the CCCII+ is shown in Figures 4.2 [87]. A current controlled conveyor with negative current transfer (CCCII−) can also be obtained easily, by adding two cross-coupled current mirrors, in order to reverse the sign of current I_z as shown in Figure 4.3.

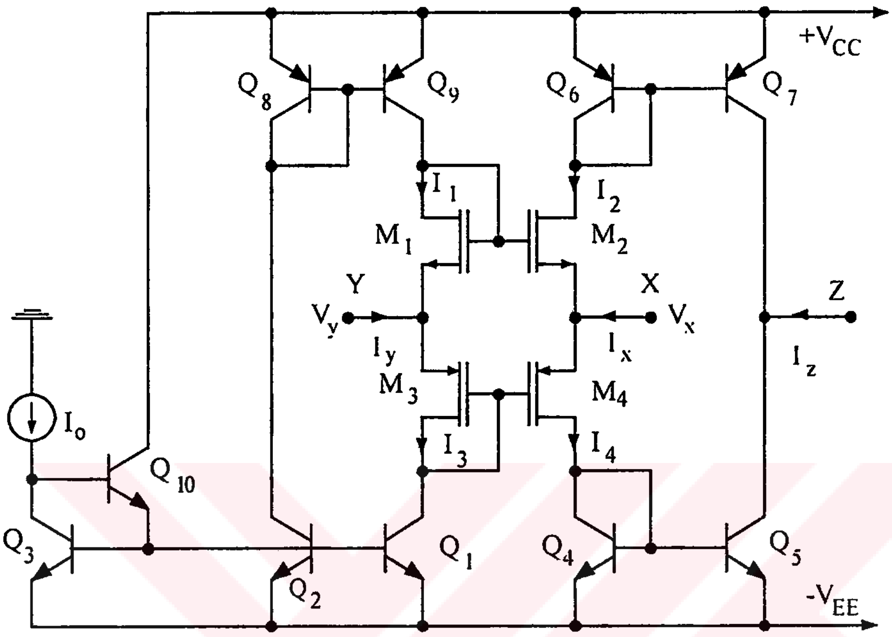

Figure 4.2: BiCMOS implementation for the CCCII+

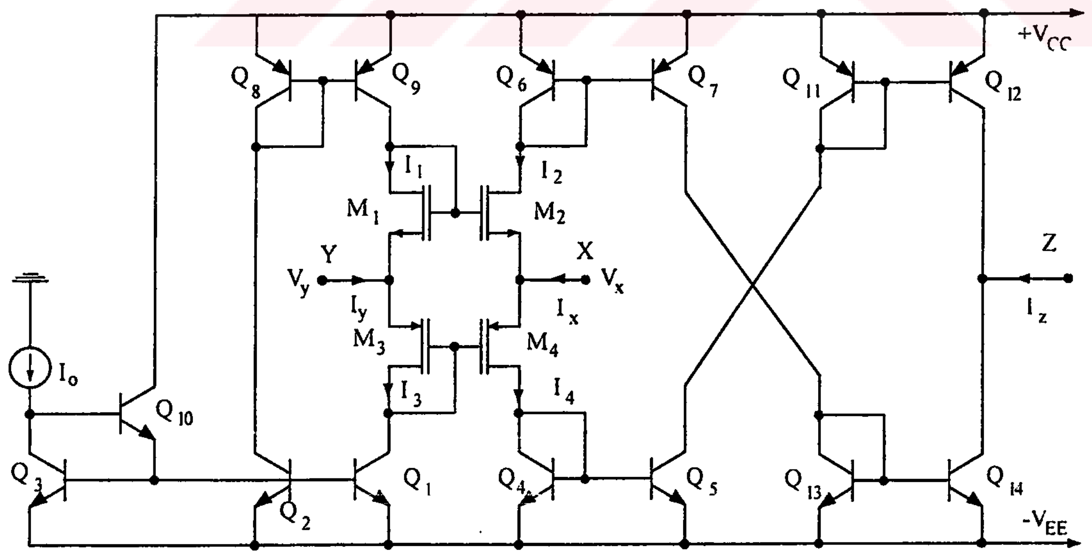

Figure 4.3: BiCMOS implementation for the CCCII−

4.2 Simulation Results

The performance of the proposed circuit of BiCMOS CCCII+ is verified by PSPICE simulation program using the transistor model of 0.8μ BiCMOS technology [88]. The voltage supply used for the CCCII+ is ±2.5V and the bias current is I_o=50μA. The dimensions of transistors M_1-M_4 are W=50μm and L=0.8μm (perfectly matched transistors).

When the circuit is used as a voltage follower, the input voltage is applied on terminal Y. The output voltage is then obtained on X, with an infinite load resistance connected at X; output Z being grounded. When the circuit is used as a current follower, the input current is applied on terminal X of the conveyor, terminals Y and Z being grounded. The DC transfer characteristic of the voltage follower is shown in Figure 4.4. The voltage clipping limits at the terminal X are obtained as: V_{xmax}= 2.14V and V_{xmin}= −2.14V.

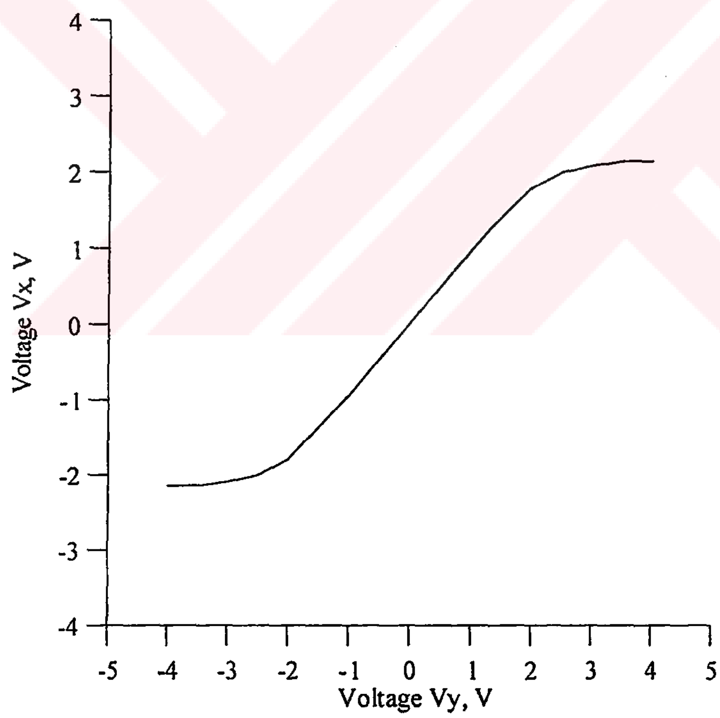

Figure 4.4: V_x-V_y, DC transfer characteristic of the BiCMOS CCCII+

Figure 4.5 shows the voltage DC transfer characteristic V_y–V_z from input terminal Y to the output terminal Z for R_z =∞ (open-circuited) and short-circuited terminal X. The voltage clipping limits are determined as: V_{zmax}= 2.49V and V_{zmin}= −2.49V.

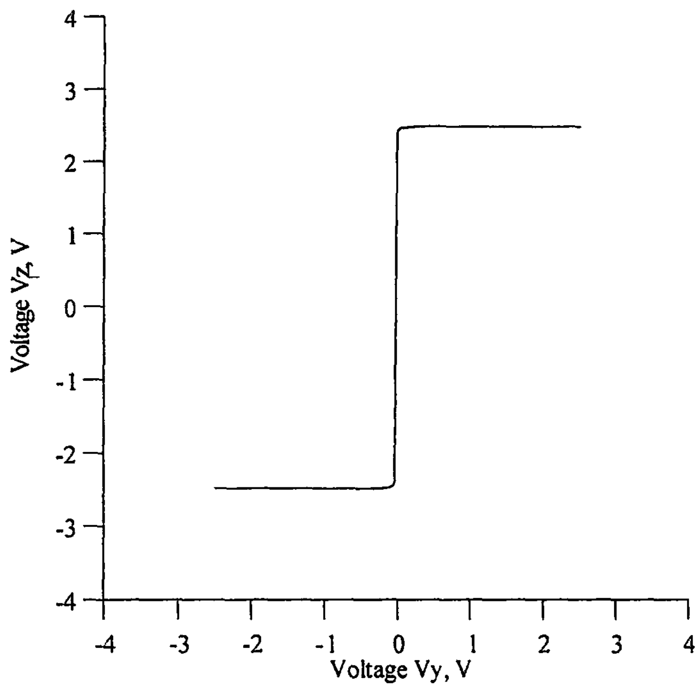

Figure 4.5: V_z-V_y, DC transfer characteristic of the BiCMOS CCCII+

Figure 4.6 shows the frequency response of the current follower. An excellent bandwidth with –3dB cutoff frequency of 1.22GHz can be seen. The frequency response of the voltage follower is shown in Figure 4.7. It indicates that this circuit is quite useful for a voltage follower configuration.

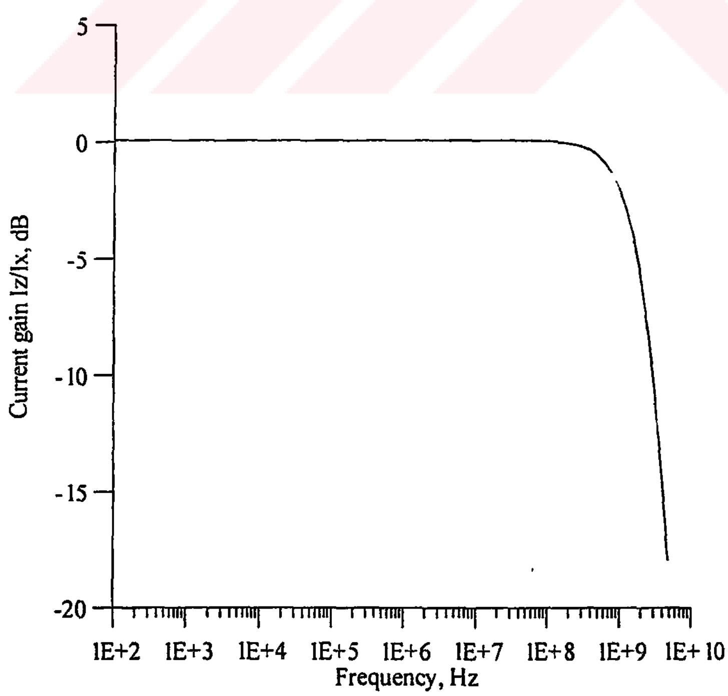

Figure 4.6: Frequency responses of the current follower (I_z/I_x)

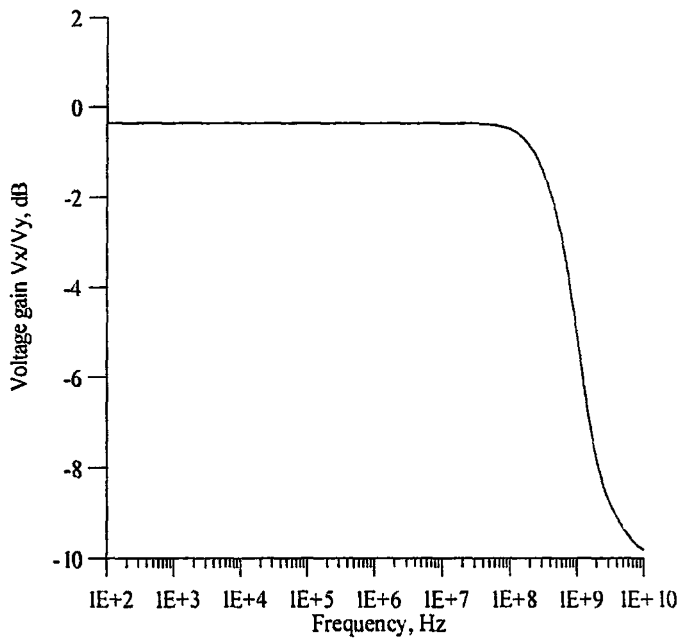

Figure 4.7: Frequency responses of the voltage follower (V_x/V_y)

Also the variation of the resistance R_x with the bias current I_o is shown in Figure 4.8. The simulation results obtained for the voltage follower and current follower configurations are summarized in Table 4.1. The results confirm high performance of the circuit.

Although the simulation results show good performance for the proposed circuit, it must be noticed that because of bad performance of the PNP transistors in standard BiCMOS technology the actual performance of the circuit is less than simulation one. However, by using special BiCMOS processes [59] high frequency performance for the proposed circuit can be achieved.

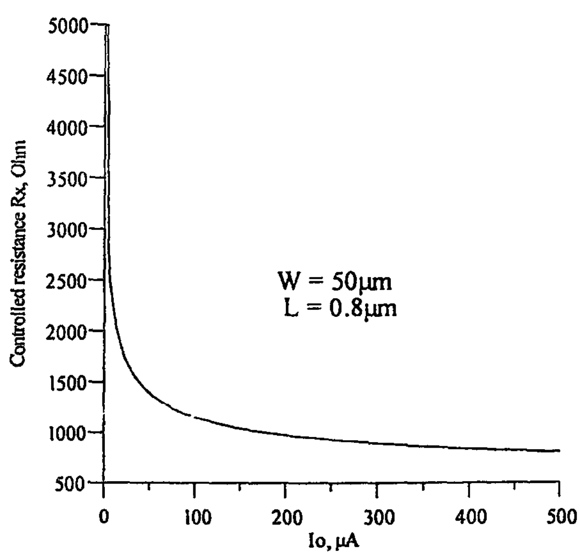

Figure 4.8: Variation of the resistance R_x with the bias current I_o

Table. 4.1: Basic characteristics of the BiCMOS CCCII+

Parameter	Voltage follower	Current follower
Gain	0.966	1.01
–3dB Bandwidth	672 MHz	1.22 GHz
Input impedance	422 kΩ // 0.13 pF	1.39 kΩ
Output impedance	1.37 kΩ	383 kΩ // 0.08 pF

4.3. Application

As an application, the proposed BiCMOS current controlled conveyor is used to build a tunable second order bandpass filter as shown in Figure 4.9 [55]. The filter consists of two CCCII+ and two grounded capacitors.

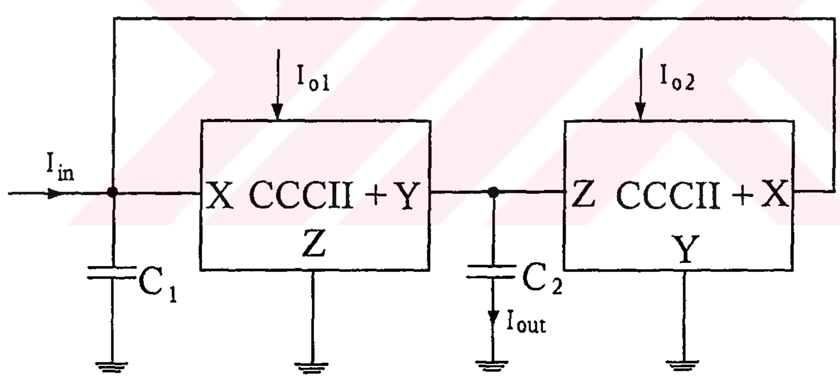

Figure 4.9: Current-mode current controlled bandpass filter

When both control currents I_{o1} and I_{o2} of the conveyors are equal to I_o (R_{x1}=R_{x2}=R_x), the transfer function of the filter can be characterized by [55]:

$$\frac{I_{out}}{I_{in}} = \frac{-R_x C_2 s}{R_x^2 C_1 C_2 s^2 + 2R_x C_2 s + 1} \tag{4.10}$$

$$\omega_o = \frac{1}{R_x}\sqrt{\frac{1}{C_1 C_2}} \tag{4.11}$$

$$Q = \frac{1}{2}\sqrt{\frac{C_1}{C_2}} \tag{4.12}$$

From (4.11) and (4.12) it can be seen that the value of ω_o is adjustable by I_0 without disturbing the quality factor Q_o. The circuit in Figure 4.9 has been simulated using SPICE with DC supply voltage=±2.5V. Figure 4.10 represents the frequency responses of the filter obtained with C_1=100pF, C_2=10pF for biasing current equal to 10μA, 30μA and 80μA. Thus, the simulated values of the center frequency f_0 are 2.23MHz, 3.01MHz and 4MHz, respectively.

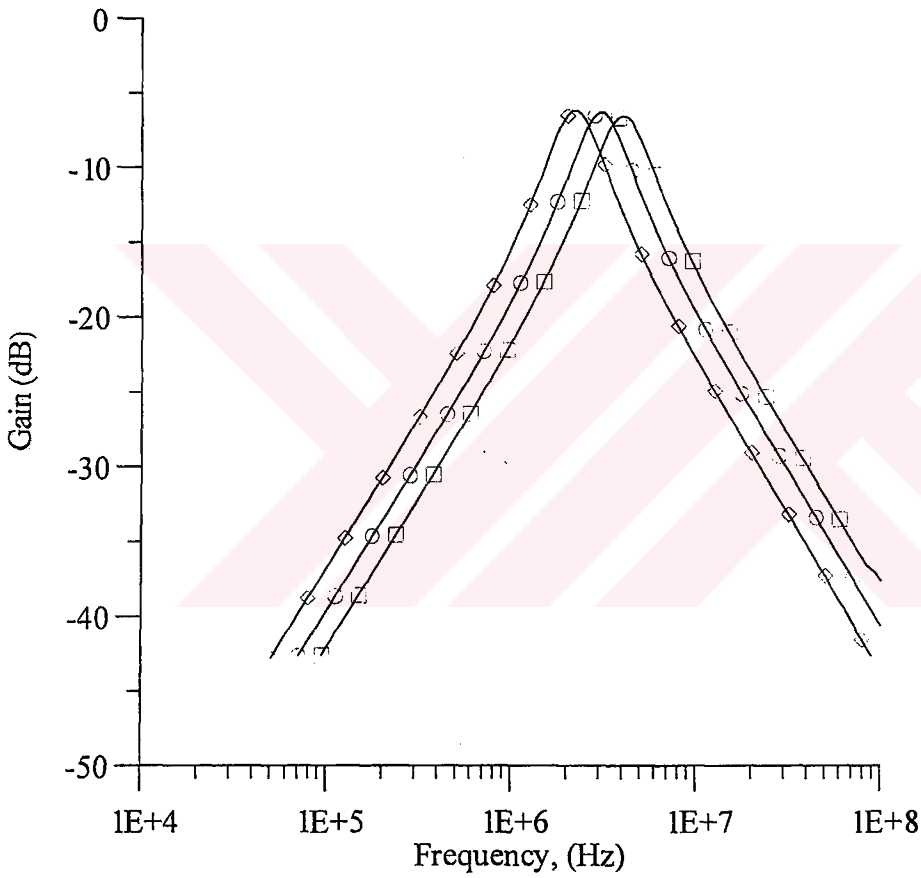

Figure 4.10: SPICE simulation results of the proposed circuit

◊ Simulated bandpass filter response for I_0=10μA

O Simulated bandpass filter response for I_0=30μA

□ Simulated bandpass filter response for I_0=80μA

5. SECOND ORDER ACTIVE FILTERS CONSTRUCTED WITH SINGLE NON-IDEAL CURRENT CONTROLLED CONVEYOR

Several multiple CCCII based filter circuits that employed grounded capacitors have been reported in the literature [61–63, 67]. However in some applications it may be desired to have an economical single CCCII wideband filters. In this chapter, a new configuration for realizing the second order current-mode current controlled filters using only one CCCII is proposed. Then the dominant non-ideality effects of the current controlled conveyor in transfer function, resonant angular frequency, quality factor and sensitivities of the second order current-mode filters constructed with single CCCII are investigated. New relations for calculating the resonant angular frequency and quality factor for the second order lowpass, and bandpass filters, which gives accurate values, are presented.

5.1 The Transfer Function Of The Second Order Active Filters Constructed With Single Non-Ideal CCCII

The block diagram of an active filter constructed with single current controlled conveyor is shown in Figure 5.1. The input and output of the block are defined I_{in} and I_{out}, respectively as shown in Figure 5.1. The passive network (N) can be comprised of passive elements like resistance and capacitors. Attending the definition of the ideal CCCII, relation between input and output currents is given by

$$\frac{I_{out}}{I_{in}} = \frac{I_{out}}{I_X}\frac{I_X}{I_{in}} \tag{5.1}$$

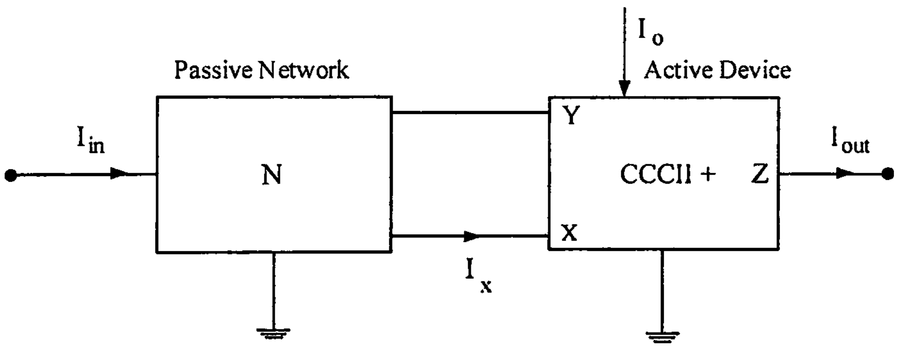

Figure. 5.1: Proposed block diagram of an active filter using single CCCII

The proposed circuit configuration suitable for realizing second order bandpass and lowpass filter is shown in Figure 5.2 [70]. The ideal transfer function of the filter is found as:

$$H(s) = \frac{I_{out}}{I_{in}} = \frac{G_x(Y_1Y_4 - Y_2Y_3)}{Y_1Y_2(Y_5 + Y_3 + Y_4) + Y_2Y_3(G_x + Y_4) + Y_1Y_3Y_4} \tag{5.2}$$

For realizing a bandpass filter

$$Y_1 = \infty \quad Y_2 = G_2 \quad Y_3 = sC_3 \quad Y_4 = sC_4 \tag{5.3}$$

and for realizing a lowpass filter

$$Y_1 = sC_1 \quad Y_2 = G_2 \quad Y_3 = \infty \quad Y_4 = sC_4 \tag{5.4}$$

can be selected.

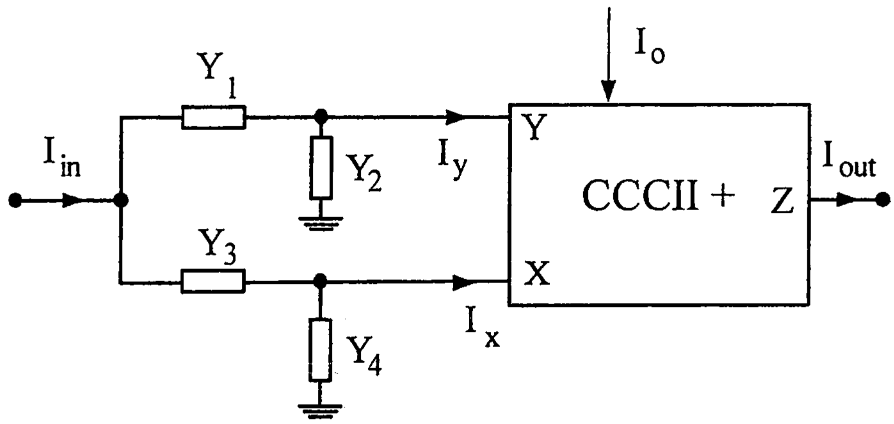

Figure 5.2: Proposed configuration for realizing bandpass and lowpass filters

Taking into account the non-idealities of the voltage and current transfer of the CCCII the transfer function of the circuit is found as:

$$H(s)=\frac{I_{out}}{I_{in}}=\frac{\alpha(s)G_x\left((\beta(s)Y_1Y_4-Y_2Y_3)+(\beta(s)-1)Y_1Y_3\right)}{Y_1Y_2(Y_5+Y_3+Y_4)+Y_2Y_3(G_x+Y_4)+Y_1Y_3Y_4+(1-\beta(s))G_xY_1Y_3} \tag{5.5}$$

In this circuit, the parasitic impedance at terminal Y of the CCCII is accommodated in Y_2. Regarding the current-mode operation of the circuit and connecting the small value load impedance at output of the circuit, the parasitic impedance at terminal Z of the CCCII can be assumed negligible.

The ideal current transfer function of a second order active filter can be given by

$$H_i(s)=\frac{I_{out}}{I_{in}}=\frac{N_i(s)}{D_i(s)}=\frac{N_i(s)}{s^2+\frac{\omega_{oi}}{Q_i}s+\omega_{oi}{}^2} \tag{5.6}$$

where ω_{oi} and Q_i are resonant angular frequency and quality factor of the ideal filter, respectively. By normalizing the transfer function of the filter with respect to ideal angular frequency (ω_{oi}), the normalized transfer function becomes

$$H_i(x)=\frac{N_i(x)}{D_i(x)}=\frac{N_i(x)}{x^2+a_1x+a_o} \tag{5.7}$$

where $x=\frac{s}{\omega_{oi}}$ is defined as the normalized angular frequency.

However the non-idealities of the CCCII change the order of denominator and nominator polynomials in equation (5.7). For the proposed configuration given in Figures 5.2, considering that the ladder branches contain a resistor or a capacitor using the non-ideal model of the CCCII given in Chapter 2, it can be easily seen that the denominator of equation (5.4), will be a fourth order polynomial. In this case, the normalized transfer function of the filter can be written as

$$H(x)=\frac{I_{out}}{I_{in}}=\frac{N(x)}{D(x)}=\frac{N(x)}{x^4+b_3x^3+b_2x^2+b_1x+b_o} \tag{5.8}$$

From (5.8), it is clearly observed that the denominator polynomial $D(x)$ can be written as

$$D(x) = x^4 + b_3x^3 + b_2x^2 + b_1x + b_o \tag{5.9}$$

5.1.1 Stability

For stability of a given circuit, the roots of the denominator polynomial of the transfer function must be in left half side of $(j\omega)$ axis in complex plane. The Routh-Hurwitz criterion can be used to determine the stability of the circuit. We know that for a system to be stable, all the coefficients in the first column of the Routh table must have the same sign. This leads to the following conditions:

$$b_1 - \frac{b_o b_3^2}{b_3 b_2 - b_1} \rangle 0 \quad \text{and} \quad b_2 b_3 - b_1 \rangle 0 \tag{5.10}$$

5.2 Second Order Bandpass Filter Using Single Non-Ideal CCCII

In this section the resonant angular frequency, quality factor and their sensitivities for the normalized bandpass filter constructed with single non-ideal CCCII is investigated.

By substituting equations (2.12) and (2.13) into equation (5.5) and considering the selection for realizing bandpass filter given in equation (5.3), the transfer function of the second order normalized bandpass filter constructed with single non-ideal current controlled conveyor can be found as:

$$H(x) = \frac{N(x)}{D(x)} = \frac{a_1 x(x + a_o)}{x^4 + b_3x^3 + b_2x^2 + b_1x + b_o} \tag{5.11}$$

5.2.1 Normalized resonant angular frequency in bandpass filter

In normalized transfer function of the bandpass filter, the normalized resonant angular frequency and quality factor are defined as:

$$\hat{x}_o = \frac{\omega_o}{\omega_{oi}} \qquad \text{and} \qquad q = \frac{Q}{Q_i} \tag{5.12}$$

where the ω_o and ω_{oi} are resonant angular frequency of the ideal and non-ideal filter, respectively. Similarly Q and Q_i are the quality factor of the ideal and non-ideal filter, respectively.

By using $x = j\hat{x} = j\dfrac{\omega}{\omega_{oi}}$ in (5.11) and defining $\hat{x}^2 = z$ as a new parameter, square module of equation (5.11) can be written as

$$G(z) = \frac{P(z)}{M(z)} = \frac{A_1 z(z + A_o)}{z^4 + B_3 z^3 + B_2 z^2 + B_1 z + B_o} \tag{5.13}$$

In this function, coefficients of the denominator can be calculated as

$$B_o = b_o^2,\ B_1 = b_1^2 - 2b_o b_2,\ B_2 = b_2^2 + 2b_o - 2b_1 b_3,\ B_3 = b_3^2 - 2b_2,\ A_o = a_o^2,\ A_1 = a_1^2 \tag{5.14}$$

To find the normalized resonant angular frequency of the non-ideal bandpass filter, the value of z which maximizes $G(z)$ must be calculated. The value of z which maximizes equation (5.13), can be found from

$$\frac{dG(z)}{dz} = 0 \tag{5.15}$$

Therefore by solving equation (5.15) it can be seen that

$$g(z_o) = 2z_o^5 + (B_3 + 3A_o)z_o^4 + 2A_o B_3 z_o^3 + (B_2 A_o - B_1)z_o^2 - 2B_o z_o - A_o B_o = 0 \tag{5.16}$$

The root of the equation (5.16), which is in the vicinity of 1 ($z_o = \hat{x}_o^2$), can be found using MATHCAD program as given in Appendix B. This root is the square of the normalized angular frequency of the bandpass filter in non-ideal case ($z_o = \hat{x}_o^2$).

5.2.2 Quality factor of non-ideal bandpass filter

From Equation (5.11), denominator polynomial can be rewritten as

$$D(x) = (x^2 + \frac{\hat{x}'_o}{Q}x + \hat{x}_o'^2)(x^2 + 2klx + k^2) \tag{5.17}$$

Where l is the damping factor due to the additional roots caused by non-idealities of the CCCII. Because of the non-idealities of the CCCII the value of $\hat{x}_o$ is different from $\hat{x}'_o$ in equation (5.17). By normalizing the denominator polynomial $D(x)$ with respect to $\hat{x}'_o$, which is the resonant angular frequency of the normalized filter, the following polynomial is found:

$$\frac{D(y)}{\hat{x}'^4_o} = y^4 + e_3 y^3 + e_2 y^2 + e_1 y + m^2 \tag{5.18}$$

where $m = \dfrac{k}{\hat{x}'_o}$, $y = \dfrac{x}{\hat{x}'_o}$ and $e_i\,(i = 1,2,3)$ are

$$e_1 = 2ml + \frac{m^2}{Q},\; e_2 = m^2 + 1 + \frac{2ml}{Q},\; e_3 = 2ml + \frac{1}{Q} \tag{5.19}$$

Therefore equation (5.11) can be rewritten again as:

$$H(y) = \frac{f_1 y(y + f_o)}{y^4 + e_3 y^3 + e_2 y^2 + e_1 y + m^2} \tag{5.20}$$

where $f_1 = \dfrac{a_1}{\hat{x}'^2_o}$ and $f_o = \dfrac{a_o}{\hat{x}'_o}$.

The value of $\hat{y}_o = \dfrac{\hat{x}_o}{\hat{x}'_o}$ which maximizes the module of $H(y)$ and presents the deviation of the resonant angular frequency ($\hat{x}_o$) from its ideal value ($\hat{x}'_o$), can be found by the method presented in section 5.2.1. For different values of m and Q it can be seen that the value of $\hat{y}_o$ is smaller than %0.1. Therefore $\hat{x}_o$ can be used in equation (5.17) instead of $\hat{x}'_o$. From (5.9) and (5.17) the quality factor Q of the filter can be easily found as [89]:

$$Q = \frac{b_o - \hat{x}^4_o}{\hat{x}_o(b_1 - b_3\hat{x}^2_o)} \tag{5.21}$$

5.2.3 Sensitivities of the normalized resonant angular frequency and quality factor

The sensitivities of the normalized angular frequency ($\hat{x}_o$) with respect to coefficients b_o, b_1, b_2, b_3 can be found from equations (5.14) and (5.16). By defining the sensitivity of a parameter F to the variable x_i as $S_{x_i}^{F}=(\frac{x_i}{F})\frac{dF}{dx_i}$, it can be seen that

$$\left.\begin{aligned}
S_{b_o}^{\hat{x}_o} &= \frac{2\hat{x}_o^8+h_3\hat{x}_o^6+2h_2\hat{x}_o^4+(h_1-a_o^2b_o-b_2b_o)\hat{x}_o^2}{10\hat{x}_o^8+4h_3\hat{x}_o^6+6h_2\hat{x}_o^4+2h_1\hat{x}_o^2-2b_o^2}\\
S_{b_1}^{\hat{x}_o} &= \frac{(b_3a_o^2+b_1)b_1\hat{x}_o^2}{10\hat{x}_o^8+4h_3\hat{x}_o^6+6h_2\hat{x}_o^4+2h_1\hat{x}_o^2-2b_o^2}\\
S_{b_2}^{\hat{x}_o} &= \frac{b_2\hat{x}_o^6+2a_o^2b_2\hat{x}_o^4-(b_2a_o^2+b_o)b_2\hat{x}_o^2}{10\hat{x}_o^8+4h_3\hat{x}_o^6+6h_2\hat{x}_o^4+2h_1\hat{x}_o^2-2b_o^2}\\
S_{b_3}^{\hat{x}_o} &= -\frac{b_3^2\hat{x}_o^6+2a_o^2b_3^2\hat{x}_o^4-b_1b_3a_o^2\hat{x}_o^2}{10\hat{x}_o^8+4h_3\hat{x}_o^6+6h_2\hat{x}_o^4+2h_1\hat{x}_o^2-2b_o^2}
\end{aligned}\right\} \qquad (5.22)$$

where

$$h_1=a_o^2(b_2^2+2b_o-2b_1b_3)-b_1^2+2b_ob_2,\; h_2=a_o^2(b_3^2-2b_2),\; h_3=b_3^2-2b_2+3a_o^2 \qquad (5.23)$$

Also the sensitivities of the quality factor with respect to coefficients b_i (i=0…3) can be found from equation (5.21) as:

$$\left.\begin{aligned}
S_{bo}^{Q} &= \frac{b_o}{b_o-\hat{x}_o^4}+S_{\hat{x}_o}^{Q}.S_{b_o}^{\hat{x}_o}\\
S_{b1}^{Q} &= S_{\hat{x}_o}^{Q}.S_{b_1}^{\hat{x}_o}-\frac{b_1}{b_1-b_3\hat{x}_o^2}\\
S_{b2}^{Q} &= S_{\hat{x}_o}^{Q}.S_{b_2}^{\hat{x}_o}\\
S_{b3}^{Q} &= S_{\hat{x}_o}^{Q}.S_{b_3}^{\hat{x}_o}+\frac{b_3\hat{x}_o^2}{b_1-b_3\hat{x}_o^2}\\
S_{\hat{x}_o}^{Q} &= \frac{2b_3\hat{x}_o^2}{b_1-b_3\hat{x}_o^2}-\frac{b_o+3\hat{x}_o^4}{b_o-\hat{x}_o^4}
\end{aligned}\right\} \qquad (5.24)$$

5.2.4 Design of a bandpass filter

As mentioned in section 5.1, selecting $Y_1=\infty$, $Y_2=G_2$, $Y_3=sC_3$, $Y_4=sC_4$ in Figure 5.2, a bandbass filter can be realized. This filter is shown in Figure 5.3.

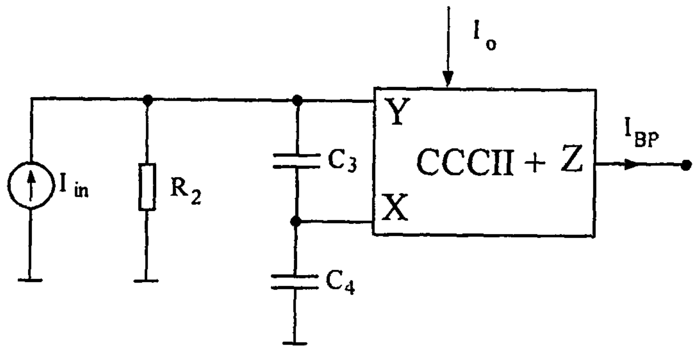

Figure 5.3: Bandpass filter realization using single CCCII

Ideal analysis of this circuit yields the following transfer function:

$$H_i(s) = \frac{I_{BP}}{I_{in}} = \frac{\frac{1}{R_x C_3} s}{s^2 + \frac{C_3 + C_4}{R_2 C_3 C_4} s + \frac{1}{R_2 R_x C_3 C_4}} \tag{5.25}$$

In this equation the parameters ω_{oi}, Q_i and $\frac{\omega_{oi}}{Q}$ can be calculated as:

$$\omega_{oi} = \frac{1}{\sqrt{R_2 R_x C_3 C_4}}, \; Q_i = \frac{1}{C_1 + C_3}\sqrt{\frac{C_1 C_3 R_2}{R_x}}, \; \frac{\omega_{oi}}{Q_i} = \frac{C_3 + C_4}{R_2 C_3 C_4} \tag{5.26}$$

To find a transfer function in terms of Q_i in normalized form in which ideal resonant angular frequency is equal to unity, we define $R^2 = R_2 R_x$ and $C = C_3 = C_4$, therefore:

$$H_i(s) = \frac{\frac{2Q_i}{RC} s}{s^2 + \frac{1}{Q_i RC} s + \frac{1}{R^2 C^2}} \tag{5.27}$$

By normalizing the transfer function with respect to ideal resonant angular frequency ($x = \frac{s}{\omega_{oi}}$), the normalized ideal transfer function of the bandpass filter is found as:

$$H_i(x) = \frac{2Q_i x}{x^2 + \frac{1}{Q_i} x + 1} \tag{5.28}$$

which is independent of the passive element values. Considering the fact that $R_y << R_2$ and negligible parasitic impedance at terminal Z of the CCCII the normalized transfer function of actual bandpass filter can be found as:

$$H(x)=\frac{2\alpha(x)Q_i(2\beta(x)-1)x}{\left(1+2\frac{C_y}{C}\right)x^2+\left(\frac{1}{Q_i}+(1-\beta(x))2Q_i+\frac{2Q_iC_y}{C}\right)x+1} \tag{5.29}$$

Assuming $\frac{C_y}{C} << 1$, the non-ideal transfer function of the bandpass filter is simplified as:

$$H(x)=\frac{2\alpha(x)Q_i(2\beta(x)-1)x}{x^2+\left(\frac{1}{Q_i}+(1-\beta(x))2Q_i\right)x+1} \tag{5.30}$$

where

$$\alpha(x)=\frac{\alpha_o\omega_{k\alpha}}{x+\omega_{k\alpha}} \qquad \beta(x)=\frac{\beta_o\omega_{k\beta}}{x+\omega_{k\beta}} \tag{5.31}$$

$\omega_{k\alpha}=\frac{\omega_\alpha}{\omega_{oi}}$ and $\omega_{k\beta}=\frac{\omega_\beta}{\omega_{oi}}$ are the normalized pole angular frequencies of the $\alpha(s)$ and $\beta(s)$ with respect to ideal natural frequency of the bandpass filter ω_{oi}. respectively. Substituting equation (5.31) into equation (5.30) results the transfer function in form of equation (5.11) with the following coefficients:

$$\left.\begin{aligned}
a_1&=-2Q_i\omega_{k\alpha}\\
a_o&=-\omega_{k\beta}\\
b_3&=\omega_{k\alpha}+\omega_{k\beta}+\frac{1}{Q_i}+2Q_i\\
b_2&=\omega_{k\alpha}\omega_{k\beta}+\frac{\omega_{k\alpha}+\omega_{k\beta}}{Q_i}+2Q_i\omega_{k\alpha}+1\\
b_1&=\frac{\omega_{k\alpha}\omega_{k\beta}}{Q_i}+\omega_{k\alpha}+\omega_{k\beta}\\
b_o&=\omega_{k\alpha}\omega_{k\beta}
\end{aligned}\right\} \tag{5.32}$$

Using MATHCAD program, by substituting these coefficients in the stability conditions of the filter given in equation (5.10), it can be seen that all of the terms are positive. The results are given in Appendix B. Therefore the proposed filter is unconditionally stable.

Also using MATHCAD program given in Appendix B, the normalized resonant angular frequency $\hat{x}_o(\omega_{k\alpha},\omega_{k\beta},Q_i)$ and normalized quality factor $q(\omega_{k\alpha},\omega_{k\beta},Q_i)$ which are defined as a function of $\omega_{k\alpha}$, $\omega_{k\beta}$ and Q_i, can be easily found for different values of $\omega_{k\alpha}$, $\omega_{k\beta}$ and Q_i. These different values are given as tabular forms in Appendix C.

The normalized resonant angular frequency of the non-ideal second order bandpass filter for different values of $\omega_{k\beta}$, $\omega_{k\alpha}$ and constant ideal quality factor of Q_i=5 is given Table C.1. It can be seen that $\hat{x}_o(\omega_{k\alpha},\omega_{k\beta},Q_i)$ is independent of $\omega_{k\alpha}$. Therefore the different values of $\hat{x}_o(\omega_{k\alpha},\omega_{k\beta},Q_i)$ for different values of $\omega_{k\beta}$ and Q_i with $\omega_{k\alpha}$=50 are given in Table C.2. Also Figure 5.4 shows the variation of $\hat{x}_o(\omega_{k\alpha},\omega_{k\beta},Q_i)$ with respect to $\omega_{k\beta}$ for different values of Q_i. From Table C.2 and Figure 5.4, it can be seen that for

$$\omega_{k\beta} > 20Q_i \tag{5.33}$$

the deviation of normalized resonant angular frequency from its ideal value 1 is less than %5. Therefore in this frequency range, by substituting equation (5.32) into equation (5.11) and neglecting small value terms, the following accurate and simplified equation can be given for calculating normalized resonant angular frequency of non-ideal bandpass filter.

$$\hat{x}_o \cong \sqrt{\frac{\omega_{k\beta}}{\omega_{k\beta}+2Q_i}} \tag{5.34}$$

One can see that the value of $\hat{x}_o$ calculated from equation (5.34) is in quite agreement with the values given in Table C.2. For example with $\omega_{k\alpha}$=50, $\omega_{k\beta}$=90 and Q_i=2 the value of $\hat{x}_o$ will be found from (5.34) equal to 0.9784 which is the same as given in Table C.2

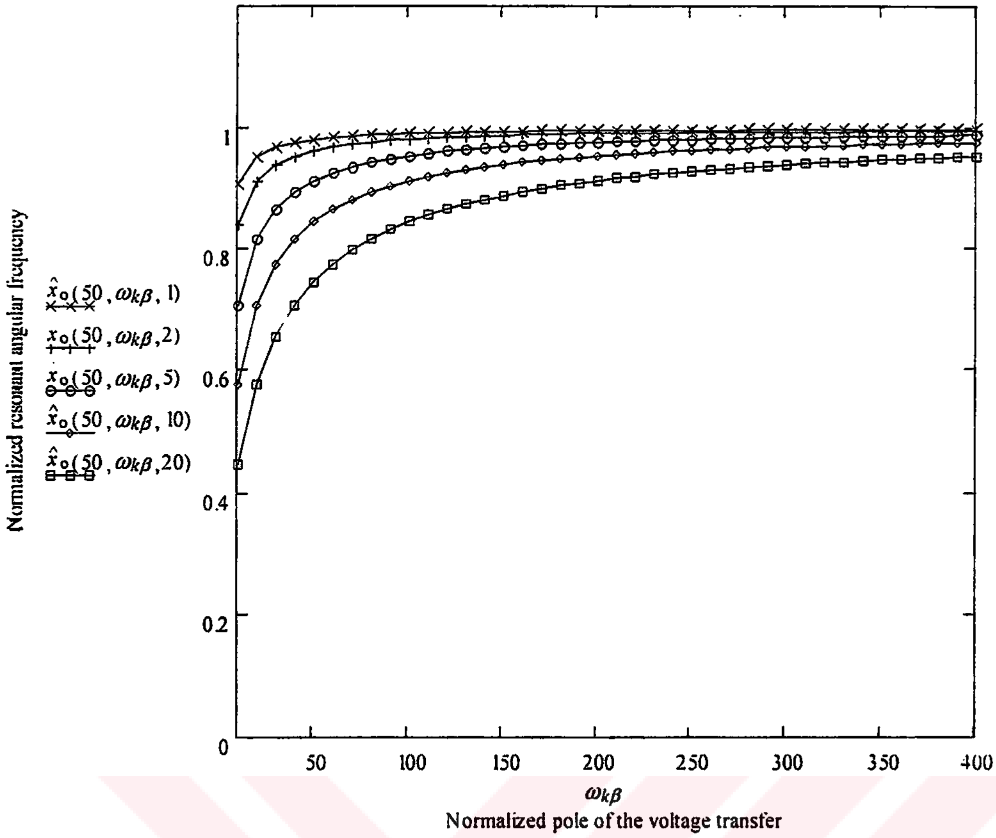

Figure 5.4: The variation of $\hat{x}_o(\omega_{k\alpha}, \omega_{k\beta}, Q_i)$ with respect to $\omega_{k\beta}$

The values of $\hat{x}'_o$ can be found from the roots of the equation (5.9). Table C.3 gives the values of $\hat{x}'_o$ for different $\omega_{k\beta}$ and Q_i with $\omega_{k\alpha}$ =50. It can be seen that the difference in the values of $\hat{x}'_o$ and $\hat{x}_o$ is less than %1 as mentioned in section 5.2.2. Therefore the approximation for finding Q in section 5.2.2 is acceptable. Also one can see that the value of Q extracted from equation (5.21) is very close to the value of Q calculated as $Q = \frac{\hat{x}_o}{B}$, where B is the bandwidth of the normalized filter. For example with $\omega_{k\alpha}$=50, $\omega_{k\beta}$=90 and Q_i=5, the values of Q from equation (5.21) and $Q = \frac{\hat{x}_o}{B}$ are found as 5.221 and 5.186, respectively.

Similarly, the normalized quality factor of the non-ideal bandpass filter which is defined as a function of $\omega_{k\alpha}$, $\omega_{k\beta}$ and Q_i, ($q(\omega_{k\alpha}, \omega_{k\beta}, Q_i)$), can be easily found for different values of $\omega_{k\alpha}$, $\omega_{k\beta}$ and Q_i. Table C.4 shows different values of the normalized quality factor for different $\omega_{k\beta}$ and $\omega_{k\alpha}$ with constant ideal quality factor of Q_i=5. It can be seen that $q(\omega_{k\alpha}, \omega_{k\beta}, Q_i)$ is also independent of $\omega_{k\alpha}$. Therefore for a constant $\omega_{k\alpha}$=50, the different values of the normalized quality factor for different values of Q_i and $\omega_{k\beta}$ are given in Table C.5. From Table C.5 it can be seen that for $\omega_{k\beta} > 20Q_i$ the deviation of normalized quality factor $q(\omega_{k\alpha}, \omega_{k\beta}, Q_i)$ from its ideal value 1, remains also less than %5. Figure 5.5 shows the variation of $q(\omega_{k\alpha}, \omega_{k\beta}, Q_i)$ with respect to $\omega_{k\beta}$ for different values of Q_i.

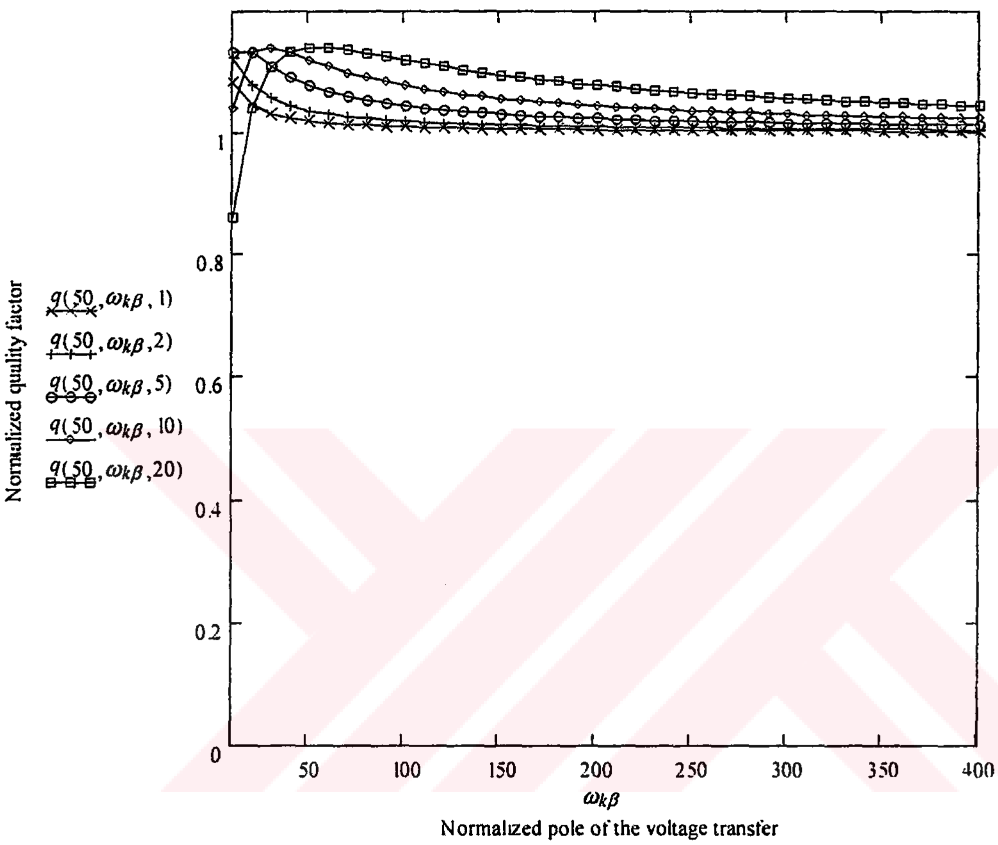

Figure 5.5: The variation of $q(\omega_{k\alpha}, \omega_{k\beta}, Q_i)$ with respect to $\omega_{k\beta}$

The sensitivities of the $\hat{x}_o$ and Q with respect to the parameters $\omega_{k\alpha}$, $\omega_{k\beta}$ and Q_i can be found as:

$$\left.\begin{aligned} S_{\omega_{k\alpha}}^{\hat{x}_o} &= \sum_{i=0}^{3} S_{b_i}^{\hat{x}_o} . S_{\omega_{k\alpha}}^{b_i}, \quad S_{\omega_{k\beta}}^{\hat{x}_o} = \sum_{i=0}^{3} S_{b_i}^{\hat{x}_o} . S_{\omega_{k\beta}}^{b_i}, \quad S_{Q_i}^{\hat{x}_o} = \sum_{i=0}^{3} S_{b_i}^{\hat{x}_o} . S_{Q_i}^{b_i} \\ S_{\omega_{k\alpha}}^{Q} &= \sum_{i=0}^{3} S_{b_i}^{Q} . S_{\omega_{k\alpha}}^{b_i}, \quad S_{\omega_{k\beta}}^{Q} = \sum_{i=0}^{3} S_{b_i}^{Q} . S_{\omega_{k\beta}}^{b_i}, \quad S_{Q_i}^{Q} = \sum_{i=0}^{3} S_{b_i}^{Q} . S_{Q_i}^{b_i} \end{aligned}\right\} \tag{5.35}$$

where

$$S_{\omega_{k\alpha}}^{b_3}=\frac{\omega_{k\alpha}}{b_3},S_{\omega_{k\alpha}}^{b_2}=\frac{\omega_{k\alpha}}{b_2}(\omega_{k\beta}+\frac{1}{Q_i}+2Q_i),S_{\omega_{k\alpha}}^{b_1}=\frac{\omega_{k\alpha}}{b_1}(\frac{\omega_{k\beta}}{Q_i}+1),S_{\omega_{k\alpha}}^{b_o}=\frac{\omega_{k\alpha}\omega_{k\beta}}{b_o} \quad (5.36)$$

$$S_{\omega_{k\beta}}^{b_3}=\frac{\omega_{k\beta}}{b_3},S_{\omega_{k\beta}}^{b_2}=\frac{\omega_{k\beta}}{b_2}(\omega_{k\alpha}+\frac{1}{Q_i}),S_{\omega_{k\beta}}^{b_1}=\frac{\omega_{k\beta}}{b_1}(\frac{\omega_{k\alpha}}{Q_i}+1),S_{\omega_{k\alpha}}^{b_o}=\frac{\omega_{k\alpha}\omega_{k\beta}}{b_o} \quad (5.37)$$

$$S_{Q_i}^{b_3}=\frac{Q_i}{b_3}(2-\frac{1}{Q_i^2}),S_{Q_i}^{b_2}=\frac{Q_i}{b_2}(2\omega_{k\alpha}-\frac{\omega_{k\alpha}+\omega_{k\beta}}{Q_i^2}),S_{Q_i}^{b_1}=-\frac{\omega_{k\alpha}\omega_{k\beta}}{b_1Q_i},S_{Q_i}^{b_o}=0 \quad (5.38)$$

The sensitivities of $\hat{x}_o$ and Q to b_i (i=0...3) were given in equations (5.22) and (5.24), respectively.

Using MATHCAD program given in Appendix B, the different values of the sensitivities of $\hat{x}_o$ with respect to the parameters $\omega_{k\alpha}$, $\omega_{k\beta}$ and Q_i can be calculated. These sensitivities are given as tabular forms in Appendix C. Table C.6 gives the sensitivities of the $\hat{x}_o$ with respect to $\omega_{k\alpha}$. It can be seen that $\hat{x}_o$ is insensitive to $\omega_{k\alpha}$. The sensitivity of $\hat{x}_o$ to $\omega_{k\beta}$ takes different values, however this sensitivity is also independent of $\omega_{k\alpha}$. The results are given in Table C.7. Therefore the variation of the sensitivity of $\hat{x}_o$ to $\omega_{k\beta}$ for different values of $\omega_{k\beta}$ and Q_i is calculated. The results are given in Table C.8 and plotted in Figure 5.6. From Figure 5.6 it can be easily observer that for $\omega_{k\beta} > 20Q_i$ the sensitivity of $\hat{x}_o$ to $\omega_{k\beta}$ remains less than 0.05.

The sensitivity values of $\hat{x}_o(\omega_{k\alpha},\omega_{k\beta},Q_i)$ with respect to Q_i in bandpass filter for different values of $\omega_{k\alpha}$ and $\omega_{k\beta}$ with Q_i=5, is given in Table C.9. From Table C.9. one can see that these sensitivities are independent of $\omega_{k\alpha}$. Therefore the sensitivity of $\hat{x}_o(\omega_{k\alpha},\omega_{k\beta},Q_i)$ with respect to Q_i for different values of $\omega_{k\beta}$ and Q_i and a constant value of $\omega_{k\alpha}$=50 is given in Table C.10. Also the results are plotted in Figure 5.7. As it can be seen from Figure 5.7, for $\omega_{k\beta} > 20Q_i$ the sensitivity values of $\hat{x}_o(\omega_{k\alpha},\omega_{k\beta},Q_i)$ to Q_i remain smaller than 0.05.

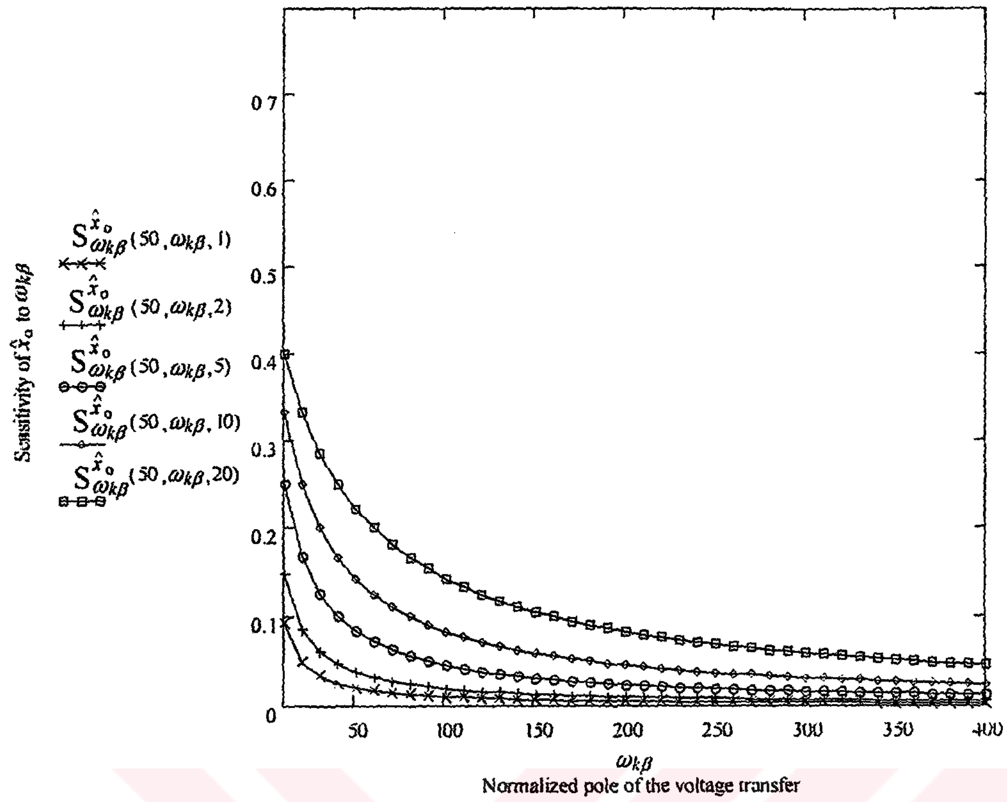

Figure 5.6: The sensitivity of $\hat{x}_o(\omega_{k\alpha},\omega_{k\beta},Q_i)$ with respect to $\omega_{k\beta}$

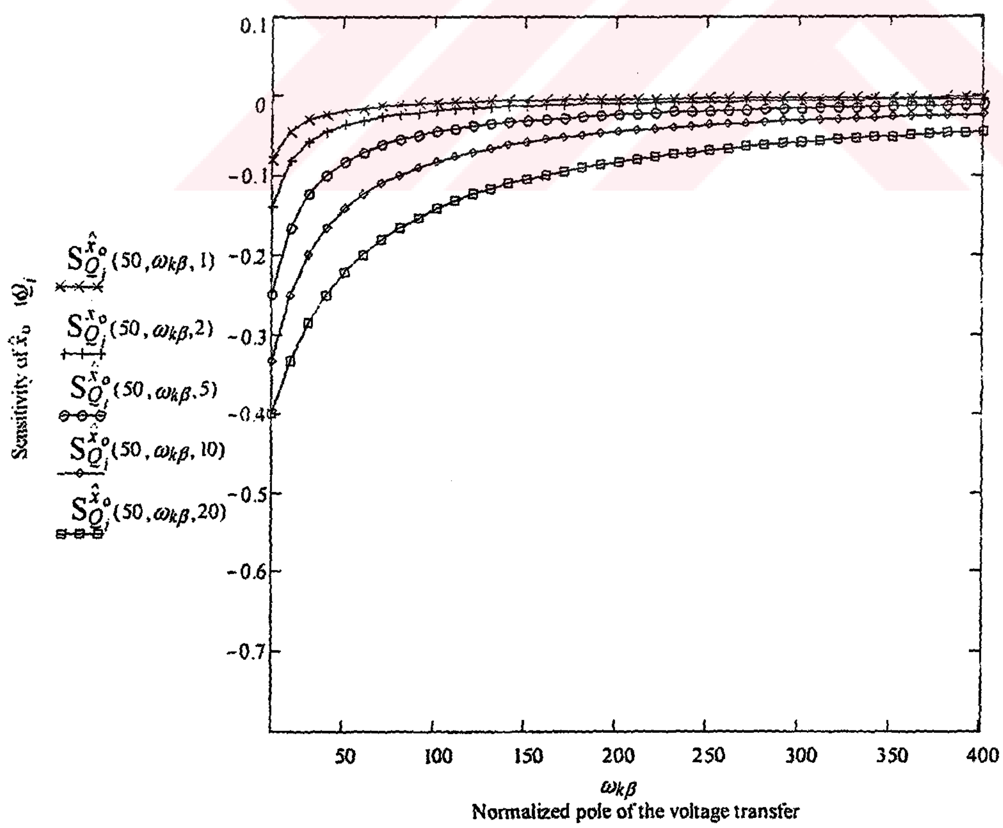

Figure 5.7: The sensitivity of $\hat{x}_o(\omega_{k\alpha},\omega_{k\beta},Q_i)$ with respect to Q_i

Table C.11 shows that the sensitivity of Q with respect to $\omega_{k\alpha}$ for different values of $\omega_{k\alpha}$ and $\omega_{k\beta}$ with Q_i=5, is very small. Table C.12 shows that the sensitivity of Q with respect to $\omega_{k\beta}$ is independent of $\omega_{k\alpha}$. Then, the sensitivity values of Q to $\omega_{k\beta}$ for different values of $\omega_{k\beta}$ and Q_i are given in Table C.13. These values are also plotted in Figure 5.8. From Figure 5.8 it can be seen that for $\omega_{k\beta} > 20Q_i$ the sensitivity values of Q to $\omega_{k\beta}$ remain smaller than 0.05.

Similarly one can see that the sensitivity of Q with respect to Q_i is independent of $\omega_{k\alpha}$. Therefore the sensitivity of Q with respect to Q_i for different values of $\omega_{k\beta}$ and Q_i is plotted in Figure 5.9. As it expected the sensitivity values are close to unity.

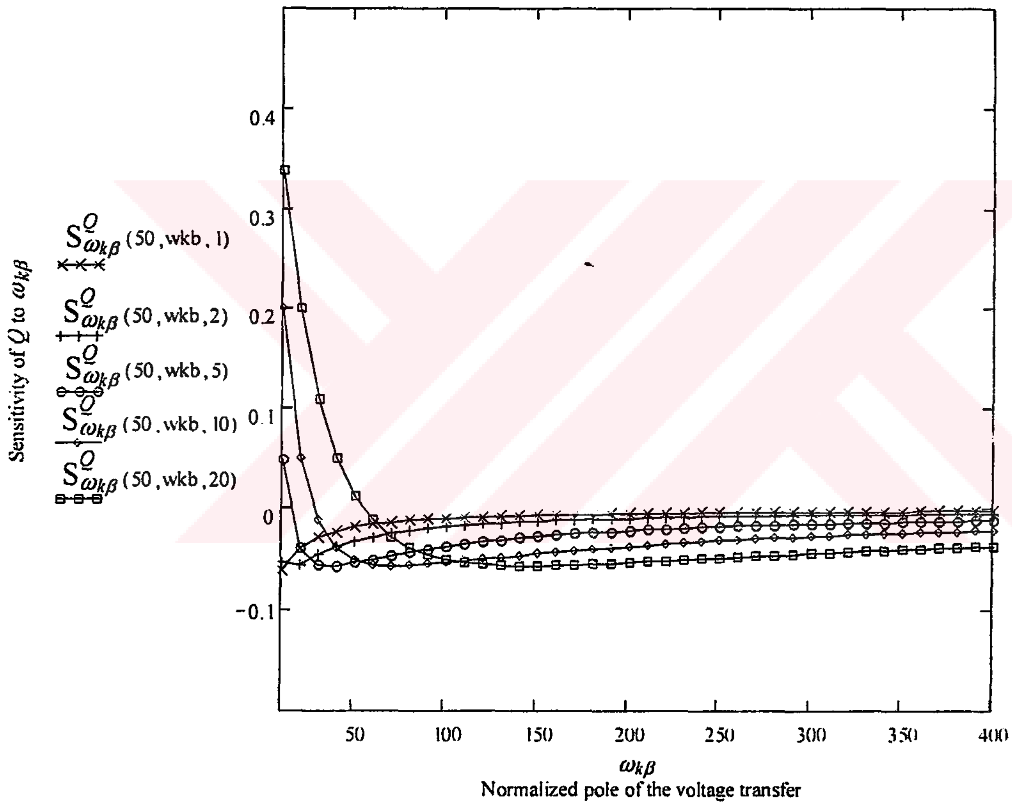

Figure 5.8: The sensitivity of $Q(\omega_{k\alpha}, \omega_{k\beta}, Q_i)$ with respect to $\omega_{k\beta}$

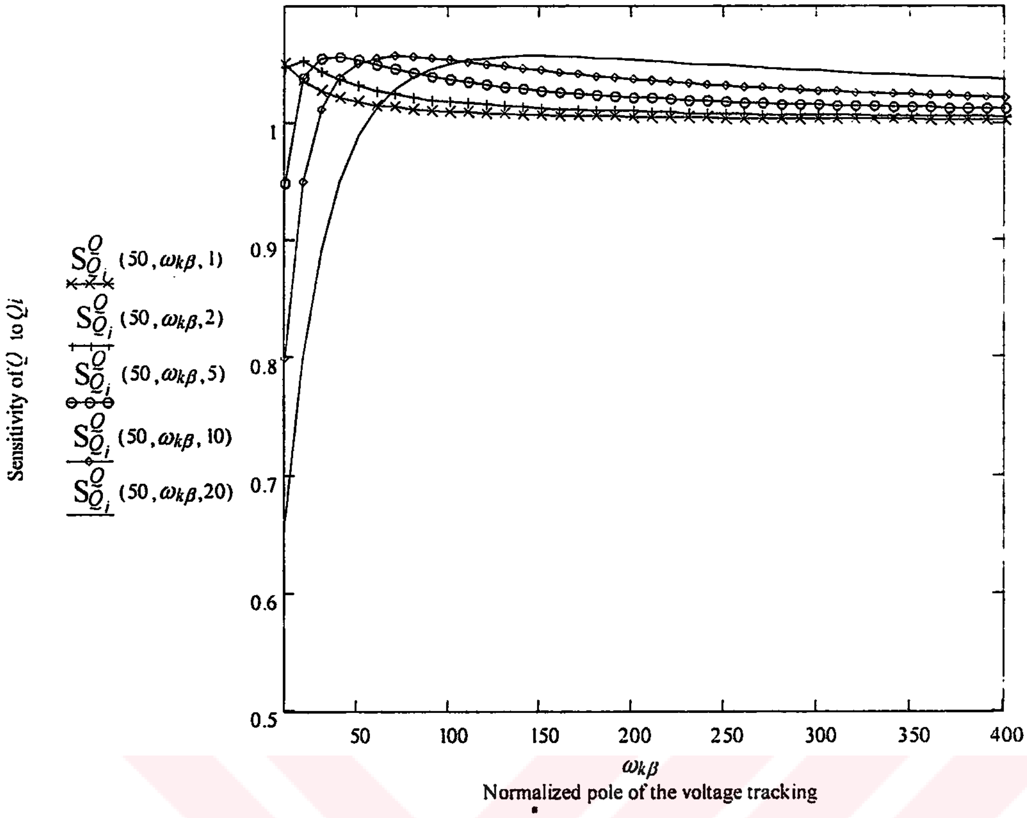

Figure 5.9: The sensitivity of $Q(\omega_{k\alpha}, \omega_{k\beta}, Q_i)$ with respect to Q_i

5.3 Second Order Lowpass Filter Using Single Non-Ideal CCCII

In this section the normalized cutoff angular frequency, quality factor and their sensitivities for the lowpass filter constructed with single non-ideal CCCII is investigated.

Considering equations (2.12), (2.13), (5.4) and (5.5) for realizing a lowpass filter, two new poles and two new zeroes will appear in the transfer function of the lowpass filter. Substituting equations (2.12) and (2.13) into (5.5), the transfer function of the second order normalized bandpass filter constructed with single non-ideal current controlled conveyor can be found as:

$$H(x)=\frac{N(x)}{D(x)}=\frac{a_2x^2+a_1x+a_o}{x^4+b_3x^3+b_2x^2+b_1x+b_o} \tag{5.39}$$

5.3.1 Normalized cutoff angular frequency in lowpass filter

The cutoff frequency of a lowpass filter and its sensitivities can be found in terms of b_j coefficients in denominator polynomial. Defining normalized cutoff frequency as $\hat{x}_c=\frac{\omega_c}{\omega_{ci}}$ and $x=j\hat{x}=j\frac{\omega}{\omega_{ci}}$, where ω_c and ω_{ci} are cutoff angular frequency of the ideal and non-ideal filter, respectively, the module of the normalized transfer function at cutoff frequency, must be equal to $|H(j\hat{x}_c)|=\frac{a_o}{\sqrt{2}b_o}$. If $z=\hat{x}^2$, the square module of the normalized transfer function can be found as

$$G(z)=\frac{P(z)}{M(z)}=\frac{A_2z^2+A_1z+A_o}{z^4+B_3z^3+B_2z^2+B_1z+B_o} \tag{5.40}$$

where

$$B_o=b_o^2,\ B_1=b_1^2-2b_ob_2,\ B_2=b_2^2+2b_o-2b_1b_3,\ B_3=b_3^2-2b_2,\ A_2=a_2^2,$$
$$A_1=a_1^2-2a_2a_o,\ A_o=a_o^2 \tag{5.41}$$

The value of $G(z)$ at $\hat{x}_c$ (cutoff frequency) must be equal to $\frac{A_o}{2B_o}$. Therefore the value of $G(z)$ in cutoff frequency can be written as:

$$\frac{A_2 z_c^2 + A_1 z_c + A_o}{z_c^4 + B_3 z_c^4 + B_2 z_c^3 + B_1 z_c + B_o} = \frac{A_o}{2B_o} \tag{5.42}$$

which results in

$$K_4 z_c^4 + K_3 z_c^3 + K_2 z_c^2 + K_1 z_c + K_o = 0 \tag{5.43}$$

where

$$K_o = -A_o B_o,\ K_1 = A_o B_1 - 2B_o A_1,\ K_2 = B_2 A_o - 2B_o A_2,\ K_3 = A_o B_3,\ K_4 = A_o \tag{5.44}$$

The root of equation (5.43), which is in the vicinity of 1 (the square of the normalized cutoff frequency) can be found using MATHCAD program given in Appendix B.

5.3.2 The peak value of the lowpass filter

The frequency, in which peak value will occur on, is obtained from derivative of the equation (5.40) with respect to z. Therefore from $\frac{dG(z)}{dz} = 0$, we obtain

$$g(z) = z_m^5 + m_4 z_m^4 + m_3 z_m^3 + m_2 z_m^2 + m_1 z_m + m_o = 0 \tag{5.45}$$

where

$$\left.\begin{aligned}
m_4 &= \frac{3A_1}{2A_2} + \frac{B_3}{2} \\
m_3 &= \frac{2A_o + A_1 B_3}{A_2} \\
m_2 &= \frac{3B_3 A_o + A_1 B_2}{2A_2} - \frac{B_1}{2} \\
m_1 &= \frac{B_2 A_o}{A_2} - B_o \\
m_o &= \frac{B_1 A_o - A_1 B_o}{2A_o}
\end{aligned}\right\} \tag{5.46}$$

If the equation (5.45) has a real and positive root (z_m) then a peak value will appear in the frequency response of the filter.

Substituting this z_m into equation (5.40), the peak value in (dB) can be calculated as

$$A_m(dB) = 10\log\frac{A_2 z_m^2 + A_1 z_m + A_o}{z_m^4 + B_3 z_m^3 + B_2 z_m^2 + B_1 z_m + B_o} \tag{5.47}$$

If the peak value remains in a reasonable range, the efficiency of damping factor will be reduced.

5.3.3 Damping factor of the lowpass filter

In a second order lowpass filter, damping factor is defined as

$$d = \frac{1}{2Q} \tag{5.48}$$

As the denominators of lowpass and bandpass filters have the same form, substituting Q from (5.21) into (5.48), damping factor can be found as

$$d = \frac{\hat{x}_o(b_1 - b_3\hat{x}_o^2)}{2(b_o - \hat{x}_o^4)} \tag{5.49}$$

5.3.4 Sensitivities of the normalized cutoff angular frequency and damping factor

The sensitivities of the normalized cutoff angular frequency can be obtained from equation (5.43). Substituting K_o, K_1, K_2, K_3 and K_4 from (5.44) into (5.43) it can be seen that

$$z_c\left(A_o z_c^3 + A_o B_3 z_c^2 + (A_o B_2 - 2B_o A_2)z_c + B_1 A_o - 2B_o A_1\right) = B_o A_o \tag{5.50}$$

Taking logarithmic differential from (5.50), the sensitivities of $\hat{x}_c$ with respect to b_j coefficients can be found as

$$\left.\begin{aligned}
S_{b_o}^{\hat{x}_c} &= \frac{1}{2} S_{b_o}^{z_c} = \frac{A_o\hat{x}_c^6 + A_oB_3\hat{x}_c^4 + (A_oB_2 - 2b_o^2A_2 - A_ob_o)\hat{x}_c^2 + B_1A_o - 2B_oA_1 + b_2b_oA_o}{4A_o\hat{x}_c^6 + 3A_oB_3\hat{x}_c^4 + 2(A_oB_2 - 2b_o^2A_2 - A_ob_o)\hat{x}_c^2 + B_1A_o - 2B_oA_1} \\
S_{b_1}^{\hat{x}_c} &= \frac{1}{2} S_{b_1}^{z_c} = \frac{(b_1b_3A_o + B_ob_1A_2)\hat{x}_c^2 + B_oA_1b_1 - b_1^2A_o}{4A_o\hat{x}_c^6 + 3A_oB_3\hat{x}_c^4 + 2(A_oB_2 - 2b_o^2A_2 - A_ob_o)\hat{x}_c^2 + B_1A_o - 2B_oA_1} \\
S_{b_2}^{\hat{x}_c} &= \frac{1}{2} S_{b_2}^{z_c} = \frac{A_ob_2\hat{x}_c^4 - A_ob_2^2\hat{x}_c^2 + b_ob_2A_o}{4A_o\hat{x}_c^6 + 3A_oB_3\hat{x}_c^4 + 2(A_oB_2 - 2b_o^2A_2 - A_ob_o)\hat{x}_c^2 + B_1A_o - 2B_oA_1} \\
S_{b_3}^{\hat{x}_c} &= \frac{1}{2} S_{b_3}^{z_c} = \frac{-b_3^2A_o\hat{x}_c^4 + b_1b_3A_o\hat{x}_c^2}{4A_o\hat{x}_c^6 + 3A_oB_3\hat{x}_c^4 + 2(A_oB_2 - 2b_o^2A_2 - A_ob_o)\hat{x}_c^2 + B_1A_o - 2B_oA_1}
\end{aligned}\right\} \quad (5.51)$$

Considering equation (5.48) the sensitivities of the damping factor to coefficients b_i (i=0...3) can be found as:

$$S_{bi}^{d} = -S_{bi}^{Q} \qquad\qquad S_{\hat{x}_o}^{d} = -S_{\hat{x}_o}^{Q} \qquad (5.52)$$

Therefore the sensitivities of the damping factor are found from (5.24) just by revising the signs of the equations.

5.3.5 Design of a lowpass filter

By selecting $Y_1=sC_1$, $Y_2=G_2$, $Y_3=\infty$, $Y_4=sC_4$ a lowpass filter can be realized. This filter is shown in Figure 5.10.

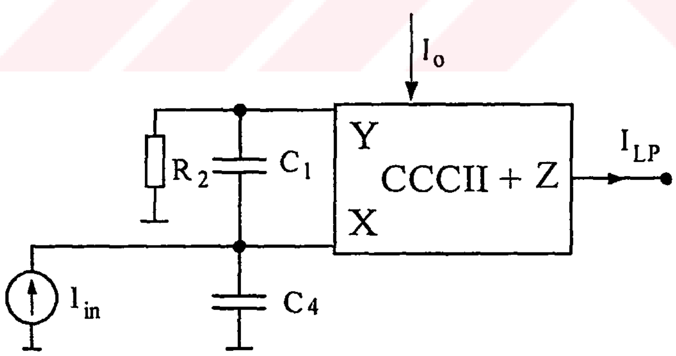

Figure 5.10: Lowpass filter realization using single CCCII

Ideal analysis of this circuit yields the following transfer function:

$$H_i(s) = \frac{I_{LP}}{I_{in}} = \frac{-\dfrac{1}{R_2R_xC_1C_4}}{s^2 + \dfrac{C_1+C_4}{R_2C_1C_4}s + \dfrac{1}{R_2R_xC_1C_4}} \qquad (5.53)$$

In this equation the parameters ω_{ci}, Q_i and $\frac{\omega_{ci}}{Q_i}$ (in maximally flat approach) can be found as:

$$\omega_{ci} = \frac{1}{\sqrt{R_2 R_x C_1 C_4}}, \; Q_i = \frac{1}{C_1 + C_4}\sqrt{\frac{C_1 C_4 R_2}{R_x}}, \; \frac{\omega_{ci}}{Q_i} = \frac{C_1 + C_4}{R_2 C_1 C_4} \tag{5.54}$$

To find a transfer function in terms of Q_i in normalized form in which ideal resonant angular frequency is equal to unity, we define $R^2 = R_2 R_x$ and $C = C_1 = C_4$, therefore:

$$H_i(s) = \frac{-\frac{1}{R^2 C^2}}{s^2 + \frac{1}{Q_i RC}s + \frac{1}{R^2 C^2}} \tag{5.55}$$

By normalizing the transfer function with respect to ideal cutoff angular frequency ($x = \frac{s}{\omega_{ci}}$), the normalized ideal transfer function of the bandpass filter is found as:

$$H_i(x) = \frac{-1}{x^2 + \frac{1}{Q_i}x + 1} \tag{5.56}$$

which is independent of the passive element values. Similarly the normalized transfer function of actual lowpass filter can be found as:

$$H(x) = \frac{\alpha(x)\left(2Q_i\left(\beta(x) - 1 - \frac{C_y}{C}\right)x - 1\right)}{\left(1 + 2\frac{C_y}{C}\right)x^2 + \left(\frac{1}{Q_i} + (1 - \beta(x))2Q_i + \frac{2Q_i C_y}{C}\right)x + 1} \tag{5.57}$$

Considering $\frac{C_y}{C} << 1$, the non-ideal transfer function of the lowpass filter is simplified as:

$$H(x) = \frac{\alpha(x)Q_i(2(\beta(x)-1)x-1)}{x^2 + \left(\frac{1}{Q_i} + (1-\beta(x))2Q_i\right)x + 1} \quad (5.58)$$

where $\alpha(x)$, $\beta(x)$ were defined in (5.31) and $\omega_{k\alpha} = \frac{\omega_\alpha}{\omega_{ci}}$ and $\omega_{k\beta} = \frac{\omega_\beta}{\omega_{ci}}$ are the normalized pole frequency of the $\alpha(s)$ and $\beta(s)$ with respect to ideal cutoff frequency of the lowpass filter ω_{ci}, respectively.

Substituting equation (5.31) into equation (5.58) results the transfer function in form of equation (5.39) with the following coefficients:

$$\left.\begin{aligned}
a_2 &= -2Q_i\omega_{k\alpha} \\
a_1 &= \omega_{k\alpha} \\
a_o &= -\omega_{k\alpha}\omega_{k\beta} \\
b_3 &= \omega_{k\alpha} + \omega_{k\beta} + \frac{1}{Q_i} + 2Q_i \\
b_2 &= \omega_{k\alpha}\omega_{k\beta} + \frac{\omega_{k\alpha} + \omega_{k\beta}}{Q_i} + 2Q_i\omega_{k\alpha} + 1 \\
b_1 &= \frac{\omega_{k\alpha}\omega_{k\beta}}{Q_i} + \omega_{k\alpha} + \omega_{k\beta} \\
b_o &= \omega_{k\alpha}\omega_{k\beta}
\end{aligned}\right\} \quad (5.59)$$

Using MATHCAD program, the amplitude of the transfer function of this lowpass filter for different values of $\omega_{k\alpha}$, $\omega_{k\beta}$ and Q_i=0.707 are given in Appendix B. As illustrated in Figures B.1 and B.2 with Q_i=0.707 there is no peak value in the frequency response of the filter.

Using the MATHCAD program given in Appendix B, the normalized cutoff angular frequency ($\hat{x}_c(\omega_{k\alpha}, \omega_{k\beta}, Q_i)$), which is defined as a function of $\omega_{k\alpha}$, $\omega_{k\beta}$ and Q_i, can be found for different values of $\omega_{k\alpha}$, $\omega_{k\beta}$ and Q_i. The values of the normalized cutoff angular frequency of the non-ideal second order lowpass filter for different values of $\omega_{k\beta}$, $\omega_{k\alpha}$ and Q_i=0.707 are given Table C.14. The ideal quality factor value Q_i is chosen 0.707 to prevent of accepting a peak value in filter characteristic. As shown in Appendix B, for different values of $\omega_{k\alpha}$, $\omega_{k\beta}$ there is no peak value in the frequency response of the filter.

From Table C.14, It can be seen that for

$$\omega_{k\alpha} > 10 \text{ and } \omega_{k\beta} > 30 \tag{5.60}$$

the deviation of the normalized cutoff frequency from its ideal value 1 is less than %5. Therefore by neglecting the small terms in equation (5.43) the following accurate equation can be given for calculating normalized cutoff angular frequency of non-ideal lowpass filter.

$$\hat{x}_c = \left(\frac{-K_1 + (K_1^2 - 4K_2K_o)^{\frac{1}{2}}}{2K_2} \right)^{\frac{1}{2}} \tag{5.61}$$

One can see that the value of $\hat{x}_c$ calculated from equation (5.61) is in quite agreement with the values given in Table C.14. For example with $\omega_{k\alpha}$=50, $\omega_{k\beta}$=90 and Q_i=0.707 the value of $\hat{x}_c$ will be found from (5.61) equal to 0.984 which is the same as given in Table C.14. Figure 5.11, shows the variation of $\hat{x}_c(\omega_{k\alpha}, \omega_{k\beta}, 0.707)$ with respect to $\omega_{k\beta}$ for different values of $\omega_{k\alpha}$. The variation of the normalized damping factor which is defined as a function of $\omega_{k\alpha}$, $\omega_{k\beta}$ and Q_i $[d_n(\omega_{k\alpha}, \omega_{k\beta}, Q_i)]$ for different values of $\omega_{k\alpha}$ and $\omega_{k\beta}$ (Q_i=0.707) is given in Table C.15. It can be seen that with non-equalities given in (5.60), the deviation of damping factor from its ideal value remains also less than %5. The variation of $d_n(\omega_{k\alpha}, \omega_{k\beta}, 0.707)$ for different values of $\omega_{k\alpha}$ and $\omega_{k\beta}$ is shown in Figure 5.12.

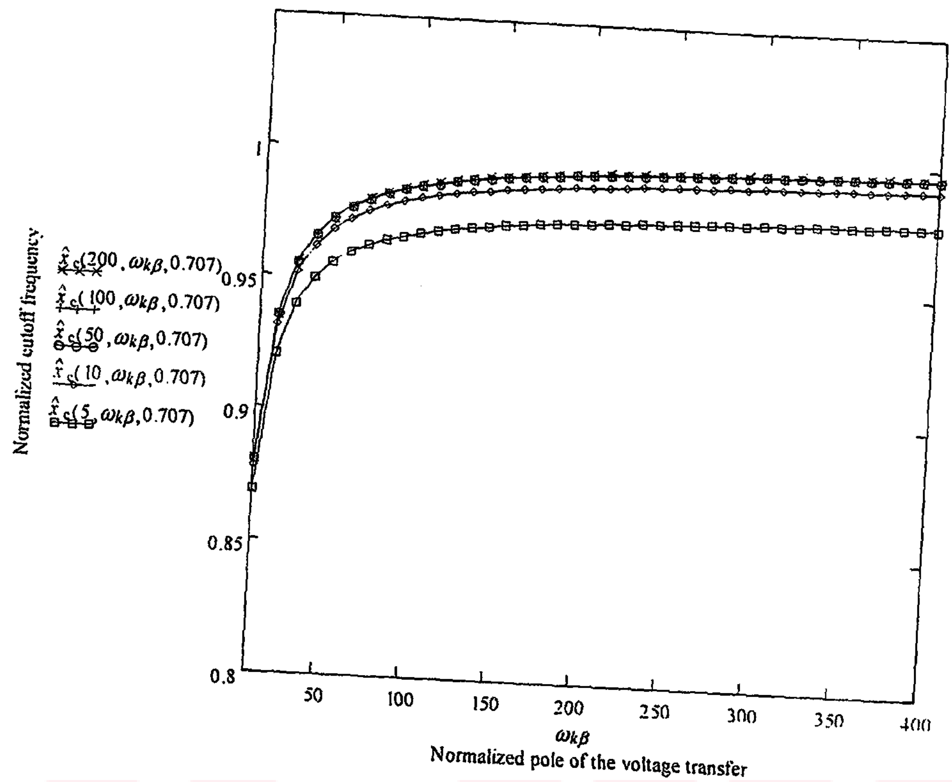

Figure 5.11: The variation of $\hat{x}_c(\omega_{k\alpha},\omega_{k\beta},0.707)$ with respect to $\omega_{k\beta}$ for different values of $\omega_{k\alpha}$

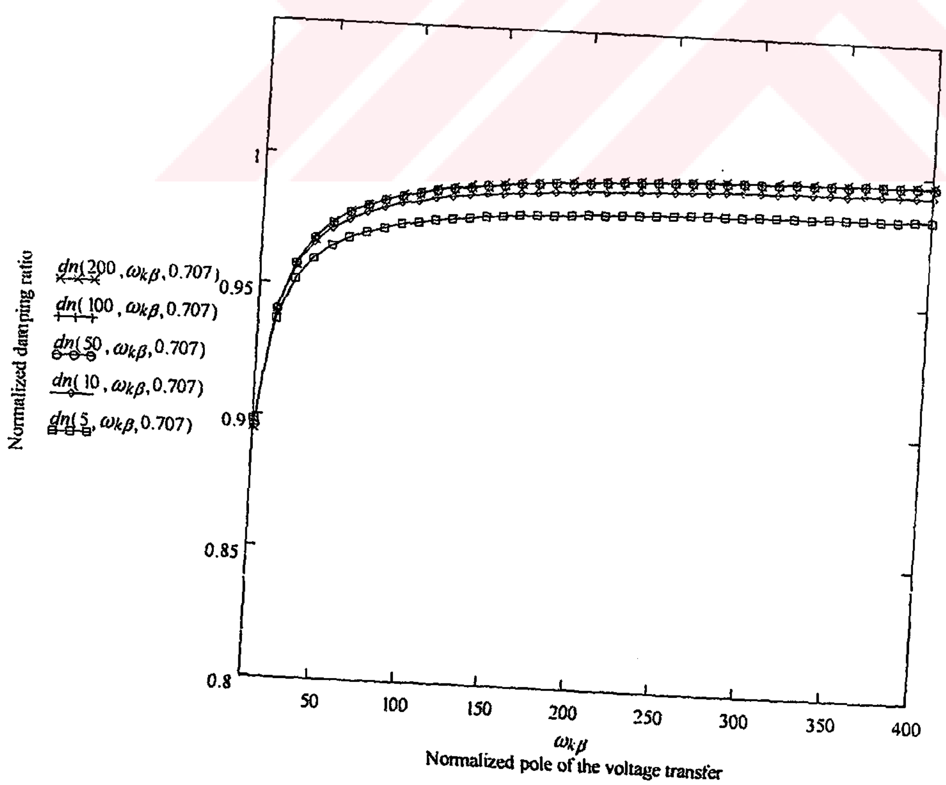

Figure 5.12: The variation of $d_n(\omega_{k\alpha},\omega_{k\beta},0.707)$ with respect to $\omega_{k\beta}$ for different values of $\omega_{k\alpha}$

The sensitivities of the $\hat{x}_c$ and d_n with respect to the parameters $\omega_{k\alpha}$, $\omega_{k\beta}$ and Q_i can be found as:

$$\left.\begin{array}{lll} S_{\omega_{k\alpha}}^{\hat{x}_c} = \sum_{i=0}^{3} S_{b_i}^{\hat{x}_c}.S_{\omega_{k\alpha}}^{b_i}, & S_{\omega_{k\beta}}^{\hat{x}_c} = \sum_{i=0}^{3} S_{b_i}^{\hat{x}_c}.S_{\omega_{k\beta}}^{b_i}, & S_{Q_i}^{\hat{x}_c} = \sum_{i=0}^{3} S_{b_i}^{\hat{x}_c}.S_{Q_i}^{b_i} \\ S_{\omega_{k\alpha}}^{d_n} = \sum_{i=0}^{3} S_{b_i}^{d_n}.S_{\omega_{k\alpha}}^{b_i}, & S_{\omega_{k\beta}}^{d_n} = \sum_{i=0}^{3} S_{b_i}^{d_n}.S_{\omega_{k\beta}}^{b_i}, & S_{Q_i}^{d_n} = \sum_{i=0}^{3} S_{b_i}^{d_n}.S_{Q_i}^{b_i} \end{array}\right\} \quad (5.62)$$

The sensitivities of $\hat{x}_c$ and d_n to b_i (i=0…3) were given in equations (5.51) and (5.52), respectively. As the b_i coefficient are the same as found in section 5.2.4, then the equations (5.36), (5.37) and (5.38) can also be used in determination of the sensitivities given in equation (5.62).

The sensitivity values of $\hat{x}_c(\omega_{k\alpha},\omega_{k\beta},0.707)$ with respect to $\omega_{k\alpha}$ for different values of $\omega_{k\alpha}$ and $\omega_{k\beta}$ are given in Table C.16. From Table C.16, one can see that these sensitivities are very small. Then the sensitivity values of $\hat{x}_c(\omega_{k\alpha},\omega_{k\beta},0.707)$ with respect to $\omega_{k\beta}$ for different values of $\omega_{k\alpha}$ and $\omega_{k\beta}$ are given in Table C.17. It can be seen that the sensitivity of $\hat{x}_c$ to $\omega_{k\beta}$ is independent of $\omega_{k\alpha}$. Also the results are plotted in Figure 5.13. As it can be seen from Figure 5.13, for the condition given in equation (5.60) the sensitivity values of $\hat{x}_c$ to $\omega_{k\beta}$ remain smaller than 0.05. Table C.18 gives the sensitivity values of $\hat{x}_c(\omega_{k\alpha},\omega_{k\beta},0.707)$ to Q_i for different values of $\omega_{k\alpha}$ and $\omega_{k\beta}$. It can be seen that these sensitivity values are independent of $\omega_{k\alpha}$. The results are plotted in Figure 5.14. From Figure 5.14, one can see that these sensitivity values are smaller than unity.

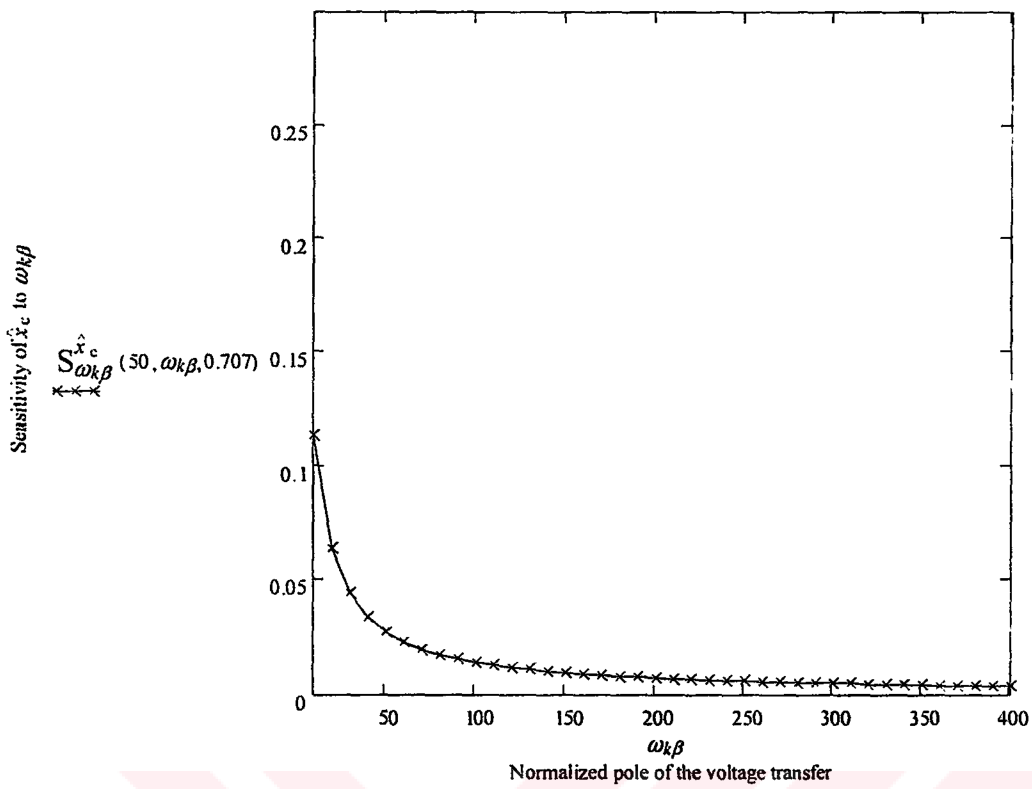

Figure 5.13: The sensitivity of $\hat{x}_c(50, \omega_{k\beta}, 0.707)$ with respect to $\omega_{k\beta}$

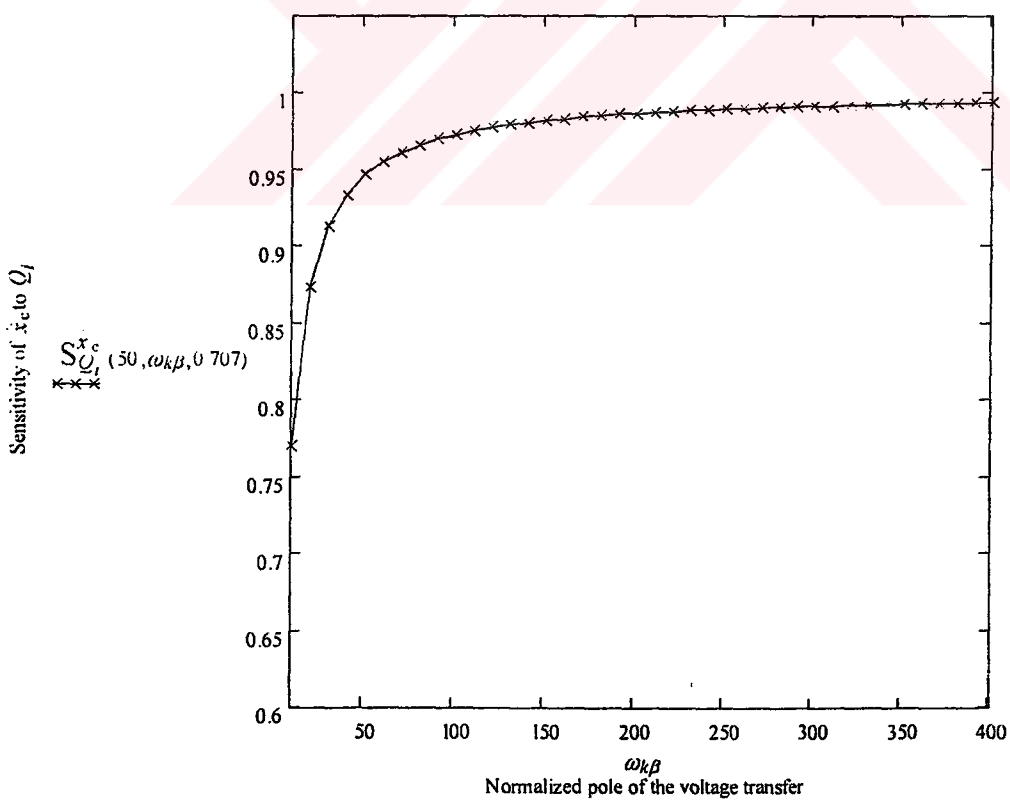

Figure 5.14: The sensitivity of $\hat{x}_c(50, \omega_{k\beta}, 0.707)$ with respect to Q_i

As given in Table C.19, the sensitivity values of $d_n(\omega_{k\alpha}, \omega_{k\beta}, 0.707)$ with respect to $\omega_{k\alpha}$ for different values of $\omega_{k\alpha}$ and $\omega_{k\beta}$ is quite small. However, the sensitivity of $d_n(\omega_{k\alpha}, \omega_{k\beta}, 0.707)$ with respect to $\omega_{k\beta}$ takes different values by changing $\omega_{k\alpha}$ and $\omega_{k\beta}$, as given in Table C.20. Also the sensitivity values of $d_n(\omega_{k\alpha}, \omega_{k\beta}, 0.707)$ with respect to Q_i for different values of $\omega_{k\alpha}$ and $\omega_{k\beta}$ are given in Table C.21. The results are given in Figure 5.15.

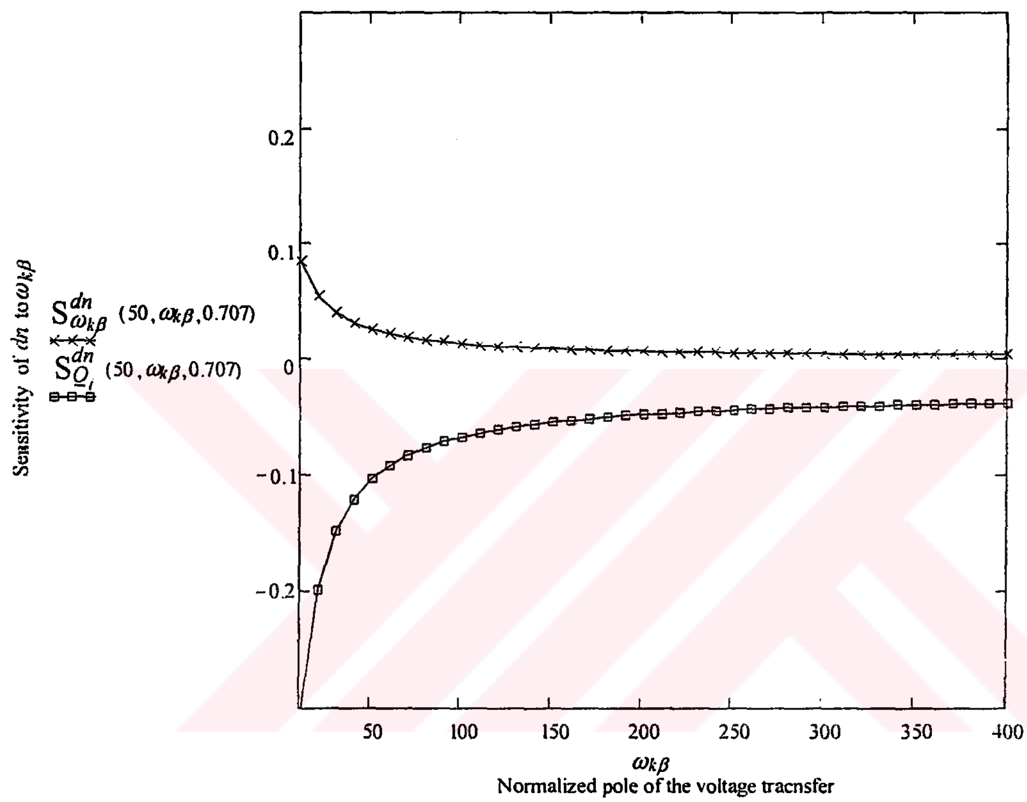

Figure 5.15: The sensitivity of $d_n(50, \omega_{k\beta}, 0.707)$ with respect to $\omega_{k\beta}$ and Q_i

5.4. Using of The Results In Design of Filter

Using the active and passive elements values of an ideal filter results a deviation characteristic of the filter in high frequencies. However in non-ideal case, by changing the element values of the filter we can expand usable range of the filter. In this section, by using the graphics plotted in section 5.2.4 and 5.3.5, we present a method for finding the element values of the non-ideal filter to make its characteristics values close to ideal one.

For example a second order bandpass filter constructed with single non-ideal CCCII is selected. For the other filter realizations the similar approach can be used in design of the filter.

First $\omega_{k\alpha} = \frac{\omega_\alpha}{\omega_{oi}}$ and $\omega_{k\beta} = \frac{\omega_\beta}{\omega_{oi}}$ of the CCCII are determined. As shown in Table C.4, the quality factor of the bandpass filter is independent of $\omega_{k\alpha}$. Therefore the different values of the normalized quality factor $q(\omega_{k\alpha}, \omega_{k\beta}, Q_i)$ for $\omega_{k\alpha} = const$ and $\omega_{k\beta} = const$ with different values of Q_i can be found from Table C.5. The value of Q_i for designing of the filter can be found by plotting $q(\omega_{k\alpha} = const, \omega_{k\beta} = const, Q_i)$ and $q = \frac{Q}{Q_i}$ (horizontal axis is Q_i) and finding intersection point of these two plots.

Similarly, the value of $\hat{x}_o$ can be found by plotting $\hat{x}_o(\omega_{k\alpha} = const, \omega_{k\beta} = const, Q_i)$ and moving this plot to plane of $q(\omega_{k\alpha} = const, \omega_{k\beta} = const, Q_i)$. The value of $\hat{x}_o$ is determined from this plot by choosing Q_i, which was found in pervious step.

Therefore the value of ω_{oi} is found from

$$\omega_{oi} = \frac{\omega_o}{\hat{x}_o} \tag{5.63}$$

These values of ω_{oi} and Q_i are used to calculate of the element values of the filter.

5.4.1 Example

As an example, we design a bandpass filter constructed with single CCCII shown in Figure 5.2 with a resonant frequency of f_o=1MHz and quality factor of Q=5. As shown in Table 2.1, the pole of the voltage and current tracking gain of the bipolar CCCII+ implemented with the transistor model of PR100N (PNP) and NR100N (NPN) [74] are found as: ω_α=3.12 E+8 rad/s and ω_β=5.68 E+8 rad/s. Therefore

$$\omega_{k\alpha} = \frac{\omega_\alpha}{\omega_{oi}} = \frac{3.12\times \mathrm{E}+8}{2\pi\times 1\times \mathrm{E}+6} = 49.6 \qquad \omega_{k\beta} = \frac{\omega_\beta}{\omega_{oi}} = \frac{5.68\times \mathrm{E}+8}{2\pi\times 1\times \mathrm{E}+6} = 90.4$$

From Figures 5.3 and 5.4 and considering $\omega_{k\alpha} = 49.6$ and $\omega_{k\beta} = 90.4$ and Q_i=5 one can find $\hat{x}_o = 0.949$ and $q = 1.048$. However, this is not the desired solution. As explained in section 5.5, using the plots of $q(\omega_{k\alpha} = 49.6, \omega_{k\beta} = 90.4, Q_i)$, $q = \frac{5}{Q_i}$ and $\hat{x}_o(\omega_{k\alpha} = 49.6, \omega_{k\beta} = 90.4, Q_i)$ as shown in Figure 5.16, the value of Q_i is found from intersection of the $q(\omega_{k\alpha} = 49.6, \omega_{k\beta} = 90.4, Q_i)$ and $q = \frac{5}{Q_i}$ as: Q_i=4.779. Using this value of Q_i from plot of $\hat{x}_o(\omega_{k\alpha} = 49.6, \omega_{k\beta} = 90.4, Q_i)$ the value of $\hat{x}_o$ will be $\hat{x}_o = 0.951$. Therefore the filter must be designed for $f_{oi} = \frac{f_o}{\hat{x}_o} = \frac{1}{0.951} = 1.052\,\mathrm{MHz}$ and Q_i=4.779.

The passive and active element values in Figure 5.3 for f_{oi}=1.052MHz and Q_i=4.779 are selected as: C_3=C_4=100pF, R_2=15.2kΩ and I_o=85.92μA. The simulation results are given in Figure 5.17. As it was desired, the resonant frequency and quality factor of the filter are 1MHz and 5, respectively.

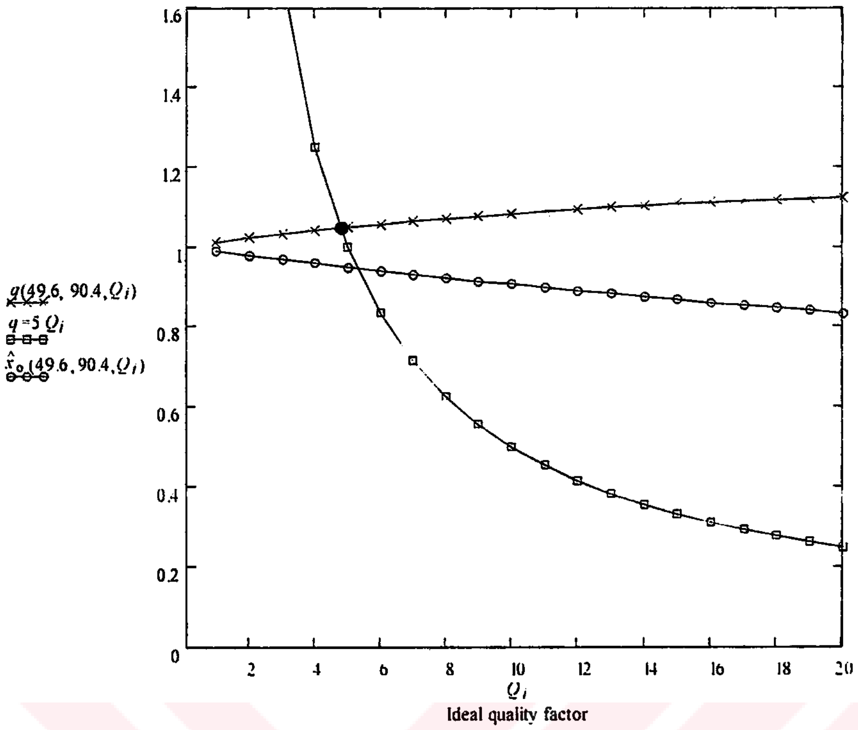

Figure 5.16: The plots of $q(\omega_{k\alpha} = 49.6, \omega_{k\beta} = 90.4, Q_i)$, $q = \dfrac{5}{Q_i}$ and $\hat{x}_o(\omega_{k\alpha} = 49.6, \omega_{k\beta} = 90.4, Q_i)$ as a function of Q_i

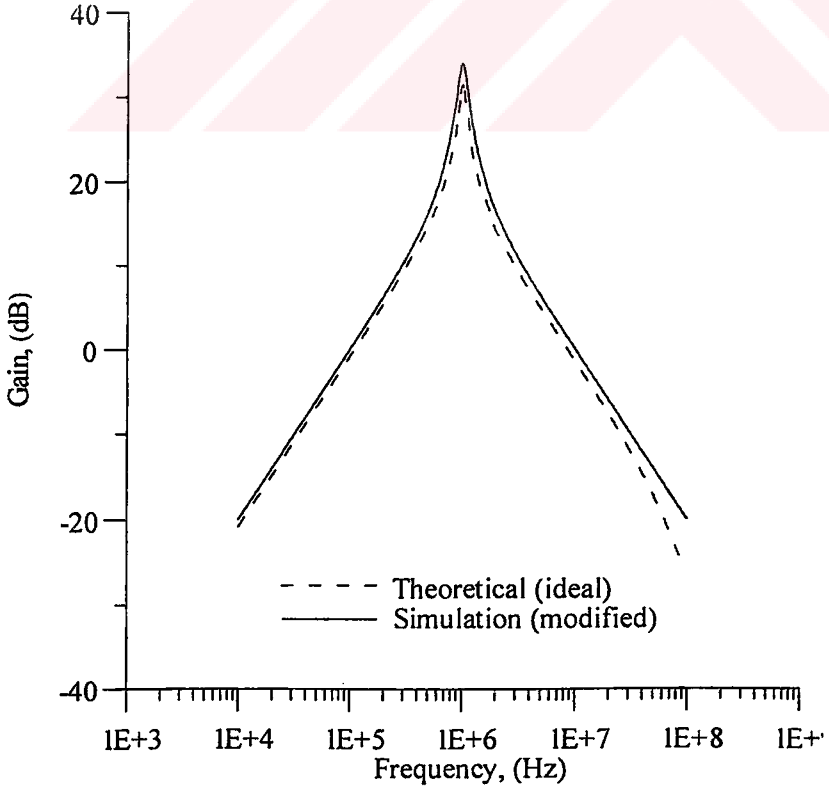

Figure 5.17: The modified frequency response of the circuit proposed in Figure 5.2

5.5 Highpass Filter Using Single CCCII

Considering that the cutoff frequency in highpass filters is very low with respect to the frequency range of the CCCII non-idealities, the effects of the non-ideality on the parameters of the high pass filter is quite negligible. In this section this fact is shown on a second order highpass filter constructed with single CCCII.

The proposed configuration for highpass filter using single CCCII is shown in Figure 5.18.

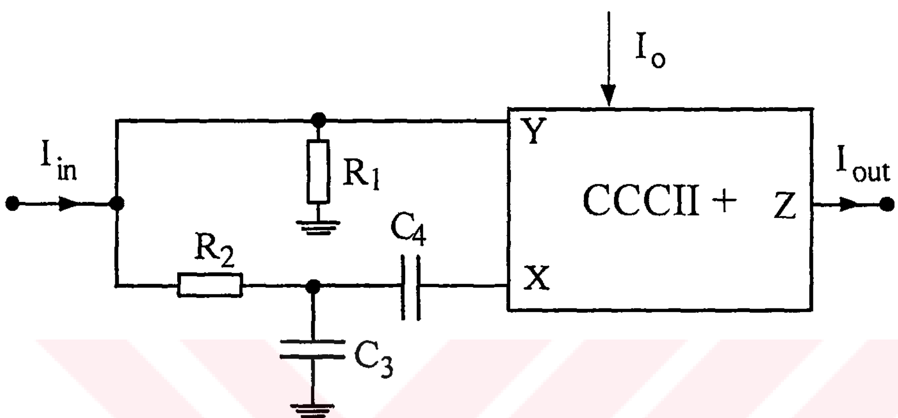

Figure 5.18: Proposed configuration for realizing highpass filter

Routine analysis of the circuit gives the ideal transfer function as:

$$H_i(s) = \frac{I_{HP}}{I_{in}} = \frac{\frac{R_1 R_2}{R_x(R_1+R_2)} s^2}{s^2 + \frac{C_4(R_x+R_2)+C_3(R_1+R_2)}{C_3C_4R_x(R_1+R_2)} s + \frac{1}{C_3C_4R_x(R_1+R_2)}} \tag{5.64}$$

Therefore the parameters ω_o and Q of the filter are found as:

$$\omega_o = \frac{1}{\sqrt{C_3C_4R_x(R_1+R_2)}}, \quad Q = \frac{\sqrt{C_3C_4R_x(R_1+R_2)}}{C_4(R_x+R_2)+C_3(R_1+R_2)} \tag{5.65}$$

The simulation and ideal response of the proposed high pass filter are given in Figure 5.19. The active and passive elements are selected as: $R_1 = R_2 = 1.95\,\mathrm{k\Omega}$. $C_3 = C_4 = 10\,\mathrm{nF}$, $I_o = 20\mu A$, which results in a cutoff frequency of 37.05kHz. The CCCII+ has been simulated using the schematic implementation proposed in Figure

2.4 with DC supply voltage $= \pm 2.5\,V$. The PNP and the NPN transistors have been simulated using the parameters of the PR100N and NR100N bipolar transistors [74]. As it can be seen from the Figure 5.19 the simulation results and ideal response of the filter are in quite agreement.

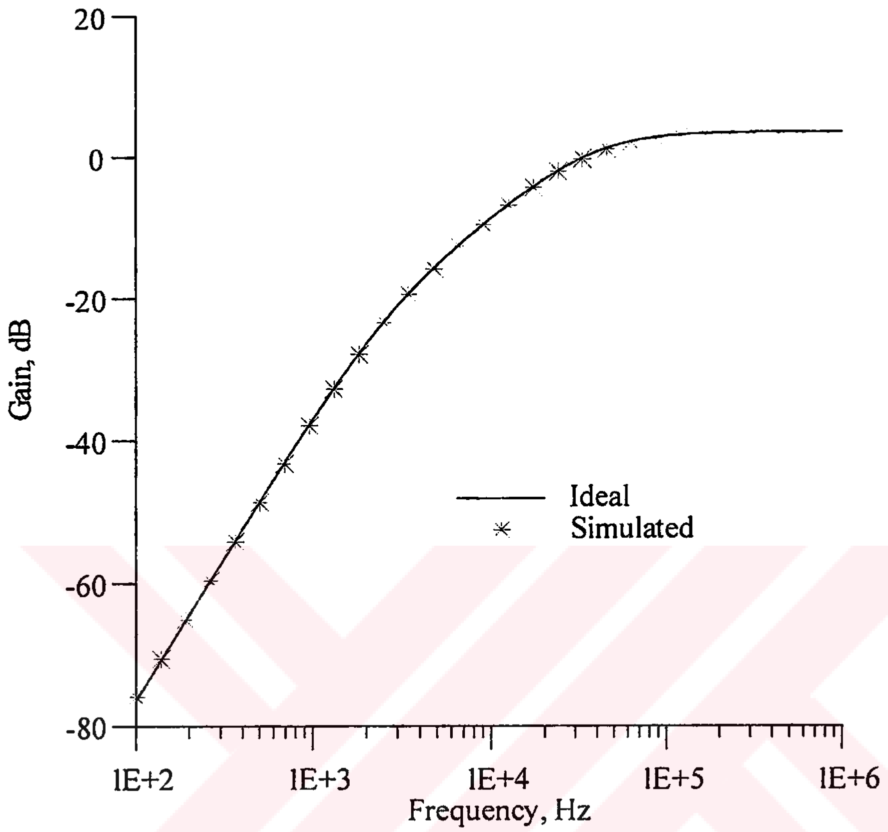

Figure 5.19: Frequency response of the highpass filter using single CCCII

6. CONCLUSION AND FUTURE WORKS

6.1 Conclusion

In this thesis, at first a detailed study in bipolar realization of the current controlled conveyor (CCCII) is performed. The DC and AC characteristics of the bipolar CCCII are extracted and non-ideality parameters of the CCCII are given. Also the bipolar realization of the CCCII is slightly modified which results in a wider tuning range. Then to illustrate the usefulness of the CCCII many new CCCII-based applications are proposed. These are current-mode single-input three-output universal filter, first order all-pass filters, floating inductance simulator and oscillator.

Moreover in order to take the advantages of the BiCMOS technology such as requiring small silicon area and high frequency performance together with high input resistance a BiCMOS realization for the CCCII is presented. The AC and DC characteristics of the proposed realization are given and the circuit is tested on a bandpass filter.

The most important section of the thesis is the investigation of the dominant non-ideality effects of the CCCII in resonant angular frequency and quality factor of the second order bandpass and lowpass filter constructed with single CCCII. The graphics of the normalized resonant angular frequency and quality factor of these filters are extracted and simplified formulas for calculating these parameters are given. The effects of the non-idealities on the stability and sensitivities of the proposed filters are investigated in details. Also as an example, a method for modifying the values of passive elements of the filter in order to minimize the deviation of the filter parameters from their ideal values are given.

6.2 Future Works

In this thesis bipolar and BiCMOS implementations of the CCCII are investigated. However the CMOS implementation of the CCCII is open for investigation. Although many new CCCII-based analog signal processing applications have been presented in this thesis, the design of neural networks, fuzzy controllers, and nonlinear circuits are not considered. Today these applications are implemented with OP-AMP and CCIIs. The electronically control advantage of the CCCII in analog neural and fuzzy circuits could be interesting for IC designers. Also the effects of the CCCII non-idealities in high order active filters are open for investigation.

REFERENCES

[1] **Wilson, B.**, 1990. Recent developments in current-mode circuits, *Proceedings of the Institution of Electrical Engineering, Pt G,* **137,** 63–67.

[2] **Kumar, U.**, 1981. Current conveyor: a review of state of the art, *IEEE Circuits and System Magazine*, **3,** 10–13.

[3] **Toumazou, C., Lidgey, F.J. and Haigh, D.G.,** 1990. Analog IC design: The current-mode approach. London: Peregrinus.

[4] **Smith, K.C. and Sedra, A.**, 1968. The current conveyor- a new circuit building block, *IEEE Proc.*, **56**, 1368–1369.

[5] **Wadsworth, D.C.,** 1990. Accurate current conveyor topology and monolithic implementation. *IEE Proc. G*, **137 (2)**, 88–94.

[6] **Sedra, A. and Smith, K.C.,** 1970. A second generation current conveyor and its applications. *IEEE Trans. Circuit Theory*, **CT-17**, 132–134.

[7] **Liu, S.I., Tsao, H.W. and Wu, J.**, 1990. Cascadable current-mode single CCII biquad, *Electronics Letters*, **26 (24)**, 2005–2006.

[8] **Chang, C.M, Chien, C.C. and Wang, H.Y.,** 1993. Universal active current filters using single second-generation current conveyor. *Electronics Letters*, **29 (13),** 1159–1160.

[9] **Senani, R.**, 1992. New current-mode biquad filter, *International Journal of Electronics*, **73 (4)**, 735–742.

[10] **Chang, C.M.**. 1993. Universal active current filter with single input and three outputs using CCIIs, *Electronics Letters*, **29 (22),** 1932–1933.

[11] **Fabre, A. and Alami, M.**, 1995. Universal current mode biquad implemented from two second generation current conveyors, *IEEE Transactions on Circuits and Systems–I: Fundamental Theory and Applications*, **42 (7)**, 383–385.

[12] **Özoğuz, S. and Acar, C.**, 1997. Universal current mode filter with reduced number of active and passive components, *Electronics Letters*, **33 (11),** 948–949.

[13] **Abuelma'atti, M.T. and Shabra, A.M.**, 1996. A novel current-conveyor-based universal current-mode filter. *Microelectronics Journal*, **27 (6)**, 471–475.

[14] **Papazoglou, C.A. and Karybakas, C.A.**, 1997. Noninteracting electronically tunable CCII-Based current-mode biquadratic filters, *IEEE Proceedings–Circuits, Devices and Systems*, **144 (3)**, 178–184.

[15] **Chang, C.M.**, 1997. Universal active current filter with three inputs and one output using plus-type CCIIs, *Electronics Letters*, **33 (14)**, 1207–1208.

[16] **Chang, C.M. and Chen, P.C.**, 1991. Universal active current filter with three Inputs and One Output Using Current Conveyors, *International Journal of Electronics*, **71 (5)**, 817–819.

[17] **Chang, C.M., Chien, C.C. and Wang, H.Y.**, 1994. Universal active current filter with three inputs using current conveyors–Part 2. *International Journal of Electronics*, **76 (1)**, 87–89.

[18] **Abuelma'atti, M.T., Al-Ghumaiz, A.A. and Khan, M.H.**, 1995. Novel CCII–Based single-element controlled oscillators employing grounded resistors and capacitors. *International Journal of Electronics*, **78 (6)**, 1107–1112.

[19] **Bhaskar, D.R. and Senani, R.**, 1993. New current-conveyor-based single-resistance-controlled/voltage-controlled oscillator employing grounded capacitors. *Electronics Letters*, **29 (7)**, 612–614.

[20] **Celma, S., Martinez, P.A. and Gutierrez, I.**, 1994. Generation of current conveyor based sinusoidal oscillators for integrated circuits, *Microelectronics Journal*, **25 (6)**, 407–414.

[21] **Liu, S.I.**, 1995. Single-resistance-controlled/voltage-controlled oscillator using current conveyors and grounded capacitors. *Electronics Letters*, **31 (5)**, 337–338.

[22] **Chang, C.M.**, 1995. Novel current-conveyor-based single-resistance-controlled/voltage-controlled oscillator employing grounded resistors and capacitors. *Electronics Letters*, **30 (3)**, 181–183.

[23] **Senani, R. and Singh, V.K.**, 1992. Single-element-controlled sinusoidal oscillator employing single current conveyor IC. *Electronics Letters*, **28 (4)**, 414–415.

[24] **Nandi, R.**, 1996. Current-mode tunable low-frequency oscillators using current conveyors. *Frequenz*, **50 (5-6)**, 128–130.

[25] **Çam, U. and Kuntman, H.**, 1998. A new CCII-based sinusoidal oscillator providing fully independent control of oscillation condition and frequency. *Microelectronics Journal*, **29 (11)**, 913–919.

[26] **Minaei, S., Kuntman, H., Çiçekoğlu, O., Türköz, S. and Tarım, N.**, 2000. High output impedance current-mode multifunction filter employing CMOS dual output CCIIs and All grounded passive elements. *Proceedings of the 12th International Conference on Microelectronics (ICM2000)*, October, Tehran, Iran, 83–86.

[27] **Minaei, S., Kuntman, H., Çiçekoğlu, O., Türköz, S. and Tarım, N.**, 2000. A new high output impedance current-mode universal filter with single input and three outputs using dual output CCIIs. *Proceedings of the 7th IEEE International Conference on Electronics, Circuits and Systems (ICECS 2000)*, December, Beirut, Lebanon, 379–382.

[28] **Pal, K. and Singh, R.**, 1982. Inductorless current conveyor allpass filter using grounded capacitors. *Electronics Letters*, **18 (1)**, 47.

[29] **Pal, K.** 1981. Realization of current conveyor all-pass network. *International Journal of Electronics*, **50 (2)**, 165–168.

[30] **Higashimura, M. and Fukui, Y.**, 1988. Realization of all-pass networks using a Current Conveyor. *International Journal of Electronics*, **65 (2)**, 249–250.

[31] **Çiçekoğlu, O., Kuntman, H. and Berk, S.**, 1999. All-Pass filters using a single current conveyor. *International Journal of Electronics*, **86, (8)**, 947–955.

[32] **Soliman, A.M.**, 1997. Generation of current conveyor based all-pass filters from op-amp based circuits. *IEEE Transactions on Circuits and Systems-II: Analog and Digital Signal Processing,* **44 (4)**, 324–330.

[33] **Higashimura, M. and Fukui, Y.** 1990. Realization of current mode all-pass networks using a current conveyor. *IEEE Transactions on Circuits and Systems*, **37 (5)**, 660–661.

[34] **Senani, R.** 1978. Active simulation of inductors using current conveyor. *Electronics Letters*, **14 (15)**, 483–484.

[35] **Senani, R.** 1979. Novel active RC circuit for floating-inductor simulation. *Electronics Letters*, **15 (21)**, 679–680.

[36] **Senani, R.** 1980. New tunable synthetic floating inductors. *Electronics Letters*, **16 (10)**, 382–383.

[37] **PAL, K.** 1981. Novel floating inductance using current conveyors. *Electronics Letters*, **17 (18)**, 683.

[38] **PAL, K.** 1981. New inductance and capacitor floatation schemes using current conveyors. *Electronics Letters*, **17 (21),** 807–808.

[39] **Singh, V.** 1981. Active RC single-resistance-controlled lossless floating inductance simulation using single grounded capacitor. *Electronics Letters*, **17 (24),** 920–921.

[40] **Senani, R.** 1982. Novel lossless synthetic floating inductor employing a grounded capacitor. *Electronics Letters*, **18 (10),** 413.

[41] **Toumazou, C. and Lidgey, F.J.,** 1985. Floating-impedance convertors using current conveyors. *Electronics Letters*, 21 **(15),** 640–642.

[42] **Higashimura, M. and Fukui, Y.,** 1987. Novel method for realizing lossless floating immitance using current conveyors. *Electronics Letters*, 23 (10), 498–499.

[43] **Senani, R.** 1987. Generation of new two-amplifier synthetic floating inductors. *Electronics Letters*, **23 (22),** 1202–1203.

[44] **Khan, I.A., Ahmed, M.T. and Minhaj, N.,** 1992. Novel technique for immittance simulation realization of some all-active simulators. *International Journal of Electronics*, **72 (3)**, 431–441.

[45] **Hou, C.L., Wu, Y.P. and Lu, F.C.,** 1993. Synthetic methods for floating immitances of one-ports and *z* and *y* parameters of multiports using CCII-. *International Journal of Electronics*, **74 (4)**. 577–586.

[46] **Chang, C.M, Wang, H.Y and Chien, C.C,** 1994. Realization of series impedance functions using one CCII+. *International Journal of Electronics*, **76 (1)**, 83–85.

[47] **Hou, C.L., Chen, R.D., Wu, Y.P. and Hu, P.C.,** 1993. Realization of grounded and floating immitance function simulators using current conveyors. *International Journal of Electronics*, **74 (6)**, 917–923.

[48] **Kwan, T. and Martin, K.,** 1991. An adaptive analog continuous-time CMOS biquadratic filter. *IEEE J. Solid-State circuits*, **26 (6)**, 859–867.

[49] **Khan, I.A and Ahmed, M.T.,** 1987. Wide-rage electronically tunable multifunctional OTA-C filter for instrumentation applications. *IEEE Trans. Instrum. Meas*, **36 (1),** 13–17.

[50] **Sanchez-Sinencio, E., Geiger, R.L. and Nevarez-Lozano, H.,** 1988. Generation of continuous-time two integrator loop OTA filter structures. *IEEE Trans. Circuits Syst*, **35 (8)**, 936–946.

[51] **Vanpeteghem, P.M. and Song, R.,** 1989. Tuning strategies in high-frequency integrated continuous-time filters. *IEEE Trans. Circuits Syst*, **36 (1),** 136–139.

[52] **Zwan, E.J., Klumperink, E.A.M. and Seevinck, E.** 1991. A CMOS OTA for HF filters with programmable transfer function. *IEEE J. Solid-State Circuits*, **26 (11),** 1720–1723.

[53] **Tan, M.A. and Schaumann, R.** 1989. Simulating general-parameter LC-ladder filters for monolithic realizations with only Transconductance elements and grounded capacitors. *IEEE Trans. Circuits Syst*, **36 (2)**, 299–307.

[54] **Abuelma'atti, M.T., Khan, M.H. and Al-Zaher, H.A.** 1998. Simulation of active-only floating inductance. *Frequenz*, **52 (7-8)**, 161–164.

[55] **Fabre, A., Saaid, O., Wiest, F. and Boucheron, C.,** 1995. Current controlled bandpass filter based on translinear conveyors, *Electronics Letters*, **31 (20)**, 1727–1728.

[56] **Fabre, A., Saaid, O., Wiest, F. and Boucheron, C.,** 1996. High frequency applications based on a new current controlled conveyor. *IEEE Transactions on Circuits and Systems–I: Fundamental Theory and Applications*. **43 (2)**, 82–91.

[57] **Kiranon, W., Kerson, J. and Wardkein, P.,** 1996. Current controlled oscillator based on translinear conveyors. *Electronics Letters*, **32 (15)**, 1330–1331.

[58] **Kiranon, W., and Pawarangkoon, P.,** 1997. Floating inductance simulation based on current conveyors. *Electronics Letters*, **33 (21)**, 1748–1749.

[59] **Fabre, A., Saaid, O., Wiest, F. and Boucheron, C.,** 1998. High frequency high-Q BiCMOS current-mode bandpass filter and mobile communication application. *IEEE Journal of Solid-State Circuits*, **33 (4)**, 614–625.

[60] **Abuelma'atti, M.T. and Al-Qahtani, M.A.,** 1998. A current-mode current-controlled current-conveyor based analogue multiplier/divider. *International Journal of Electronics*, **85 (1),** 71–77.

[61] **Abuelma'atti, M.T., and Tasadduq, N.M.,** 1998. A novel single-input multiple-output current-mode current-controlled universal filter. *Microelectronics Journal*, **29**, 901–905.

[62] **Abuelma'atti, M.T., and Tasadduq, N.M.,** 1998. New current-mode current-controlled filters using the current-controlled conveyor. *International Journal of Electronics*, **85 (4),** 483–488.

[63] **Abuelma'atti, M.T., and Tasadduq, N.M.,** 1998. Universal current-controlled current-mode filter using the multiple-output translinear current conveyor. *Frequenz*, **52 (11-12),** 252–254.

[64] **Abuelma'atti, M.T. and Tasadduq, N.A.**, 1998. A novel current-controlled oscillator using translinear current conveyors. *Frequenz*, **52 (5-6)**, 123–124.

[65] **Abuelma'atti, M.T., and Tasadduq, N.M.,** 1999. Electronically tunable capacitance multiplier and frequency-dependent negative-resistance simulator using the current-controlled current conveyor. *Microelectronics Journal,* **30,** 869–873.

[66] **Minaei, S., and Türköz, S.,** 2000. New current-mode current-controlled universal filter implemented from single-output current controlled conveyors. *Frequenz*, **54 (5-6)**,138–140.

[67] **Türköz, S. and Minaei, S.,** 2000. A new current-controlled sinusoidal oscillator using the current controlled conveyor. *Frequenz*, **54, (5-6)**, 132–133.

[68] **Khan, I. and Maheshwari, S.** 2000. Simple first order all-pass section using a single CCII". *International Journal of Electronics*, **87 (3)**, 303–306.

[69] **Minaei, S., and Türköz, S.,** 2001. New current-mode current-controlled universal filter with single input and three outputs. *International Journal of Electronics,* **88 (3)**, 333–337.

[70] **Minaei, S., Çiçekoğlu, O., Kuntman, H., and Türköz,** S., 2001. High output impedance current-mode lowpass, bandpass and highpass filters using current controlled conveyors. *International Journal of Electronics*, **88 (8)**, 915–922.

[71] **Fabre, A.**, 1983. Dual translinear voltage/current convertor. *Electronics Letters*, **19 (24)**, 1030–1031.

[72] **Kardontchik, J.E,** 1992. Introduction to the design of transconductor capacitor filters. Boston, MA. Kluwer Academic.

[73] **Ashburn, P.,** 1988. Design and realization of bipolar transistors. New York: Wiley.

[74] **Frey, D.R.,** 1993. Log-domain filtering: An approach to current-mode filtering. *IEE Proceedings–G, Circuits, Devices and Systems,* **140 (6)**, 406–416.

[75] **Wilson, B.**, 1990. Current-mode circuits: analysis and CAD modeling. *IEEE International Symposium on Circuits and Systems*, New Orleans, May, 3242–3245.

[76] **Wilson, B.**, 1989. Performance analysis of current conveyors. *Electronics Letters,* **25**, 1596–1598.

[77] **Celma, S., Martinez, P.A and Carlosena, A.**, 1992. Minimal realization for single resistor controlled sinusoidal oscillator using single CCII. *Electronics Letters,* **25,** 443–444.

[78] **Martinez, P.A. and Celma, S.**, 1993. Design condition for sinusoidal oscillators using single CCII+. *International Journal of Electronics,* **75,** 87–90.

[79] **Fabre, A., Saaid, O., Barthelemy, H.**, 1995. On the frequency limitations of the circuits based on second generation current conveyors. *Analog Integrated Circuits and Signal Processing,* 7, 113–129.

[80] **Minaei, S., Çiçekoğlu, O., Kuntman, H., Türköz, S.**, 2001. New current-mode all-pass configuration using CCCIIs. *Accepted for presentation in 13th International Conference on Microelectronics (ICM 2001)*, October, Moroco.

[81] **Minaei, S., Çiçekoğlu, O., Kuntman, H., Türköz, S.**, 2001. First order current-mode all-pass filters using CCCIIs. *Proceedings of the International Symposium on Signals, Circuits and Systems (SCS 2001)*, July, Iasi, Romania, 417–420.

[82] **Abuelma'atti, M.T. and Almaskati, R.H.**, 1988. Two novel voltage (current) controlled integrable oscillators. *International Journal of Electronics,* **64 (4),** 611–615.

[83] **Filoramo, P., Giustolisi, G., Palmisano, G. and Palumbo, G.**, 2000. Approach to the design of low-voltage SC filters. *IEE Proc.-Circuits Devices Syst.*, **147 (3),** 196–200.

[84] **Cheng, M.C.H. and Toumazou, C.**, 1993. 3V MOS current conveyor cell for VLSI technology. *Electronics Letters,* **29,** 317–319.

[85] **Bruun, E.**, 1993. CMOS High Speed, High precision current conveyor and current feedback amplifier structures. *International Journal of Electronics,* **74,** 93–100.

[86] **Kaulberg, T.**, 1993. A CMOS current-mode operational amplifier. *IEEE Journal of Solid State Circuits,* **28,** 849-852.

[87] **Minaei, S.**, 2001. BiCMOS realization of the second-generation current controlled conveyor (CCCII) and its application. *Proceedings of the International Symposium on Signals, Circuits and Systems (SCS 2001)*, July, Iasi, Romania, 421–424.

[88] **Embabi S.H.K., Bellaouar A. and Elmasry M.I.**, 1993. Digital BiCMOS integrated circuit design. *Kluwer Academic Publishers.*

[89] **Türköz, S.**, 1981. İdeal olmayan tek kuvvetlendirici ile kurulan ikinci dereceden aktif filtreler, *Doktora Tezi*, İstanbul Teknik Üniversitesi.

APPENDIX A

1. SPICE Ideal Model of the CCCII+.

```
.SUBCKT ICCCIIP 1 5 3
RY 1 0 1E12
RZ 3 0 1E12
RX 5 2 260
VK 2 4 DC 0
E1 4 0 1 0 1
F1 3 0 VK 1
.ENDS ICCCIIP
```

2. SPICE Ideal Model of the CCCII–.

```
.SUBCKT ICCCIIN 1 5 3
RY 1 0 1E12
RZ 3 0 1E12
RX 5 2 260
VK 2 4 DC 0
E1 4 0 1 0 1
F1 3 0 VK -1
.ENDS ICCCIIN
```

3. SPICE Device Model of the CCCII+.

```
.SUBCKT CCCII 5 6 10 8 3 11
Q1 1 1 5 NR100N
Q15 1 2 3 PR100N
Q16 2 2 3 PR100N
Q17 4 4 3 PR100N
Q19 4 1 6 NR100N
Q20 7 7 8 NR100N
Q21 11 7 8 NR100N
Q22 7 9 6 PR100N
Q23 9 9 5 PR100N
Q24 9 12 8 NR100N
Q25 2 12 8 NR100N
Q26 10 12 8 NR100N
Q27 11 4 3 PR100N
Q28 3 10 12 NR100N
```

4. SPICE Device model of the CCCII–.

```
.SUBCKT CCCII- 5 6 10 8 3 13
Q1 1 1 5 NR100N
Q15 1 2 3 PR100N
Q16 2 2 3 PR100N
Q17 4 4 3 PR100N
Q19 4 1 6 NR100N
Q20 7 7 8 NR100N
Q21 112 7 8 NR100N
Q22 7 9 6 PR100N
Q23 9 9 5 PR100N
Q24 9 12 8 NR100N
Q25 2 12 8 NR100N
Q26 10 12 8 NR100N
Q27 11 4 3 PR100N
Q28 11 11 8 NR100N
Q29 13 11 8 NR100N
Q30 112 112 3 PR100N
Q31 13 112 3 PR100N
Q32 3 10 12 NR100N
.ENDS
```

5. SPICE Device Model of the BiCMOS CCCII+.

```
.SUBCKT CCCII 5 6 10 8 3 11
M1 1 1 5 5 MN W=500U L=2U
Q15 1 2 3 PNP
Q16 2 2 3 PNP
Q17 4 4 3 PNP
M19 4 1 6 6 MN W=500U L=2U
Q20 7 7 8 NPN
Q21 11 7 8 NPN
M22 7 9 6 6 MP W=500U L=2U
M23 9 9 5 5 MP W=500U L=2U
Q24 9 12 8 NPN
Q25 2 12 8 NPN
Q26 10 12 8 NPN
Q27 11 4 3 PNP
Q28 3 10 12 NPN
.ENDS CCCII
```

6. SPICE Device Model of the BiCMOS CCCII–.

```
.SUBCKT CCCII- 5 6 10 8 3 13
M1 1 1 5 5 MN W=500U L=2U
Q15 1 2 3 PR100N
Q16 2 2 3 PR100N
Q17 4 4 3 PR100N
M19 4 1 6 6 MN W=500U L=2U
```

```
Q20 7 7 8 NR100N
Q21 112 7 8 NR100N
M22 7 9 6 6 MP W=500U L=2U
M23 9 9 5 5 MP W=500U L=2U
Q24 9 12 8 NR100N
Q25 2 12 8 NR100N
Q26 10 12 8 NR100N
Q27 11 4 3 PR100N
Q28 11 11 8 NR100N
Q29 13 11 8 NR100N
Q30 112 112 3 PR100N
Q31 13 112 3 PR100N
Q32 3 10 12 NR100N
.ENDS
```

7. The Parameters of The PR100N and NR100N Bipolar Transistors

```
.MODEL PR100N PNP (IS=73.5E-018 BF=110 VAF=51.8 IKF=2.359E-3
+ISE=25.1E-16 NE=1.650 BR=0.4745 VAR=9.96 IKR=6.478E-3 RE=3 RB=327
+RBM=24.55 RC=50 CJE=0.180E-12 VJE=0.5 MJE=0.28 CJC=0.164E-12 VJC=0.8
+MJC=0.4 XCJC=0.037 CJS=1.03E-12 VJS=0.55 MJS=0.35 FC=0.5 TF=0.610E-9
+TR=0.610E-8 EG=1.206 XTB=1.866 XTI=1.7)

.MODEL NR100N NPN (IS=121E-018 BF=137.5 VAF=159.4 IKF=6.974E-3
+ISE=36E-16 NE=1.713 BR=0.7258 VAR=10.73 IKR=2.198E-3 RE=1 RB=524.6
+RBM=25 RC=50 CJE=0.214E-12 VJE=0.5 MJE=0.28 CJC=0.983E-13 VJC=0.5
+MJC=0.3 XCJC=0.034 CJS=0.913E-12 VJS=0.64 MJS=0.4 FC=0.5 TF=0.425E-9
+TR=0.425E-8 EG=1.206 XTB=1.538 XTI=2)
```

APPENDIX B

MATHCAD PROGRAM FOR CALCULATING THE EFFECTS OF THE CCCII NON-IDEALITIES ON RESONANT ANGULAR FREQUENCY AND QUALITY FACTOR OF THE BANDPASS-LOWPASS FILTER PROPOSED IN FIGURES 5.3 AND 5.10.

In MATHCAD program, $\omega_{k\alpha}$ and $\omega_{k\beta}$ are shown with wka and wkb, respectively.

1. The normalized resonant angular frequency and quality factor of the bandpass filter

Coefficients of the transfer function

$Qi := 1,2..20 \qquad wka := 10,20..200 \qquad wkb := 10,20..400$

$a0(wkb) := -wkb \qquad a1(wka,Qi) := -2\cdot Qi\cdot wka$

$b0(wka,wkb) := wka\cdot wkb$

$$b1(wka,wkb,Qi) := wka + wkb + \frac{wka\cdot wkb}{Qi}$$

$$b2(wka,wkb,Qi) := wka\cdot wkb + \frac{wka + wkb}{Qi} + 2\cdot Qi\cdot wka + 1$$

$$b3(wka,wkb,Qi) := wka + wkb + 2\cdot Qi + \frac{1}{Qi}$$

$A0(wkb) := a0(wkb)^2 \qquad A1(wka,Qi) := a1(wka,Qi)^2$

$B0(wka,wkb) := b0(wka,wkb)^2$

$B1(wka,wkb,Qi) := b1(wka,wkb,Qi)^2 - 2\cdot b0(wka,wkb)\cdot b2(wka,wkb,Qi)$

$B2(wka,wkb,Qi) := b2(wka,wkb,Qi)^2 + 2\cdot b0(wka,wkb) - 2b1(wka,wkb,Qi)\cdot b3(wka,wkb,Qi)$

$B3(wka,wkb,Qi) := b3(wka,wkb,Qi)^2 - 2\cdot b2(wka,wkb,Qi)$

Normalized resonant angular frequency

$$G(z) := \frac{A1z\cdot(z+A0)}{z^4 + B3\cdot z^3 + B2\cdot z^2 + B1\cdot z + B0}$$

$$\frac{d}{dz}G(z) \text{ simplify } \rightarrow -A1\cdot\frac{(2\cdot z^5 + B3\cdot z^4 - B1\cdot z^2 - 2\cdot z\cdot B0 + 3\cdot A0\cdot z^4 + 2\cdot A0\cdot B3\cdot z^3 + A0\cdot B2\cdot z^2 - A0\cdot B0)}{(z^4 + B3\cdot z^3 + B2\cdot z^2 + B1\cdot z + B0)^2}$$

$$v(wka, wkb, Qi) := \begin{pmatrix} -A0(wkb)\cdot B0(wka, wkb) \\ -2\cdot B0(wka, wkb) \\ -B1(wka, wkb, Qi) + A0(wkb)\cdot B2(wka, wkb, Qi) \\ 2\cdot A0(wkb)\cdot B3(wka, wkb, Qi) \\ 3\cdot A0(wkb) + B3(wka, wkb, Qi) \\ 2 \end{pmatrix}$$

$$r(wka, wkb, Qi) := \text{polyroots}(v(wka, wkb, Qi))$$

$$r(50, 90, 5) = \begin{pmatrix} -8.563\times 10^3 - 2.472i\times 10^3 \\ -8.563\times 10^3 + 2.472i\times 10^3 \\ -1.274\times 10^3 \\ -0.9 \\ 0.9 \end{pmatrix}$$

$$xo(wka, wkb, Qi) := \sqrt{r(wka, wkb, Qi)_4}$$

$$xo(50, 90, 5) = 0.949$$

Finding of the normalized resonant angular frequency from denominator polynomial of the bandpass transfer function ($\hat{x}'_o$ =xxo).

$$D(x, wka, wkb, Qi) := x^4 + b3(wka, wkb, Qi)\cdot x^3 + b2(wka, wkb, Qi)\cdot x^2 + b1(wka, wkb, Qi)\cdot x + b0(wka, wkb)$$

$$co(wka,wkb,Qi) := \begin{pmatrix} b0(wka,wkb) \\ b1(wka,wkb,Qi) \\ b2(wka,wkb,Qi) \\ b3(wka,wkb,Qi) \\ 1 \end{pmatrix}$$

$$ro(wka,wkb,Qi) := polyroots(co(wka,wkb,Qi))$$

$$ro(50,90,5) = \begin{pmatrix} -100.019 \\ -50 \\ -0.09 - 0.944i \\ -0.09 + 0.944i \end{pmatrix}$$

$$xxo(wka,wkb,Qi) := \sqrt{\left(ro(wka,wkb,Qi)_2 \cdot ro(wka,wkb,Qi)_3\right)}$$

$$xxo(50,90,5) = 0.949$$

Quality factor of the bandpass filter

$$Q(wka,wkb,Qi) := \frac{b0(wka,wkb) - xo(wka,wkb,Qi)^4}{xo(wka,wkb,Qi) \cdot \left(b1(wka,wkb,Qi) - b3(wka,wkb,Qi) \cdot xo(wka,wkb,Qi)^2\right)}$$

$$q(wka,wkb,Qi) := \frac{Q(wka,wkb,Qi)}{Qi}$$

2. The normalized cutoff angular frequency, quality factor damping factor and amplitude of the lowpass filter

Coefficients of The Transfer Function

$Qi := 1,2..20 \qquad wka := 10,20..200 \qquad wkb := 10,20..400$

$b0(wka,wkb) := wka \cdot wkb \qquad b1(wka,wkb,Qi) := wka + wkb + \dfrac{wka \cdot wkb}{Qi}$

$$b2(wka,wkb,Qi) := \frac{wka + wkb}{Qi} + 2 \cdot Qi \cdot wka + wka \cdot wkb + 1$$

$$b3(wka,wkb,Qi) := wka + wkb + 2 \cdot Qi + \frac{1}{Qi}$$

$a0(wka,wkb) := -wka \cdot wkb \qquad a1(wka) := -wka \qquad a2(wka,Qi) := -wka \cdot 2 \cdot Qi$

$$B0(wka,wkb) := b0(wka,wkb)^2$$

$$B1(wka,wkb,Qi) := b1(wka,wkb,Qi)^2 - 2 \cdot b2(wka,wkb,Qi) \cdot b0(wka,wkb)$$

$$B2(wka,wkb,Qi) := b2(wka,wkb,Qi)^2 + 2 \cdot b0(wka,wkb) - 2 \cdot b1(wka,wkb,Qi) \cdot b3(wka,wkb,Qi)$$

$$B3(wka,wkb,Qi) := b3(wka,wkb,Qi)^2 - 2 \cdot b2(wka,wkb,Qi)$$

$$A0(wka,wkb) := a0(wka,wkb)^2$$

$$A1(wka,wkb,Qi) := a1(wka)^2 - 2 \cdot a0(wka,wkb) \cdot a2(wka,Qi)$$

$$A2(wka,Qi) := a2(wka,Qi)^2$$

Amplitude of the transfer function

$j := \sqrt{-1}$

$$H(wka,wkb,Qi,x) := \frac{a2(wka,Qi) \cdot x^2 + a1(wka) \cdot x + a0(wka,wkb)}{x^4 + b3(wka,wkb,Qi) \cdot x^3 + b2(wka,wkb,Qi) \cdot x^2 + b1(wka,wkb,Qi) \cdot x + b0(wka,wkb)}$$

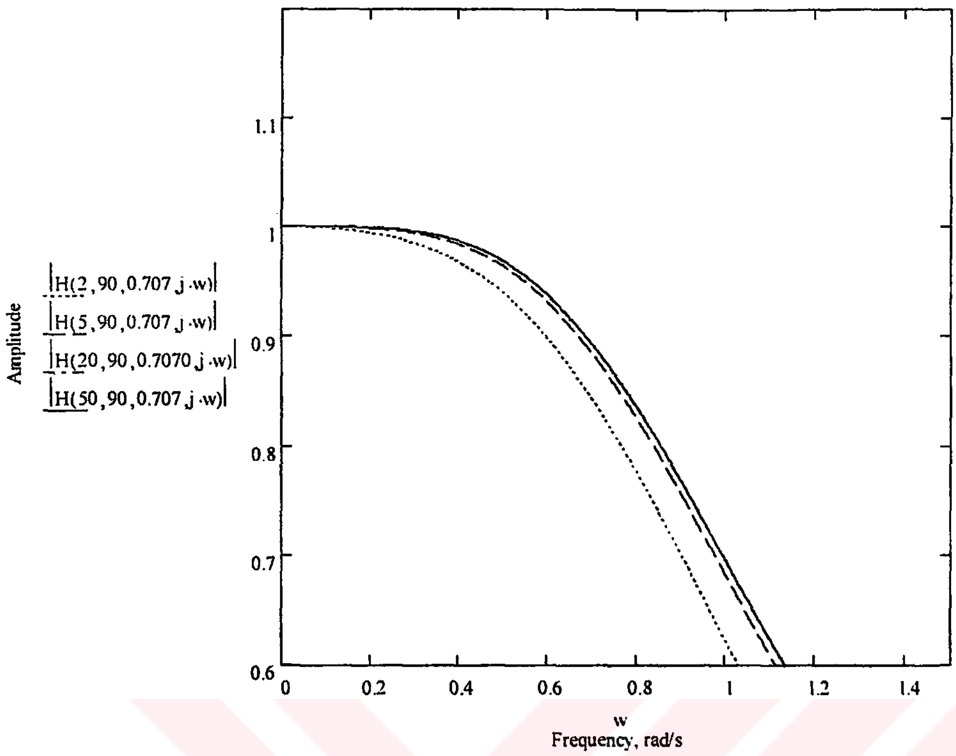

Figure B.1: Amplitude of the lowpass filter for different values of $\omega_{k\alpha}$ with $\omega_{k\beta}$=90

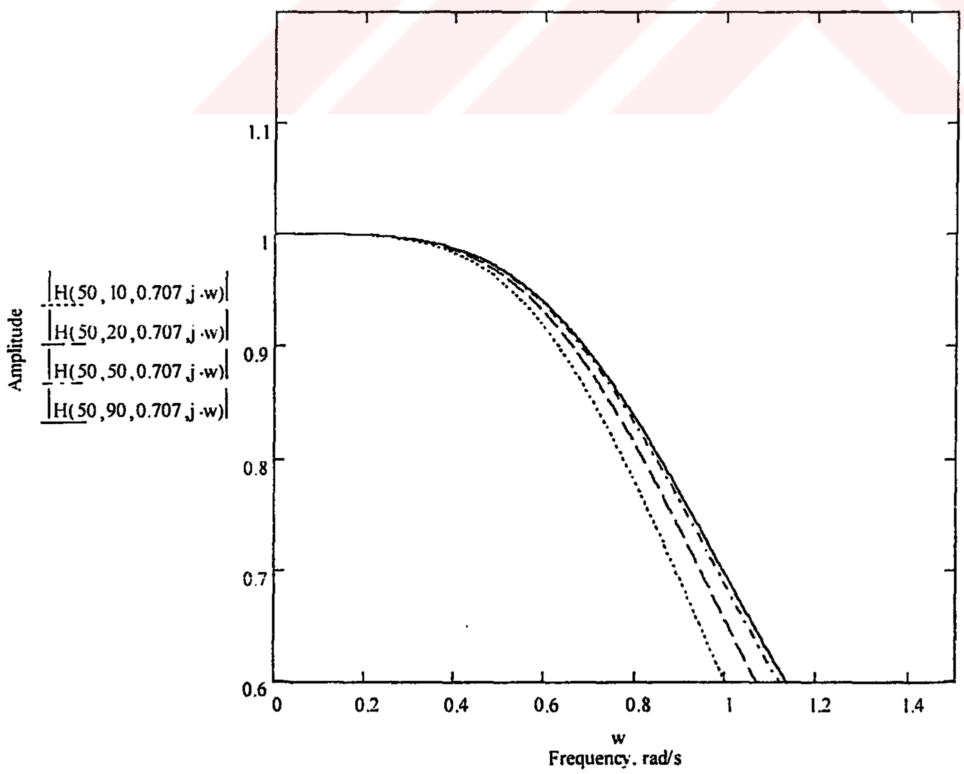

Figure B.2: Amplitude of the lowpass filter for different values of $\omega_{k\beta}$ with $\omega_{k\alpha}$=50

Normalized cutoff angular frequency

$$f(z) := A0\cdot z^4 + A0\cdot B3\cdot z^3 + (A0\cdot B2 - 2\cdot B0\cdot A2)\cdot z^2 + (A0 B1 - 2B0\cdot A1)\cdot z - A0\cdot B0$$

$$v(wka,wkb,Qi) := \begin{pmatrix} -A0(wka,wkb)\cdot B0(wka,wkb) \\ A0(wka,wkb)\cdot B1(wka,wkb,Qi) - 2\cdot B0(wka,wkb)\cdot A1(wka,wkb,Qi) \\ A0(wka,wkb)\cdot B2(wka,wkb,Qi) - 2\cdot B0(wka,wkb)\cdot A2(wka,Qi) \\ A0(wka,wkb)\, B3(wka,wkb,Qi) \\ A0(wka,wkb) \end{pmatrix}$$

$$r(wka,wkb,Qi) := \text{polyroots}(v(wka,wkb,Qi))$$

$$\sqrt{r(50,90,0.707)} = \begin{pmatrix} 91.446i \\ 49.982i \\ i \\ 0.984 \end{pmatrix}$$

$$xc(wka,wkb,Qi) := \sqrt{r(wka,wkb,Qi)_3}$$

$$xc(50,90,0.707) = 0.984$$

Finding of the normalized cutoff angular frequency from equation (5.61) ($\hat{x}_c$ = xcc).

$$K2(wka,wkb,Qi) := A0(wka,wkb)\cdot B2(wka,wkb,Qi) - 2\cdot B0(wka,wkb)\cdot A2(wka,Qi)$$

$$K1(wka,wkb,Qi) := A0(wka,wkb)\cdot B1(wka,wkb,Qi) - 2\cdot B0(wka,wkb)\cdot A1(wka,wkb,Qi)$$

$$K0(wka,wkb) := -A0(wka,wkb)\cdot B0(wka,wkb)$$

$$xcc(wka,wkb,Qi) := \left(\frac{-K1(wka,wkb,Qi) + \sqrt{K1(wka,wkb,Qi)^2 - 4\cdot K2(wka,wkb,Qi)\cdot K0(wka,wkb)}}{2\cdot K2(wka,wkb,Qi)}\right)^{0.5}$$

$$xcc(50,90,0.707) = 0.984$$

Quality factor and damping factor

$$Q(wka,wkb,Qi) := \frac{b0(wka,wkb) - xc(wka,wkb,Qi)^4}{xc(wka,wkb,Qi)\cdot\left(b1(wka,wkb,Qi) - b3(wka,wkb,Qi)\cdot xc(wka,wkb,Qi)^2\right)}$$

$$d(wka,wkb,Qi) := \frac{1}{2\cdot Q(wka,wkb,Qi)} \qquad dn(wka,wkb,Qi) := d(wka,wkb,Qi)\cdot\sqrt{2}$$

3. Stability of the Filter

First condition:

$$b2(wka,wkb,Qi)\cdot b3(wka,wkb,Qi) - b1(wka,wkb,Qi)\ \left|\begin{array}{l}\text{convert},\text{parfrac},Qi\\ \text{collect},Qi,wka,wkb\end{array}\right. \rightarrow$$

$$4\cdot Qi^2\cdot wka + \left(4\cdot wka\cdot wkb + 2\cdot wka^2 + 2\right)\cdot Qi + wka^2\cdot wkb + \left(wkb^2 + 4\right)\cdot wka + 2\cdot wkb +$$
$$+ \frac{\left(2\cdot wka\cdot wkb + wka^2 + wkb^2 + 1\right)}{Qi} + \frac{(wka + wkb)}{Qi^2}$$

which all of are positive.

Second condition

Multiplying the second condition by the following term, which is always positive:

$$b2(wka,wkb,Qi)\cdot b3(wka,wkb,Qi) - b1(wka,wkb,Qi)$$

The second condition is investigated as:

$$b1(wka,wkb,Qi)\cdot(b2(wka,wkb,Qi)\cdot b3(wka,wkb,Qi) - b1(wka,wkb,Qi)) - b0(wka,wkb)\cdot b3(wka,wkb,Qi)^2 \ \text{collect},Qi,wka,wkb \rightarrow$$

$$4\cdot wka^2\cdot Qi^2 + \left(2\cdot wka^3 + 6\cdot wka^2\cdot wkb + 2\cdot wka + 2\cdot wkb\right)\cdot Qi + 2\cdot wkb\cdot wka^3 + \left(4\cdot wkb^2 + 4\right)\cdot wka^2 +$$
$$+ 4\cdot wka\cdot wkb + 2\cdot wkb^2 + \frac{\left[\left(1 + wkb^2\right)\cdot wka^3 + \left(wkb^3 + 5\cdot wkb\right)\cdot wka^2 + \left(3\cdot wkb^2 + 1\right)\cdot wka + wkb^3 + wkb\right]}{Qi} +$$
$$+ \frac{\left[wkb\cdot wka^3 + \left(2\cdot wkb^2 + 1\right)\cdot wka^2 + \left(wkb^3 + 2\cdot wkb\right)\cdot wka + wkb^2\right]}{Qi^2} + \frac{\left(wka^2\cdot wkb + wkb^2\cdot wka\right)}{Qi^3}$$

which all of are positive. Therefore the filter is unconditionally stable.

APPENDIX C

Effects of CCCII non-idealities on normalized resonant angular frequency, quality factor and their sensitivities in the bandpass filter proposed in Figure 5.3.

Table C.1: The different values of normalized resonant angular frequency $\hat{x}_o(\omega_{k\alpha}, \omega_{k\beta}, Q_i)$ by changing $\omega_{k\alpha}$ and $\omega_{k\beta}$ for bandpass filter

$\omega_{k\beta}$	$\hat{x}_o(200, \omega_{k\beta}, 5)$	$\hat{x}_o(100, \omega_{k\beta}, 5)$	$\hat{x}_o(50, \omega_{k\beta}, 5)$	$\hat{x}_o(10, \omega_{k\beta}, 5)$	$\hat{x}_o(5, \omega_{k\beta}, 5)$	$\hat{x}_o(2, \omega_{k\beta}, 5)$
10	0.706	0.706	0.706	0.706	0.706	0.705
20	0.816	0.816	0.816	0.816	0.816	0.815
30	0.866	0.866	0.866	0.866	0.865	0.864
40	0.894	0.894	0.894	0.894	0.894	0.893
50	0.913	0.913	0.913	0.913	0.912	0.911
60	0.926	0.926	0.926	0.926	0.925	0.924
70	0.935	0.935	0.935	0.935	0.935	0.934
80	0.943	0.943	0.943	0.943	0.942	0.941
90	0.949	0.949	0.949	0.949	0.948	0.947
100	0.953	0.953	0.953	0.953	0.953	0.952
110	0.957	0.957	0.957	0.957	0.957	0.956
120	0.961	0.961	0.961	0.961	0.96	0.959
130	0.964	0.964	0.964	0.963	0.963	0.962
140	0.966	0.966	0.966	0.966	0.966	0.964
150	0.968	0.968	0.968	0.968	0.968	0.966
160	0.97	0.97	0.97	0.97	0.97	0.968
170	0.972	0.972	0.972	0.972	0.971	0.97
180	0.973	0.973	0.973	0.973	0.973	0.972
190	0.975	0.975	0.975	0.975	0.974	0.973
200	0.976	0.976	0.976	0.976	0.976	0.974
210	0.977	0.977	0.977	0.977	0.977	0.975
220	0.978	0.978	0.978	0.978	0.978	0.976
230	0.979	0.979	0.979	0.979	0.979	0.977
240	0.98	0.98	0.98	0.98	0.979	0.978
250	0.981	0.981	0.981	0.98	0.98	0.979
260	0.981	0.981	0.981	0.981	0.981	0.979
270	0.982	0.982	0.982	0.982	0.982	0.98
280	0.983	0.983	0.983	0.983	0.982	0.981
290	0.983	0.983	0.983	0.983	0.983	0.981
300	0.984	0.984	0.984	0.984	0.983	0.982
310	0.984	0.984	0.984	0.984	0.984	0.982
320	0.985	0.985	0.985	0.985	0.984	0.983
330	0.985	0.985	0.985	0.985	0.985	0.983
340	0.986	0.986	0.986	0.986	0.985	0.984
350	0.986	0.986	0.986	0.986	0.986	0.984
360	0.986	0.986	0.986	0.986	0.986	0.985
370	0.987	0.987	0.987	0.987	0.986	0.985
380	0.987	0.987	0.987	0.987	0.987	0.985
390	0.987	0.987	0.987	0.987	0.987	0.986
400	0.988	0.988	0.988	0.988	0.987	0.986

Table C.2: The different values normalized resonant angular frequency ($\hat{x}_o$) by changing $\omega_{k\beta}$ and Q_i with $\omega_{k\alpha}$ =50 for bandpass filter

$\omega_{k\beta}$	$\hat{x}_o(50, \omega_{k\beta}, 1)$	$\hat{x}_o(50, \omega_{k\beta}, 2)$	$\hat{x}_o(50, \omega_{k\beta}, 5)$	$\hat{x}_o(50, \omega_{k\beta}, 10)$	$\hat{x}_o(50, \omega_{k\beta}, 20)$
10	0.907	0.842	0.706	0.577	0.447
20	0.952	0.911	0.816	0.707	0.577
30	0.967	0.939	0.866	0.774	0.655
40	0.975	0.953	0.894	0.816	0.707
50	0.98	0.962	0.913	0.845	0.745
60	0.983	0.968	0.926	0.866	0.775
70	0.986	0.972	0.935	0.882	0.798
80	0.987	0.976	0.943	0.894	0.816
90	0.989	0.978	0.949	0.904	0.832
100	0.99	0.98	0.953	0.913	0.845
110	0.991	0.982	0.957	0.92	0.856
120	0.992	0.984	0.961	0.926	0.866
130	0.992	0.985	0.964	0.931	0.874
140	0.993	0.986	0.966	0.935	0.882
150	0.993	0.987	0.968	0.939	0.889
160	0.994	0.988	0.97	0.943	0.894
170	0.994	0.988	0.972	0.946	0.9
180	0.994	0.989	0.973	0.949	0.905
190	0.995	0.99	0.975	0.951	0.909
200	0.995	0.99	0.976	0.953	0.913
210	0.995	0.991	0.977	0.956	0.917
220	0.995	0.991	0.978	0.957	0.92
230	0.996	0.991	0.979	0.959	0.923
240	0.996	0.992	0.98	0.961	0.926
250	0.996	0.992	0.981	0.962	0.928
260	0.996	0.992	0.981	0.964	0.931
270	0.996	0.993	0.982	0.965	0.933
280	0.996	0.993	0.983	0.966	0.935
290	0.996	0.993	0.983	0.967	0.937
300	0.997	0.993	0.984	0.968	0.939
310	0.997	0.994	0.984	0.969	0.941
320	0.997	0.994	0.985	0.97	0.943
330	0.997	0.994	0.985	0.971	0.944
340	0.997	0.994	0.986	0.972	0.946
350	0.997	0.994	0.986	0.973	0.947
360	0.997	0.994	0.986	0.973	0.949
370	0.997	0.995	0.987	0.974	0.95
380	0.997	0.995	0.987	0.975	0.951
390	0.997	0.995	0.987	0.975	0.952
400	0.997	0.995	0.988	0.976	0.953

Table C.3: The different values of normalized resonant angular frequency ($\hat{x}'_o$) by changing $\omega_{k\beta}$ and Q_i with $\omega_{k\alpha}$ =50 for bandpass filter

$\omega_{k\beta}$	$\hat{x}_o(50, \omega_{k\beta}, 1)$	$\hat{x}_o(50, \omega_{k\beta}, 2)$	$\hat{x}_o(50, \omega_{k\beta}, 5)$	$\hat{x}_o(50, \omega_{k\beta}, 10)$	$\hat{x}_o(50, \omega_{k\beta}, 20)$
10	0.907	0.841	0.706	0.577	0.447
20	0.952	0.911	0.816	0.707	0.577
30	0.967	0.939	0.866	0.774	0.655
40	0.975	0.953	0.894	0.816	0.707
50	0.98	0.962	0.913	0.845	0.745
60	0.983	0.968	0.926	0.866	0.775
70	0.986	0.972	0.935	0.882	0.798
80	0.988	0.976	0.943	0.894	0.816
90	0.989	0.978	0.949	0.904	0.832
100	0.99	0.98	0.953	0.913	0.845
110	0.991	0.982	0.957	0.92	0.856
120	0.992	0.984	0.961	0.926	0.866
130	0.992	0.985	0.964	0.931	0.874
140	0.993	0.986	0.966	0.935	0.882
150	0.993	0.987	0.968	0.939	0.889
160	0.994	0.988	0.97	0.943	0.894
170	0.994	0.988	0.972	0.946	0.9
180	0.994	0.989	0.973	0.949	0.905
190	0.995	0.99	0.975	0.951	0.909
200	0.995	0.99	0.976	0.953	0.913
210	0.995	0.991	0.977	0.956	0.917
220	0.995	0.991	0.978	0.957	0.92
230	0.996	0.991	0.979	0.959	0.923
240	0.996	0.992	0.98	0.961	0.926
250	0.996	0.992	0.981	0.962	0.928
260	0.996	0.992	0.981	0.964	0.931
270	0.996	0.993	0.982	0.965	0.933
280	0.996	0.993	0.983	0.966	0.935
290	0.997	0.993	0.983	0.967	0.937
300	0.997	0.993	0.984	0.968	0.939
310	0.997	0.994	0.984	0.969	0.941
320	0.997	0.994	0.985	0.97	0.943
330	0.997	0.994	0.985	0.971	0.944
340	0.997	0.994	0.986	0.972	0.946
350	0.997	0.994	0.986	0.973	0.947
360	0.997	0.994	0.986	0.973	0.949
370	0.997	0.995	0.987	0.974	0.95
380	0.997	0.995	0.987	0.975	0.951
390	0.997	0.995	0.987	0.975	0.952
400	0.998	0.995	0.988	0.976	0.953

Table C.4: The different values of normalized quality factor ($q(\omega_{k\alpha}, \omega_{k\beta}, Q_l)$) by changing $\omega_{k\alpha}$ and $\omega_{k\beta}$ with Q_l=5 for bandpass filter

$\omega_{k\beta}$	$q(200, \omega_{k\beta}, 5)$	$q(100, \omega_{k\beta}, 5)$	$q(50, \omega_{k\beta}, 5)$	$q(10, \omega_{k\beta}, 5)$	$q(5, \omega_{k\beta}, 5)$	$q(2, \omega_{k\beta}, 5)$
10	1.133	1.133	1.133	1.133	1.133	1.129
20	1.131	1.131	1.131	1.131	1.131	1.126
30	1.109	1.109	1.109	1.109	1.109	1.103
40	1.091	1.091	1.091	1.091	1.091	1.085
50	1.078	1.078	1.078	1.078	1.077	1.071
60	1.068	1.068	1.068	1.068	1.067	1.061
70	1.06	1.06	1.06	1.06	1.059	1.053
80	1.053	1.053	1.053	1.053	1.053	1.046
90	1.048	1.048	1.048	1.048	1.048	1.041
100	1.044	1.044	1.044	1.044	1.044	1.037
110	1.041	1.041	1.041	1.041	1.04	1.033
120	1.038	1.038	1.038	1.038	1.037	1.03
130	1.035	1.035	1.035	1.035	1.035	1.028
140	1.033	1.033	1.033	1.033	1.032	1.025
150	1.031	1.031	1.031	1.031	1.03	1.023
160	1.029	1.029	1.029	1.029	1.029	1.022
170	1.027	1.027	1.027	1.027	1.027	1.02
180	1.026	1.026	1.026	1.026	1.026	1.018
190	1.025	1.025	1.025	1.025	1.024	1.017
200	1.023	1.023	1.024	1.023	1.023	1.016
210	1.022	1.022	1.022	1.022	1.022	1.015
220	1.021	1.021	1.021	1.021	1.021	1.014
230	1.021	1.021	1.021	1.021	1.02	1.013
240	1.02	1.02	1.02	1.02	1.019	1.012
250	1.019	1.019	1.019	1.019	1.019	1.011
260	1.018	1.018	1.018	1.018	1.018	1.011
270	1.018	1.018	1.018	1.018	1.017	1.01
280	1.017	1.017	1.017	1.017	1.017	1.009
290	1.017	1.017	1.017	1.017	1.016	1.009
300	1.016	1.016	1.016	1.016	1.016	1.008
310	1.015	1.015	1.016	1.015	1.015	1.008
320	1.015	1.015	1.015	1.015	1.015	1.007
330	1.015	1.015	1.015	1.015	1.014	1.007
340	1.014	1.014	1.014	1.014	1.014	1.007
350	1.014	1.014	1.014	1.014	1.013	1.006
360	1.013	1.013	1.013	1.013	1.013	1.006
370	1.013	1.013	1.013	1.013	1.013	1.005
380	1.013	1.013	1.013	1.013	1.012	1.005
390	1.012	1.012	1.012	1.012	1.012	1.005
400	1.012	1.012	1.012	1.012	1.012	1.004

Table C.5: The different values of the normalized quality factor (q) by changing $\omega_{k\beta}$ and Q_i with $\omega_{k\alpha}$=50 for bandpass filter

$\omega_{k\beta}$	$q(50, \omega_{k\beta}, 1)$	$q(50, \omega_{k\beta}, 2)$	$q(50, \omega_{k\beta}, 5)$	$q(50, \omega_{k\beta}, 10)$	$q(50, \omega_{k\beta}, 20)$
10	1.083	1.123	1.133	1.04	0.86
20	1.046	1.079	1.131	1.132	1.039
30	1.032	1.057	1.109	1.139	1.106
40	1.024	1.045	1.091	1.131	1.131
50	1.019	1.036	1.078	1.119	1.139
60	1.016	1.031	1.068	1.109	1.139
70	1.014	1.027	1.06	1.099	1.136
80	1.012	1.024	1.053	1.091	1.131
90	1.011	1.021	1.048	1.084	1.125
100	1.01	1.019	1.044	1.078	1.119
110	1.009	1.017	1.041	1.072	1.114
120	1.008	1.016	1.038	1.067	1.109
130	1.008	1.015	1.035	1.063	1.104
140	1.007	1.014	1.033	1.06	1.099
150	1.007	1.013	1.031	1.056	1.095
160	1.006	1.012	1.029	1.053	1.091
170	1.006	1.011	1.027	1.051	1.087
180	1.006	1.011	1.026	1.048	1.084
190	1.005	1.01	1.025	1.046	1.08
200	1.005	1.01	1.024	1.044	1.078
210	1.005	1.009	1.022	1.042	1.075
220	1.005	1.009	1.021	1.041	1.072
230	1.004	1.009	1.021	1.039	1.07
240	1.004	1.008	1.02	1.038	1.067
250	1.004	1.008	1.019	1.036	1.065
260	1.004	1.008	1.018	1.035	1.063
270	1.004	1.007	1.018	1.034	1.061
280	1.004	1.007	1.017	1.033	1.06
290	1.004	1.007	1.017	1.032	1.058
300	1.003	1.007	1.016	1.031	1.056
310	1.003	1.006	1.016	1.03	1.055
320	1.003	1.006	1.015	1.029	1.053
330	1.003	1.006	1.015	1.028	1.052
340	1.003	1.006	1.014	1.027	1.051
350	1.003	1.006	1.014	1.027	1.049
360	1.003	1.006	1.013	1.026	1.048
370	1.003	1.005	1.013	1.025	1.047
380	1.003	1.005	1.013	1.025	1.046
390	1.003	1.005	1.012	1.024	1.045
400	1.003	1.005	1.012	1.023	1.044

Table C.6: The sensitivity values of $\hat{x}_o(\omega_{k\alpha},\omega_{k\beta},Q_i)$ with respect to $\omega_{k\alpha}$. in bandpass filter for different values of $\omega_{k\alpha}$ and $\omega_{k\beta}$ with Q_i=5

$\omega_{k\beta}$	$S^{\hat{x}_o}_{\omega_{k\alpha}}(200,\omega_{k\beta},5)$	$S^{\hat{x}_o}_{\omega_{k\alpha}}(100,\omega_{k\beta},5)$	$S^{\hat{x}_o}_{\omega_{k\alpha}}(50,\omega_{k\beta},5)$	$S^{\hat{x}_o}_{\omega_{k\alpha}}(10,\omega_{k\beta},5)$	$S^{\hat{x}_o}_{\omega_{k\alpha}}(5,\omega_{k\beta},5)$
10	$1.941\cdot10^{-7}$	$7.766\cdot10^{-7}$	$3.105\cdot10^{-6}$	$7.688\cdot10^{-5}$	$2.985\cdot10^{-4}$
20	$2.599\cdot10^{-7}$	$1.04\cdot10^{-6}$	$4.158\cdot10^{-6}$	$1.026\cdot10^{-4}$	$3.944\cdot10^{-4}$
30	$3.048\cdot10^{-7}$	$1.218\cdot10^{-6}$	$4.87\cdot10^{-6}$	$1.2\cdot10^{-4}$	$4.59\cdot10^{-4}$
40	$3.248\cdot10^{-7}$	$1.311\cdot10^{-6}$	$5.448\cdot10^{-6}$	$1.321\cdot10^{-4}$	$5.039\cdot10^{-4}$
50	$3.516\cdot10^{-7}$	$1.418\cdot10^{-6}$	$5.892\cdot10^{-6}$	$1.41\cdot10^{-4}$	$5.367\cdot10^{-4}$
60	$3.706\cdot10^{-7}$	$1.497\cdot10^{-6}$	$6.222\cdot10^{-6}$	$1.478\cdot10^{-4}$	$5.616\cdot10^{-4}$
70	$3.858\cdot10^{-7}$	$1.558\cdot10^{-6}$	$6.476\cdot10^{-6}$	$1.53\cdot10^{-4}$	$5.811\cdot10^{-4}$
80	$3.978\cdot10^{-7}$	$1.607\cdot10^{-6}$	$6.402\cdot10^{-6}$	$1.573\cdot10^{-4}$	$5.967\cdot10^{-4}$
90	$4.078\cdot10^{-7}$	$1.646\cdot10^{-6}$	$6.545\cdot10^{-6}$	$1.608\cdot10^{-4}$	$6.095\cdot10^{-4}$
100	$4.157\cdot10^{-7}$	$1.679\cdot10^{-6}$	$6.665\cdot10^{-6}$	$1.637\cdot10^{-4}$	$6.203\cdot10^{-4}$
110	$4.226\cdot10^{-7}$	$1.706\cdot10^{-6}$	$6.766\cdot10^{-6}$	$1.662\cdot10^{-4}$	$6.293\cdot10^{-4}$
120	$4.28\cdot10^{-7}$	$1.729\cdot10^{-6}$	$6.854\cdot10^{-6}$	$1.683\cdot10^{-4}$	$6.371\cdot10^{-4}$
130	$4.337\cdot10^{-7}$	$1.75\cdot10^{-6}$	$6.929\cdot10^{-6}$	$1.701\cdot10^{-4}$	$6.439\cdot10^{-4}$
140	$4.376\cdot10^{-7}$	$1.767\cdot10^{-6}$	$6.996\cdot10^{-6}$	$1.717\cdot10^{-4}$	$6.498\cdot10^{-4}$
150	$4.408\cdot10^{-7}$	$1.783\cdot10^{-6}$	$7.054\cdot10^{-6}$	$1.732\cdot10^{-4}$	$6.55\cdot10^{-4}$
160	$4.45\cdot10^{-7}$	$1.797\cdot10^{-6}$	$7.106\cdot10^{-6}$	$1.744\cdot10^{-4}$	$6.597\cdot10^{-4}$
170	$4.481\cdot10^{-7}$	$1.809\cdot10^{-6}$	$7.153\cdot10^{-6}$	$1.756\cdot10^{-4}$	$6.638\cdot10^{-4}$
180	$4.508\cdot10^{-7}$	$1.82\cdot10^{-6}$	$7.195\cdot10^{-6}$	$1.766\cdot10^{-4}$	$6.675\cdot10^{-4}$
190	$4.529\cdot10^{-7}$	$1.83\cdot10^{-6}$	$7.233\cdot10^{-6}$	$1.775\cdot10^{-4}$	$6.709\cdot10^{-4}$
200	$4.555\cdot10^{-7}$	$1.839\cdot10^{-6}$	$7.267\cdot10^{-6}$	$1.783\cdot10^{-4}$	$6.74\cdot10^{-4}$
210	$4.575\cdot10^{-7}$	$1.847\cdot10^{-6}$	$7.299\cdot10^{-6}$	$1.791\cdot10^{-4}$	$6.768\cdot10^{-4}$
220	$4.593\cdot10^{-7}$	$1.855\cdot10^{-6}$	$7.328\cdot10^{-6}$	$1.798\cdot10^{-4}$	$6.794\cdot10^{-4}$
230	$4.611\cdot10^{-7}$	$1.862\cdot10^{-6}$	$7.354\cdot10^{-6}$	$1.805\cdot10^{-4}$	$6.818\cdot10^{-4}$
240	$4.623\cdot10^{-7}$	$1.868\cdot10^{-6}$	$7.379\cdot10^{-6}$	$1.811\cdot10^{-4}$	$6.84\cdot10^{-4}$
250	$4.642\cdot10^{-7}$	$1.874\cdot10^{-6}$	$7.402\cdot10^{-6}$	$1.816\cdot10^{-4}$	$6.86\cdot10^{-4}$
260	$4.655\cdot10^{-7}$	$1.88\cdot10^{-6}$	$7.423\cdot10^{-6}$	$1.821\cdot10^{-4}$	$6.879\cdot10^{-4}$
270	$4.667\cdot10^{-7}$	$1.885\cdot10^{-6}$	$7.442\cdot10^{-6}$	$1.826\cdot10^{-4}$	$6.896\cdot10^{-4}$
280	$4.678\cdot10^{-7}$	$1.89\cdot10^{-6}$	$7.461\cdot10^{-6}$	$1.83\cdot10^{-4}$	$6.912\cdot10^{-4}$
290	$4.691\cdot10^{-7}$	$1.894\cdot10^{-6}$	$7.478\cdot10^{-6}$	$1.835\cdot10^{-4}$	$6.928\cdot10^{-4}$
300	$4.702\cdot10^{-7}$	$1.898\cdot10^{-6}$	$7.494\cdot10^{-6}$	$1.839\cdot10^{-4}$	$6.942\cdot10^{-4}$
310	$4.711\cdot10^{-7}$	$1.902\cdot10^{-6}$	$7.509\cdot10^{-6}$	$1.842\cdot10^{-4}$	$6.955\cdot10^{-4}$
320	$4.715\cdot10^{-7}$	$1.906\cdot10^{-6}$	$7.523\cdot10^{-6}$	$1.846\cdot10^{-4}$	$6.968\cdot10^{-4}$
330	$4.726\cdot10^{-7}$	$1.909\cdot10^{-6}$	$7.537\cdot10^{-6}$	$1.849\cdot10^{-4}$	$6.98\cdot10^{-4}$
340	$4.733\cdot10^{-7}$	$1.913\cdot10^{-6}$	$7.549\cdot10^{-6}$	$1.852\cdot10^{-4}$	$6.991\cdot10^{-4}$
350	$4.738\cdot10^{-7}$	$1.916\cdot10^{-6}$	$7.562\cdot10^{-6}$	$1.855\cdot10^{-4}$	$7.002\cdot10^{-4}$
360	$4.748\cdot10^{-7}$	$1.919\cdot10^{-6}$	$7.573\cdot10^{-6}$	$1.858\cdot10^{-4}$	$7.012\cdot10^{-4}$
370	$4.759\cdot10^{-7}$	$1.922\cdot10^{-6}$	$7.584\cdot10^{-6}$	$1.86\cdot10^{-4}$	$7.022\cdot10^{-4}$
380	$4.764\cdot10^{-7}$	$1.924\cdot10^{-6}$	$7.594\cdot10^{-6}$	$1.863\cdot10^{-4}$	$7.031\cdot10^{-4}$
390	$4.772\cdot10^{-7}$	$1.927\cdot10^{-6}$	$7.604\cdot10^{-6}$	$1.865\cdot10^{-4}$	$7.04\cdot10^{-4}$
400	$4.775\cdot10^{-7}$	$1.929\cdot10^{-6}$	$7.613\cdot10^{-6}$	$1.867\cdot10^{-4}$	$7.048\cdot10^{-4}$

Table C.7: The sensitivity values of $\hat{x}_o(\omega_{k\alpha}, \omega_{k\beta}, Q_i)$ with respect to $\omega_{k\beta}$ in bandpass filter for different values of $\omega_{k\alpha}$ and $\omega_{k\beta}$ with Q_i=5

$\omega_{k\beta}$	$S^{\hat{x}_o}_{\omega_{k\beta}}(200, \omega_{k\beta}, 5)$	$S^{\hat{x}_o}_{\omega_{k\beta}}(100, \omega_{k\beta}, 5)$	$S^{\hat{x}_o}_{\omega_{k\beta}}(50, \omega_{k\beta}, 5)$	$S^{\hat{x}_o}_{\omega_{k\beta}}(10, \omega_{k\beta}, 5)$	$S^{\hat{x}_o}_{\omega_{k\beta}}(5, \omega_{k\beta}, 5)$
10	0.252	0.252	0.252	0.251	0.251
20	0.168	0.168	0.168	0.168	0.168
30	0.126	0.126	0.126	0.126	0.126
40	0.101	0.101	0.101	0.101	0.1
50	0.084	0.084	0.084	0.084	0.084
60	0.072	0.072	0.072	0.072	0.072
70	0.063	0.063	0.063	0.063	0.063
80	0.056	0.056	0.056	0.056	0.056
90	0.05	0.05	0.05	0.05	0.05
100	0.046	0.046	0.046	0.046	0.046
110	0.042	0.042	0.042	0.042	0.042
120	0.039	0.039	0.039	0.039	0.039
130	0.036	0.036	0.036	0.036	0.036
140	0.033	0.033	0.033	0.033	0.033
150	0.031	0.031	0.031	0.031	0.031
160	0.029	0.029	0.029	0.029	0.029
170	0.028	0.028	0.028	0.028	0.028
180	0.026	0.026	0.026	0.026	0.026
190	0.025	0.025	0.025	0.025	0.025
200	0.024	0.024	0.024	0.024	0.024
210	0.023	0.023	0.023	0.023	0.023
220	0.022	0.022	0.022	0.022	0.022
230	0.021	0.021	0.021	0.021	0.021
240	0.02	0.02	0.02	0.02	0.02
250	0.019	0.019	0.019	0.019	0.019
260	0.019	0.019	0.019	0.019	0.019
270	0.018	0.018	0.018	0.018	0.018
280	0.017	0.017	0.017	0.017	0.017
290	0.017	0.017	0.017	0.017	0.017
300	0.016	0.016	0.016	0.016	0.016
310	0.016	0.016	0.016	0.016	0.016
320	0.015	0.015	0.015	0.015	0.015
330	0.015	0.015	0.015	0.015	0.015
340	0.014	0.014	0.014	0.014	0.014
350	0.014	0.014	0.014	0.014	0.014
360	0.014	0.014	0.014	0.014	0.014
370	0.013	0.013	0.013	0.013	0.013
380	0.013	0.013	0.013	0.013	0.013
390	0.013	0.013	0.013	0.013	0.012
400	0.012	0.012	0.012	0.012	0.012

Table C.8: The sensitivity values of $\hat{x}_o(\omega_{k\alpha}, \omega_{k\beta}, Q_i)$ with respect to $\omega_{k\beta}$ in bandpass filter for different values of $\omega_{k\beta}$ and Q_i with $\omega_{k\alpha}$=50

$\omega_{k\beta}$	$S^{\hat{x}_o}_{\omega_{k\beta}}(50, \omega_{k\beta}, 1)$	$S^{\hat{x}_o}_{\omega_{k\beta}}(50, \omega_{k\beta}, 2)$	$S^{\hat{x}_o}_{\omega_{k\beta}}(50, \omega_{k\beta}, 5)$	$S^{\hat{x}_o}_{\omega_{k\beta}}(50, \omega_{k\beta}, 10)$	$S^{\hat{x}_o}_{\omega_{k\beta}}(50, \omega_{k\beta}, 20)$
10	0.093	0.148	0.252	0.334	0.4
20	0.049	0.086	0.188	0.25	0.333
30	0.033	0.06	0.126	0.2	0.286
40	0.025	0.046	0.101	0.167	0.25
50	0.02	0.038	0.084	0.143	0.222
60	0.017	0.032	0.072	0.125	0.2
70	0.014	0.027	0.063	0.111	0.182
80	0.012	0.024	0.056	0.1	0.167
90	0.011	0.021	0.05	0.091	0.154
100	$9.986\cdot 10^{-3}$	0.019	0.046	0.083	0.143
110	$9.08\cdot 10^{-3}$	0.018	0.042	0.077	0.133
120	$8.324\cdot 10^{-3}$	0.016	0.039	0.072	0.125
130	$7.685\cdot 10^{-3}$	0.015	0.036	0.067	0.118
140	$7.136\cdot 10^{-3}$	0.014	0.033	0.063	0.111
150	$6.661\cdot 10^{-3}$	0.013	0.031	0.059	0.105
160	$6.245\cdot 10^{-3}$	0.012	0.029	0.056	0.1
170	$5.878\cdot 10^{-3}$	0.012	0.028	0.053	0.095
180	$5.552\cdot 10^{-1}$	0.011	0.026	0.05	0.091
190	$5.26\cdot 10^{-3}$	0.01	0.025	0.048	0.087
200	$4.997\cdot 10^{-3}$	$9.849\cdot 10^{-3}$	0.024	0.045	0.083
210	$4.759\cdot 10^{-3}$	$9.387\cdot 10^{-3}$	0.023	0.044	0.08
220	$4.543\cdot 10^{-3}$	$8.966\cdot 10^{-3}$	0.022	0.042	0.077
230	$4.345\cdot 10^{-3}$	$8.582\cdot 10^{-3}$	0.021	0.04	0.074
240	$4.164\cdot 10^{-3}$	$8.229\cdot 10^{-3}$	0.02	0.038	0.071
250	$3.998\cdot 10^{-3}$	$7.903\cdot 10^{-3}$	0.019	0.037	0.069
260	$3.844\cdot 10^{-3}$	$7.603\cdot 10^{-3}$	0.019	0.036	0.067
270	$3.702\cdot 10^{-3}$	$7.325\cdot 10^{-3}$	0.018	0.035	0.065
280	$3.57\cdot 10^{-3}$	$7.066\cdot 10^{-3}$	0.017	0.033	0.063
290	$3.446\cdot 10^{-3}$	$6.825\cdot 10^{-3}$	0.017	0.032	0.061
300	$3.332\cdot 10^{-3}$	$6.599\cdot 10^{-3}$	0.016	0.031	0.059
310	$3.224\cdot 10^{-3}$	$6.389\cdot 10^{-3}$	0.016	0.03	0.057
320	$3.123\cdot 10^{-3}$	$6.191\cdot 10^{-3}$	0.015	0.029	0.056
330	$3.029\cdot 10^{-3}$	$6.005\cdot 10^{-3}$	0.015	0.029	0.054
340	$2.94\cdot 10^{-3}$	$5.83\cdot 10^{-3}$	0.014	0.028	0.053
350	$2.856\cdot 10^{-3}$	$5.665\cdot 10^{-3}$	0.014	0.027	0.051
360	$2.776\cdot 10^{-3}$	$5.509\cdot 10^{-3}$	0.014	0.026	0.05
370	$2.701\cdot 10^{-3}$	$5.361\cdot 10^{-3}$	0.013	0.026	0.049
380	$2.63\cdot 10^{-3}$	$5.221\cdot 10^{-3}$	0.013	0.025	0.048
390	$2.563\cdot 10^{-3}$	$5.088\cdot 10^{-3}$	0.013	0.024	0.047
400	$2.499\cdot 10^{-3}$	$4.962\cdot 10^{-3}$	0.012	0.024	0.045

Table C.9: The sensitivity values of $\hat{x}_o(\omega_{k\alpha}, \omega_{k\beta}, Q_i)$ with respect to Q_i in bandpass filter for different values of $\omega_{k\alpha}$ and $\omega_{k\beta}$ with Q_i=5

$\omega_{k\beta}$	$S_{Q_i}^{\hat{x}_o}(200, \omega_{k\beta}, 5)$	$S_{Q_i}^{\hat{x}_o}(100, \omega_{k\beta}, 5)$	$S_{Q_i}^{\hat{x}_o}(50, \omega_{k\beta}, 5)$	$S_{Q_i}^{\hat{x}_o}(10, \omega_{k\beta}, 5)$	$S_{Q_i}^{\hat{x}_o}(5, \omega_{k\beta}, 5)$
10	-0.248	-0.248	-0.248	-0.248	-0.247
20	-0.166	-0.166	-0.166	-0.166	-0.165
30	-0.125	-0.125	-0.125	-0.125	-0.124
40	-0.1	-0.1	-0.1	-0.1	-0.099
50	-0.083	-0.083	-0.083	-0.083	-0.083
60	-0.071	-0.071	-0.071	-0.071	-0.071
70	-0.062	-0.062	-0.062	-0.062	-0.062
80	-0.056	-0.056	-0.056	-0.055	-0.055
90	-0.05	-0.05	-0.05	-0.05	-0.049
100	-0.045	-0.045	-0.045	-0.045	-0.045
110	-0.042	-0.042	-0.042	-0.041	-0.041
120	-0.038	-0.038	-0.038	-0.038	-0.038
130	-0.036	-0.036	-0.036	-0.036	-0.035
140	-0.033	-0.033	-0.033	-0.033	-0.033
150	-0.031	-0.031	-0.031	-0.031	-0.031
160	-0.029	-0.029	-0.029	-0.029	-0.029
170	-0.028	-0.028	-0.028	-0.028	-0.027
180	-0.026	-0.026	-0.026	-0.026	-0.026
190	-0.025	-0.025	-0.025	-0.025	-0.024
200	-0.024	-0.024	-0.024	-0.024	-0.023
210	-0.023	-0.023	-0.023	-0.023	-0.022
220	-0.022	-0.022	-0.022	-0.022	-0.021
230	-0.021	-0.021	-0.021	-0.021	-0.02
240	-0.02	-0.02	-0.02	-0.02	-0.019
250	-0.019	-0.019	-0.019	-0.019	-0.018
260	-0.019	-0.019	-0.019	-0.018	-0.018
270	-0.018	-0.018	-0.018	-0.018	-0.017
280	-0.017	-0.017	-0.017	-0.017	-0.016
290	-0.017	-0.017	-0.017	-0.016	-0.016
300	-0.016	-0.016	-0.016	-0.016	-0.015
310	-0.016	-0.016	-0.016	-0.015	-0.015
320	-0.015	-0.015	-0.015	-0.015	-0.014
330	-0.015	-0.015	-0.015	-0.015	-0.014
340	-0.014	-0.014	-0.014	-0.014	-0.014
350	-0.014	-0.014	-0.014	-0.014	-0.013
360	-0.014	-0.014	-0.014	-0.013	-0.013
370	-0.013	-0.013	-0.013	-0.013	-0.012
380	-0.013	-0.013	-0.013	-0.013	-0.012
390	-0.012	-0.012	-0.012	-0.012	-0.012
400	-0.012	-0.012	-0.012	-0.012	-0.011

Table C.10: The sensitivity values of $\hat{x}_o(\omega_{k\alpha},\omega_{k\beta},Q_i)$ with respect to Q_i in bandpass filter for different values of Q_i and $\omega_{k\beta}$ with $\omega_{k\alpha}$ =50

$\omega_{k\beta}$	$S_{Q_i}^{\hat{x}_o}(50,\omega_{k\beta},1)$	$S_{Q_i}^{\hat{x}_o}(50,\omega_{k\beta},2)$	$S_{Q_i}^{\hat{x}_o}(50,\omega_{k\beta},5)$	$S_{Q_i}^{\hat{x}_o}(50,\omega_{k\beta},10)$	$S_{Q_i}^{\hat{x}_o}(50,\omega_{k\beta},20)$
10	-0.081	-0.14	-0.248	-0.332	-0.4
20	-0.045	-0.083	-0.166	-0.249	-0.333
30	-0.031	-0.059	-0.125	-0.2	-0.286
40	-0.024	-0.045	-0.1	-0.166	-0.25
50	-0.019	-0.037	-0.083	-0.143	-0.222
60	-0.016	-0.031	-0.071	-0.125	-0.2
70	-0.014	-0.027	-0.062	-0.111	-0.182
80	-0.012	-0.024	-0.056	-0.1	-0.167
90	-0.011	-0.021	-0.05	-0.091	-0.154
100	$-9.604\cdot10^{-3}$	-0.019	-0.045	-0.083	-0.143
110	$-8.729\cdot10^{-3}$	-0.017	-0.042	-0.077	-0.133
120	$-7.998\cdot10^{-3}$	-0.016	-0.038	-0.071	-0.125
130	$-7.377\cdot10^{-3}$	-0.015	-0.036	-0.067	-0.118
140	$-6.844\cdot10^{-3}$	-0.014	-0.033	-0.062	-0.111
150	$-6.38\cdot10^{-3}$	-0.013	-0.031	-0.059	-0.105
160	$-5.974\cdot10^{-3}$	-0.012	-0.029	-0.056	-0.1
170	$-5.616\cdot10^{-3}$	-0.011	-0.028	-0.053	-0.095
180	$-5.298\cdot10^{-3}$	-0.011	-0.026	-0.05	-0.091
190	$-5.01\cdot10^{-3}$	-0.01	-0.025	-0.048	-0.087
200	$-4.752\cdot10^{-3}$	$-9.754\cdot10^{-3}$	-0.024	-0.045	-0.083
210	$-4.519\cdot10^{-3}$	$-9.296\cdot10^{-3}$	-0.023	-0.043	-0.08
220	$-4.306\cdot10^{-3}$	$-8.879\cdot10^{-3}$	-0.022	-0.042	-0.077
230	$-4.112\cdot10^{-3}$	$-8.497\cdot10^{-3}$	-0.021	-0.04	-0.074
240	$-3.934\cdot10^{-3}$	$-8.147\cdot10^{-3}$	-0.02	-0.038	-0.071
250	$-3.77\cdot10^{-3}$	$-7.824\cdot10^{-3}$	-0.019	-0.037	-0.069
260	$-3.618\cdot10^{-3}$	$-7.526\cdot10^{-3}$	-0.019	-0.036	-0.067
270	$-3.478\cdot10^{-3}$	$-7.25\cdot10^{-3}$	-0.018	-0.034	-0.065
280	$-3.348\cdot10^{-3}$	$-6.993\cdot10^{-3}$	-0.017	-0.033	-0.062
290	$-3.226\cdot10^{-3}$	$-6.753\cdot10^{-3}$	-0.017	-0.032	-0.061
300	$-3.113\cdot10^{-3}$	$-6.529\cdot10^{-3}$	-0.016	-0.031	-0.059
310	$-3.006\cdot10^{-3}$	$-6.32\cdot10^{-3}$	-0.016	-0.03	-0.057
320	$-2.907\cdot10^{-3}$	$-6.123\cdot10^{-3}$	-0.015	-0.029	-0.056
330	$-2.813\cdot10^{-3}$	$-5.938\cdot10^{-3}$	-0.015	-0.029	-0.054
340	$-2.725\cdot10^{-3}$	$-5.764\cdot10^{-3}$	-0.014	-0.028	-0.053
350	$-2.642\cdot10^{-3}$	$-5.6\cdot10^{-3}$	-0.014	-0.027	-0.051
360	$-2.564\cdot10^{-3}$	$-5.445\cdot10^{-3}$	-0.014	-0.026	-0.05
370	$-2.489\cdot10^{-3}$	$-5.298\cdot10^{-3}$	-0.013	-0.026	-0.049
380	$-2.419\cdot10^{-3}$	$-5.159\cdot10^{-3}$	-0.013	-0.025	-0.048
390	$-2.352\cdot10^{-3}$	$-5.027\cdot10^{-3}$	-0.012	-0.024	-0.047
400	$-2.289\cdot10^{-3}$	$-4.901\cdot10^{-3}$	-0.012	-0.024	-0.045

Table C.11: The sensitivity values of $Q(\omega_{k\alpha}, \omega_{k\beta}, Q_i)$ with respect to $\omega_{k\alpha}$ for different values of $\omega_{k\alpha}$ and $\omega_{k\beta}$ with Q_i=5 in bandpass filter

$\omega_{k\beta}$	$S^{Q}_{\omega_{k\alpha}}(200,\mathrm{wkb},5)$	$S^{Q}_{\omega_{k\alpha}}(100,\mathrm{wkb},5)$	$S^{Q}_{\omega_{k\alpha}}(50,\mathrm{wkb},5)$	$S^{Q}_{\omega_{k\alpha}}(10,\mathrm{wkb},5)$	$S^{Q}_{\omega_{k\alpha}}(5,\mathrm{wkb},5)$
10	$-1.28 \cdot 10^{-6}$	$-2.684 \cdot 10^{-6}$	$-5.748 \cdot 10^{-6}$	$2.273 \cdot 10^{-5}$	$4.952 \cdot 10^{-4}$
20	$-4.94 \cdot 10^{-7}$	$-1.241 \cdot 10^{-6}$	$-3.083 \cdot 10^{-6}$	$6.439 \cdot 10^{-5}$	$8.161 \cdot 10^{-4}$
30	$-3.521 \cdot 10^{-7}$	$-1.035 \cdot 10^{-6}$	$-2.872 \cdot 10^{-6}$	$7.894 \cdot 10^{-5}$	$9.812 \cdot 10^{-4}$
40	$-3.119 \cdot 10^{-7}$	$-1.013 \cdot 10^{-6}$	$-3.105 \cdot 10^{-6}$	$8.583 \cdot 10^{-5}$	$1.083 \cdot 10^{-3}$
50	$-3.115 \cdot 10^{-7}$	$-1.064 \cdot 10^{-6}$	$-3.38 \cdot 10^{-6}$	$8.966 \cdot 10^{-5}$	$1.151 \cdot 10^{-3}$
60	$-3.178 \cdot 10^{-7}$	$-1.12 \cdot 10^{-6}$	$-3.628 \cdot 10^{-6}$	$9.201 \cdot 10^{-5}$	$1.2 \cdot 10^{-3}$
70	$-3.279 \cdot 10^{-7}$	$-1.171 \cdot 10^{-6}$	$-3.841 \cdot 10^{-6}$	$9.356 \cdot 10^{-5}$	$1.238 \cdot 10^{-3}$
80	$-3.372 \cdot 10^{-7}$	$-1.217 \cdot 10^{-6}$	$-3.843 \cdot 10^{-6}$	$9.463 \cdot 10^{-5}$	$1.267 \cdot 10^{-3}$
90	$-3.463 \cdot 10^{-7}$	$-1.257 \cdot 10^{-6}$	$-3.982 \cdot 10^{-6}$	$9.54 \cdot 10^{-5}$	$1.29 \cdot 10^{-3}$
100	$-3.549 \cdot 10^{-7}$	$-1.291 \cdot 10^{-6}$	$-4.103 \cdot 10^{-6}$	$9.598 \cdot 10^{-5}$	$1.31 \cdot 10^{-3}$
110	$-3.612 \cdot 10^{-7}$	$-1.321 \cdot 10^{-6}$	$-4.207 \cdot 10^{-6}$	$9.642 \cdot 10^{-5}$	$1.326 \cdot 10^{-3}$
120	$-3.674 \cdot 10^{-7}$	$-1.348 \cdot 10^{-6}$	$-4.298 \cdot 10^{-6}$	$9.677 \cdot 10^{-5}$	$1.339 \cdot 10^{-3}$
130	$-3.738 \cdot 10^{-7}$	$-1.371 \cdot 10^{-6}$	$-4.379 \cdot 10^{-6}$	$9.705 \cdot 10^{-5}$	$1.351 \cdot 10^{-3}$
140	$-3.788 \cdot 10^{-7}$	$-1.392 \cdot 10^{-6}$	$-4.45 \cdot 10^{-6}$	$9.727 \cdot 10^{-5}$	$1.361 \cdot 10^{-3}$
150	$-3.826 \cdot 10^{-7}$	$-1.41 \cdot 10^{-6}$	$-4.514 \cdot 10^{-6}$	$9.746 \cdot 10^{-5}$	$1.37 \cdot 10^{-3}$
160	$-3.878 \cdot 10^{-7}$	$-1.427 \cdot 10^{-6}$	$-4.571 \cdot 10^{-6}$	$9.761 \cdot 10^{-5}$	$1.378 \cdot 10^{-3}$
170	$-3.915 \cdot 10^{-7}$	$-1.442 \cdot 10^{-6}$	$-4.622 \cdot 10^{-6}$	$9.774 \cdot 10^{-5}$	$1.385 \cdot 10^{-3}$
180	$-3.951 \cdot 10^{-7}$	$-1.456 \cdot 10^{-6}$	$-4.669 \cdot 10^{-6}$	$9.786 \cdot 10^{-5}$	$1.391 \cdot 10^{-3}$
190	$-3.98 \cdot 10^{-7}$	$-1.468 \cdot 10^{-6}$	$-4.711 \cdot 10^{-6}$	$9.795 \cdot 10^{-5}$	$1.397 \cdot 10^{-3}$
200	$-4.006 \cdot 10^{-7}$	$-1.479 \cdot 10^{-6}$	$-4.75 \cdot 10^{-6}$	$9.803 \cdot 10^{-5}$	$1.402 \cdot 10^{-3}$
210	$-4.031 \cdot 10^{-7}$	$-1.489 \cdot 10^{-6}$	$-4.785 \cdot 10^{-6}$	$9.811 \cdot 10^{-5}$	$1.406 \cdot 10^{-3}$
220	$-4.059 \cdot 10^{-7}$	$-1.499 \cdot 10^{-6}$	$-4.818 \cdot 10^{-6}$	$9.817 \cdot 10^{-5}$	$1.411 \cdot 10^{-3}$
230	$-4.08 \cdot 10^{-7}$	$-1.507 \cdot 10^{-6}$	$-4.848 \cdot 10^{-6}$	$9.822 \cdot 10^{-5}$	$1.414 \cdot 10^{-3}$
240	$-4.097 \cdot 10^{-7}$	$-1.516 \cdot 10^{-6}$	$-4.876 \cdot 10^{-6}$	$9.827 \cdot 10^{-5}$	$1.416 \cdot 10^{-3}$
250	$-4.128 \cdot 10^{-7}$	$-1.523 \cdot 10^{-6}$	$-4.902 \cdot 10^{-6}$	$9.832 \cdot 10^{-5}$	$1.421 \cdot 10^{-3}$
260	$-4.134 \cdot 10^{-7}$	$-1.531 \cdot 10^{-6}$	$-4.926 \cdot 10^{-6}$	$9.836 \cdot 10^{-5}$	$1.424 \cdot 10^{-3}$
270	$-4.151 \cdot 10^{-7}$	$-1.537 \cdot 10^{-6}$	$-4.948 \cdot 10^{-6}$	$9.839 \cdot 10^{-5}$	$1.427 \cdot 10^{-3}$
280	$-4.174 \cdot 10^{-7}$	$-1.543 \cdot 10^{-6}$	$-4.969 \cdot 10^{-6}$	$9.842 \cdot 10^{-5}$	$1.43 \cdot 10^{-3}$
290	$-4.187 \cdot 10^{-7}$	$-1.549 \cdot 10^{-6}$	$-4.989 \cdot 10^{-6}$	$9.845 \cdot 10^{-5}$	$1.432 \cdot 10^{-3}$
300	$-4.2 \cdot 10^{-7}$	$-1.554 \cdot 10^{-6}$	$-5.008 \cdot 10^{-6}$	$9.848 \cdot 10^{-5}$	$1.435 \cdot 10^{-3}$
310	$-4.212 \cdot 10^{-7}$	$-1.559 \cdot 10^{-6}$	$-5.025 \cdot 10^{-6}$	$9.85 \cdot 10^{-5}$	$1.437 \cdot 10^{-3}$
320	$-4.221 \cdot 10^{-7}$	$-1.564 \cdot 10^{-6}$	$-5.042 \cdot 10^{-6}$	$9.852 \cdot 10^{-5}$	$1.439 \cdot 10^{-3}$
330	$-4.237 \cdot 10^{-7}$	$-1.568 \cdot 10^{-6}$	$-5.057 \cdot 10^{-6}$	$9.854 \cdot 10^{-5}$	$1.441 \cdot 10^{-3}$
340	$-4.246 \cdot 10^{-7}$	$-1.572 \cdot 10^{-6}$	$-5.072 \cdot 10^{-6}$	$9.856 \cdot 10^{-5}$	$1.442 \cdot 10^{-3}$
350	$-4.254 \cdot 10^{-7}$	$-1.576 \cdot 10^{-6}$	$-5.086 \cdot 10^{-6}$	$9.858 \cdot 10^{-5}$	$1.444 \cdot 10^{-3}$
360	$-4.266 \cdot 10^{-7}$	$-1.58 \cdot 10^{-6}$	$-5.099 \cdot 10^{-6}$	$9.859 \cdot 10^{-5}$	$1.446 \cdot 10^{-3}$
370	$-4.278 \cdot 10^{-7}$	$-1.584 \cdot 10^{-6}$	$-5.111 \cdot 10^{-6}$	$9.861 \cdot 10^{-5}$	$1.447 \cdot 10^{-3}$
380	$-4.287 \cdot 10^{-7}$	$-1.587 \cdot 10^{-6}$	$-5.123 \cdot 10^{-6}$	$9.862 \cdot 10^{-5}$	$1.449 \cdot 10^{-3}$
390	$-4.299 \cdot 10^{-7}$	$-1.591 \cdot 10^{-6}$	$-5.135 \cdot 10^{-6}$	$9.863 \cdot 10^{-5}$	$1.45 \cdot 10^{-3}$
400	$-4.303 \cdot 10^{-7}$	$-1.593 \cdot 10^{-6}$	$-5.145 \cdot 10^{-6}$	$9.865 \cdot 10^{-5}$	$1.451 \cdot 10^{-3}$

Table C.12: The sensitivity values of $Q(\omega_{k\alpha}, \omega_{k\beta}, Q_i)$ with respect to $\omega_{k\beta}$ in bandpass filter for different values of $\omega_{k\alpha}$ and $\omega_{k\beta}$ with Q_i=5

$\omega_{k\beta}$	$S^{Q}_{\omega_{k\beta}}(200, \omega_{k\beta}, 5)$	$S^{Q}_{\omega_{k\beta}}(100, \omega_{k\beta}, 5)$	$S^{Q}_{\omega_{k\beta}}(50, \omega_{k\beta}, 5)$	$S^{Q}_{\omega_{k\beta}}(10, \omega_{k\beta}, 5)$	$S^{Q}_{\omega_{k\beta}}(5, \omega_{k\beta}, 5)$
10	0.049	0.049	0.049	0.049	0.049
20	-0.039	-0.039	-0.039	-0.039	-0.039
30	-0.055	-0.055	-0.055	-0.055	-0.056
40	-0.056	-0.056	-0.056	-0.056	-0.057
50	-0.054	-0.054	-0.054	-0.054	-0.054
60	-0.05	-0.05	-0.05	-0.05	-0.05
70	-0.046	-0.046	-0.046	-0.046	-0.046
80	-0.043	-0.043	-0.043	-0.043	-0.043
90	-0.04	-0.04	-0.04	-0.04	-0.04
100	-0.037	-0.037	-0.037	-0.037	-0.037
110	-0.035	-0.035	-0.035	-0.035	-0.035
120	-0.032	-0.032	-0.032	-0.032	-0.032
130	-0.031	-0.031	-0.031	-0.031	-0.031
140	-0.029	-0.029	-0.029	-0.029	-0.029
150	-0.027	-0.027	-0.027	-0.027	-0.027
160	-0.026	-0.026	-0.026	-0.026	-0.026
170	-0.025	-0.025	-0.025	-0.025	-0.025
180	-0.024	-0.024	-0.024	-0.024	-0.024
190	-0.022	-0.022	-0.022	-0.022	-0.022
200	-0.022	-0.022	-0.022	-0.022	-0.022
210	-0.021	-0.021	-0.021	-0.021	-0.021
220	-0.02	-0.02	-0.02	-0.02	-0.02
230	-0.019	-0.019	-0.019	-0.019	-0.019
240	-0.018	-0.018	-0.018	-0.018	-0.018
250	-0.018	-0.018	-0.018	-0.018	-0.018
260	-0.017	-0.017	-0.017	-0.017	-0.017
270	-0.017	-0.017	-0.017	-0.017	-0.017
280	-0.016	-0.016	-0.016	-0.016	-0.016
290	-0.016	-0.016	-0.016	-0.016	-0.016
300	-0.015	-0.015	-0.015	-0.015	-0.015
310	-0.015	-0.015	-0.015	-0.015	-0.015
320	-0.014	-0.014	-0.014	-0.014	-0.014
330	-0.014	-0.014	-0.014	-0.014	-0.014
340	-0.013	-0.013	-0.013	-0.013	-0.013
350	-0.013	-0.013	-0.013	-0.013	-0.013
360	-0.013	-0.013	-0.013	-0.013	-0.013
370	-0.012	-0.012	-0.012	-0.012	-0.012
380	-0.012	-0.012	-0.012	-0.012	-0.012
390	-0.012	-0.012	-0.012	-0.012	-0.012
400	-0.012	-0.012	-0.012	-0.012	-0.012

Table C.13: The sensitivity values of $Q(\omega_{k\alpha}, \omega_{k\beta}, Q_i)$ with respect to $\omega_{k\beta}$ in bandpass filter for different values of $\omega_{k\beta}$ and Q_i with $\omega_{k\alpha}$=50

$\omega_{k\beta}$	$S^{Q}_{\omega_{k\beta}}(50,\omega_{k\beta},1)$	$S^{Q}_{\omega_{k\beta}}(50,\omega_{k\beta},2)$	$S^{Q}_{\omega_{k\beta}}(50,\omega_{k\beta},5)$	$S^{Q}_{\omega_{k\beta}}(50,\omega_{k\beta},10)$	$S^{Q}_{\omega_{k\beta}}(50,\omega_{k\beta},20)$
10	-0.061	-0.054	0.049	0.2	0.338
20	-0.04	-0.055	-0.039	0.05	0.2
30	-0.029	-0.045	-0.055	-0.012	0.108
40	-0.022	-0.038	-0.056	-0.039	0.05
50	-0.018	-0.032	-0.054	-0.05	0.013
60	-0.016	-0.028	-0.05	-0.055	-0.012
70	-0.013	-0.024	-0.046	-0.057	-0.028
80	-0.012	-0.022	-0.043	-0.056	-0.039
90	-0.011	-0.02	-0.04	-0.055	-0.046
100	$-9.591\cdot10^{-3}$	-0.018	-0.037	-0.053	-0.05
110	$-8.752\cdot10^{-3}$	-0.016	-0.035	-0.052	-0.053
120	$-8.049\cdot10^{-3}$	-0.015	-0.032	-0.05	-0.055
130	$-7.449\cdot10^{-3}$	-0.014	-0.031	-0.048	-0.056
140	$-6.933\cdot10^{-3}$	-0.013	-0.029	-0.046	-0.056
150	$-6.484\cdot10^{-3}$	-0.012	-0.027	-0.044	-0.056
160	$-6.089\cdot10^{-3}$	-0.012	-0.026	-0.043	-0.056
170	$-5.74\cdot10^{-3}$	-0.011	-0.025	-0.041	-0.056
180	$-5.428\cdot10^{-3}$	-0.01	-0.024	-0.04	-0.055
190	$-5.149\cdot10^{-3}$	$-9.928\cdot10^{-3}$	-0.022	-0.038	-0.054
200	$-4.897\cdot10^{-3}$	$-9.459\cdot10^{-3}$	-0.022	-0.037	-0.053
210	$-4.668\cdot10^{-3}$	$-9.033\cdot10^{-3}$	-0.021	-0.036	-0.052
220	$-4.46\cdot10^{-3}$	$-8.643\cdot10^{-3}$	-0.02	-0.034	-0.051
230	$-4.269\cdot10^{-3}$	$-8.286\cdot10^{-3}$	-0.019	-0.033	-0.051
240	$-4.095\cdot10^{-3}$	$-7.957\cdot10^{-3}$	-0.018	-0.032	-0.05
250	$-3.933\cdot10^{-3}$	$-7.652\cdot10^{-3}$	-0.018	-0.031	-0.049
260	$-3.785\cdot10^{-3}$	$-7.371\cdot10^{-3}$	-0.017	-0.03	-0.048
270	$-3.647\cdot10^{-3}$	$-7.109\cdot10^{-3}$	-0.017	-0.03	-0.047
280	$-3.518\cdot10^{-3}$	$-6.865\cdot10^{-3}$	-0.016	-0.029	-0.046
290	$-3.399\cdot10^{-3}$	$-6.638\cdot10^{-3}$	-0.016	-0.028	-0.045
300	$-3.287\cdot10^{-3}$	$-6.425\cdot10^{-3}$	-0.015	-0.027	-0.044
310	$-3.182\cdot10^{-3}$	$-6.225\cdot10^{-3}$	-0.015	-0.027	-0.043
320	$-3.084\cdot10^{-3}$	$-6.037\cdot10^{-3}$	-0.014	-0.026	-0.043
330	$-2.992\cdot10^{-3}$	$-5.86\cdot10^{-3}$	-0.014	-0.025	-0.042
340	$-2.905\cdot10^{-3}$	$-5.693\cdot10^{-3}$	-0.013	-0.025	-0.041
350	$-2.823\cdot10^{-3}$	$-5.536\cdot10^{-3}$	-0.013	-0.024	-0.04
360	$-2.745\cdot10^{-3}$	$-5.387\cdot10^{-3}$	-0.013	-0.023	-0.04
370	$-2.672\cdot10^{-3}$	$-5.246\cdot10^{-3}$	-0.012	-0.023	-0.039
380	$-2.602\cdot10^{-3}$	$-5.112\cdot10^{-3}$	-0.012	-0.022	-0.038
390	$-2.536\cdot10^{-3}$	$-4.984\cdot10^{-3}$	-0.012	-0.022	-0.037
400	$-2.474\cdot10^{-3}$	$-4.863\cdot10^{-3}$	-0.012	-0.021	-0.037

Effects of CCCII non-idealities on normalized cutoff angular frequency, quality factor and their sensitivities in the lowpass filter proposed in Figure 5.10.

Table C.14: The different values of normalized cutoff frequency ($\hat{x}_c$) by changing $\omega_{k\alpha}$ and $\omega_{k\beta}$ (Q$_i$=0.707) in lowpass filter

$\omega_{k\beta}$	$x_c(200,\omega_{k\beta},0.707)$	$x_c(100,\omega_{k\beta},0.707)$	$\dot{x}_c(50,\omega_{k\beta},0.707)$	$x_c(10,\omega_{k\beta},0.707)$	$x_c(5,\omega_{k\beta},0.707)$	$x_c(2,\omega_{k\beta},0.707)$
10	0.881	0.881	0.88	0.878	0.869	0.816
20	0.935	0.935	0.935	0.931	0.92	0.857
30	0.955	0.955	0.955	0.951	0.939	0.871
40	0.966	0.966	0.966	0.962	0.949	0.879
50	0.973	0.973	0.972	0.968	0.955	0.883
60	0.977	0.977	0.977	0.972	0.96	0.886
70	0.98	0.98	0.98	0.976	0.962	0.888
80	0.983	0.983	0.982	0.978	0.965	0.89
90	0.984	0.984	0.984	0.98	0.966	0.891
100	0.986	0.986	0.986	0.981	0.968	0.892
110	0.987	0.987	0.987	0.983	0.969	0.893
120	0.988	0.988	0.988	0.984	0.97	0.894
130	0.989	0.989	0.989	0.984	0.971	0.895
140	0.99	0.99	0.99	0.985	0.972	0.895
150	0.991	0.99	0.99	0.986	0.972	0.896
160	0.991	0.991	0.991	0.986	0.973	0.896
170	0.992	0.992	0.991	0.987	0.973	0.896
180	0.992	0.992	0.992	0.987	0.974	0.897
190	0.992	0.992	0.992	0.988	0.974	0.897
200	0.993	0.993	0.993	0.988	0.974	0.897
210	0.993	0.993	0.993	0.988	0.975	0.897
220	0.993	0.993	0.993	0.989	0.975	0.898
230	0.994	0.994	0.994	0.989	0.975	0.898
240	0.994	0.994	0.994	0.989	0.975	0.898
250	0.994	0.994	0.994	0.989	0.976	0.898
260	0.994	0.994	0.994	0.99	0.976	0.898
270	0.995	0.995	0.994	0.99	0.976	0.898
280	0.995	0.995	0.995	0.99	0.976	0.898
290	0.995	0.995	0.995	0.99	0.976	0.899
300	0.995	0.995	0.995	0.99	0.976	0.899
310	0.995	0.995	0.995	0.99	0.977	0.899
320	0.995	0.995	0.995	0.991	0.977	0.899
330	0.996	0.996	0.995	0.991	0.977	0.899
340	0.996	0.996	0.996	0.991	0.977	0.899
350	0.996	0.996	0.996	0.991	0.977	0.899
360	0.996	0.996	0.996	0.991	0.977	0.899
370	0.996	0.996	0.996	0.991	0.977	0.899
380	0.996	0.996	0.996	0.991	0.977	0.899
390	0.996	0.996	0.996	0.991	0.977	0.899
400	0.996	0.996	0.996	0.991	0.978	0.899

Table C.15: The different values of normalized damping factor (d_n) in lowpass filter for different $\omega_{k\alpha}$ and $\omega_{k\beta}$ with Q_i=0.707

$\omega_{k\beta}$	$dn(200,\omega_{k\beta},0.707)$	$dn(100,\omega_{k\beta},0.707)$	$dn(50,\omega_{k\beta},0.707)$	$dn(10,\omega_{k\beta},0.707)$	$dn(5,\omega_{k\beta},0.707)$	$dn(2,\omega_{k\beta},0.707)$
10	0.895	0.895	0.896	0.898	0.898	0.898
20	0.94	0.94	0.94	0.94	0.936	0.926
30	0.958	0.958	0.958	0.957	0.952	0.937
40	0.967	0.967	0.968	0.966	0.96	0.943
50	0.974	0.974	0.974	0.972	0.965	0.947
60	0.978	0.978	0.978	0.975	0.968	0.949
70	0.981	0.981	0.981	0.978	0.971	0.951
80	0.983	0.983	0.983	0.98	0.973	0.952
90	0.985	0.985	0.985	0.982	0.974	0.953
100	0.986	0.986	0.986	0.983	0.975	0.954
110	0.988	0.988	0.988	0.984	0.976	0.955
120	0.989	0.989	0.989	0.985	0.977	0.955
130	0.989	0.989	0.989	0.986	0.978	0.956
140	0.99	0.99	0.99	0.987	0.978	0.956
150	0.991	0.991	0.991	0.987	0.979	0.956
160	0.991	0.991	0.991	0.988	0.979	0.957
170	0.992	0.992	0.992	0.988	0.98	0.957
180	0.992	0.992	0.992	0.989	0.98	0.957
190	0.993	0.993	0.993	0.989	0.98	0.958
200	0.993	0.993	0.993	0.989	0.981	0.958
210	0.993	0.993	0.993	0.99	0.981	0.958
220	0.994	0.994	0.994	0.99	0.981	0.958
230	0.994	0.994	0.994	0.99	0.981	0.958
240	0.994	0.994	0.994	0.99	0.982	0.958
250	0.994	0.994	0.994	0.991	0.982	0.958
260	0.995	0.995	0.995	0.991	0.982	0.959
270	0.995	0.995	0.995	0.991	0.982	0.959
280	0.995	0.995	0.995	0.991	0.982	0.959
290	0.995	0.995	0.995	0.991	0.982	0.959
300	0.995	0.995	0.995	0.992	0.982	0.959
310	0.995	0.995	0.995	0.992	0.983	0.959
320	0.996	0.996	0.996	0.992	0.983	0.959
330	0.996	0.996	0.996	0.992	0.983	0.959
340	0.996	0.996	0.996	0.992	0.983	0.959
350	0.996	0.996	0.996	0.992	0.983	0.959
360	0.996	0.996	0.996	0.992	0.983	0.959
370	0.996	0.996	0.996	0.992	0.983	0.959
380	0.996	0.996	0.996	0.992	0.983	0.96
390	0.996	0.996	0.996	0.993	0.983	0.96
400	0.996	0.996	0.996	0.993	0.983	0.96

Table C.16: The sensitivity values of $\hat{x}_c(\omega_{k\alpha},\omega_{k\beta},0.707)$ with respect to $\omega_{k\alpha}$ in bandpass filter for different values of $\omega_{k\alpha}$ and $\omega_{k\beta}$

$\omega_{k\beta}$	$S^{\hat{x}_c}_{\omega_{k\alpha}}(200,\omega_{k\beta},0.707)$	$S^{\hat{x}_c}_{\omega_{k\alpha}}(100,\omega_{k\beta},0.707)$	$S^{\hat{x}_c}_{\omega_{k\alpha}}(50,\omega_{k\beta},0.707)$	$S^{\hat{x}_c}_{\omega_{k\alpha}}(10,\omega_{k\beta},0.707)$	$S^{\hat{x}_c}_{\omega_{k\alpha}}(5,\omega_{k\beta},0.707)$
10	$1.731\cdot10^{-5}$	$6.924\cdot10^{-5}$	$2.769\cdot10^{-4}$	$6.836\cdot10^{-3}$	0.028
20	$2.052\cdot10^{-5}$	$8.207\cdot10^{-5}$	$3.281\cdot10^{-4}$	$8.081\cdot10^{-3}$	0.031
30	$2.185\cdot10^{-5}$	$8.737\cdot10^{-5}$	$3.493\cdot10^{-4}$	$8.593\cdot10^{-3}$	0.033
40	$2.257\cdot10^{-5}$	$9.028\cdot10^{-5}$	$3.608\cdot10^{-4}$	$8.871\cdot10^{-3}$	0.034
50	$2.302\cdot10^{-5}$	$9.207\cdot10^{-5}$	$3.681\cdot10^{-4}$	$9.045\cdot10^{-3}$	0.034
60	$2.333\cdot10^{-5}$	$9.331\cdot10^{-5}$	$3.73\cdot10^{-4}$	$9.165\cdot10^{-3}$	0.035
70	$2.356\cdot10^{-5}$	$9.422\cdot10^{-5}$	$3.767\cdot10^{-4}$	$9.252\cdot10^{-3}$	0.035
80	$2.373\cdot10^{-5}$	$9.491\cdot10^{-5}$	$3.794\cdot10^{-4}$	$9.318\cdot10^{-3}$	0.035
90	$2.387\cdot10^{-5}$	$9.545\cdot10^{-5}$	$3.816\cdot10^{-4}$	$9.37\cdot10^{-3}$	0.036
100	$2.397\cdot10^{-5}$	$9.589\cdot10^{-5}$	$3.833\cdot10^{-4}$	$9.412\cdot10^{-3}$	0.036
110	$2.406\cdot10^{-5}$	$9.625\cdot10^{-5}$	$3.848\cdot10^{-4}$	$9.447\cdot10^{-3}$	0.036
120	$2.414\cdot10^{-5}$	$9.655\cdot10^{-5}$	$3.86\cdot10^{-4}$	$9.476\cdot10^{-3}$	0.036
130	$2.421\cdot10^{-5}$	$9.681\cdot10^{-5}$	$3.87\cdot10^{-4}$	$9.501\cdot10^{-3}$	0.036
140	$2.426\cdot10^{-5}$	$9.703\cdot10^{-5}$	$3.879\cdot10^{-4}$	$9.522\cdot10^{-3}$	0.036
150	$2.431\cdot10^{-5}$	$9.722\cdot10^{-5}$	$3.886\cdot10^{-4}$	$9.54\cdot10^{-3}$	0.036
160	$2.435\cdot10^{-5}$	$9.739\cdot10^{-5}$	$3.893\cdot10^{-4}$	$9.557\cdot10^{-3}$	0.036
170	$2.439\cdot10^{-5}$	$9.754\cdot10^{-5}$	$3.899\cdot10^{-4}$	$9.571\cdot10^{-3}$	0.036
180	$2.442\cdot10^{-5}$	$9.767\cdot10^{-5}$	$3.905\cdot10^{-4}$	$9.584\cdot10^{-3}$	0.036
190	$2.445\cdot10^{-5}$	$9.779\cdot10^{-5}$	$3.909\cdot10^{-4}$	$9.595\cdot10^{-3}$	0.036
200	$2.448\cdot10^{-5}$	$9.79\cdot10^{-5}$	$3.914\cdot10^{-4}$	$9.605\cdot10^{-3}$	0.036
210	$2.45\cdot10^{-5}$	$9.799\cdot10^{-5}$	$3.917\cdot10^{-4}$	$9.615\cdot10^{-3}$	0.036
220	$2.452\cdot10^{-5}$	$9.808\cdot10^{-5}$	$3.921\cdot10^{-4}$	$9.623\cdot10^{-3}$	0.036
230	$2.455\cdot10^{-5}$	$9.816\cdot10^{-5}$	$3.924\cdot10^{-4}$	$9.631\cdot10^{-3}$	0.036
240	$2.456\cdot10^{-5}$	$9.824\cdot10^{-5}$	$3.927\cdot10^{-4}$	$9.638\cdot10^{-3}$	0.037
250	$2.458\cdot10^{-5}$	$9.831\cdot10^{-5}$	$3.93\cdot10^{-4}$	$9.645\cdot10^{-3}$	0.037
260	$2.46\cdot10^{-5}$	$9.837\cdot10^{-5}$	$3.933\cdot10^{-4}$	$9.651\cdot10^{-3}$	0.037
270	$2.461\cdot10^{-5}$	$9.843\cdot10^{-5}$	$3.935\cdot10^{-4}$	$9.657\cdot10^{-3}$	0.037
280	$2.462\cdot10^{-5}$	$9.848\cdot10^{-5}$	$3.937\cdot10^{-4}$	$9.662\cdot10^{-3}$	0.037
290	$2.464\cdot10^{-5}$	$9.854\cdot10^{-5}$	$3.939\cdot10^{-4}$	$9.667\cdot10^{-3}$	0.037
300	$2.465\cdot10^{-5}$	$9.858\cdot10^{-5}$	$3.941\cdot10^{-4}$	$9.671\cdot10^{-3}$	0.037
310	$2.466\cdot10^{-5}$	$9.863\cdot10^{-5}$	$3.943\cdot10^{-4}$	$9.676\cdot10^{-3}$	0.037
320	$2.467\cdot10^{-5}$	$9.867\cdot10^{-5}$	$3.944\cdot10^{-4}$	$9.68\cdot10^{-3}$	0.037
330	$2.468\cdot10^{-5}$	$9.871\cdot10^{-5}$	$3.946\cdot10^{-4}$	$9.683\cdot10^{-3}$	0.037
340	$2.469\cdot10^{-5}$	$9.875\cdot10^{-5}$	$3.947\cdot10^{-4}$	$9.687\cdot10^{-3}$	0.037
350	$2.47\cdot10^{-5}$	$9.878\cdot10^{-5}$	$3.949\cdot10^{-4}$	$9.69\cdot10^{-3}$	0.037
360	$2.471\cdot10^{-5}$	$9.881\cdot10^{-5}$	$3.95\cdot10^{-4}$	$9.693\cdot10^{-3}$	0.037
370	$2.471\cdot10^{-5}$	$9.884\cdot10^{-5}$	$3.951\cdot10^{-4}$	$9.696\cdot10^{-3}$	0.037
380	$2.472\cdot10^{-5}$	$9.887\cdot10^{-5}$	$3.953\cdot10^{-4}$	$9.699\cdot10^{-3}$	0.037
390	$2.473\cdot10^{-5}$	$9.89\cdot10^{-5}$	$3.954\cdot10^{-4}$	$9.702\cdot10^{-3}$	0.037
400	$2.474\cdot10^{-5}$	$9.893\cdot10^{-5}$	$3.955\cdot10^{-4}$	$9.704\cdot10^{-3}$	0.037

Table C.17: The sensitivity values of $\hat{x}_c(\omega_{k\alpha},\omega_{k\beta},0.707)$ with respect to $\omega_{k\beta}$ in bandpass filter for different values of $\omega_{k\alpha}$ and $\omega_{k\beta}$

$\omega_{k\beta}$	$S^{\hat{x}_c}_{\omega_{k\beta}}(200,\omega_{k\beta},0.707)$	$S^{\hat{x}_c}_{\omega_{k\beta}}(100,\omega_{k\beta},0.707)$	$S^{\hat{x}_c}_{\omega_{k\beta}}(50,\omega_{k\beta},0.707)$	$S^{\hat{x}_c}_{\omega_{k\beta}}(10,\omega_{k\beta},0.707)$	$S^{\hat{x}_c}_{\omega_{k\beta}}(5,\omega_{k\beta},0.707)$
10	0.114	0.114	0.114	0.112	0.109
20	0.063	0.063	0.063	0.063	0.061
30	0.044	0.044	0.044	0.043	0.042
40	0.033	0.033	0.033	0.033	0.032
50	0.027	0.027	0.027	0.027	0.026
60	0.023	0.023	0.023	0.022	0.022
70	0.02	0.02	0.02	0.019	0.019
80	0.017	0.017	0.017	0.017	0.016
90	0.015	0.015	0.015	0.015	0.015
100	0.014	0.014	0.014	0.014	0.013
110	0.013	0.013	0.013	0.012	0.012
120	0.012	0.012	0.012	0.011	0.011
130	0.011	0.011	0.011	0.011	0.01
140	$9.945\cdot10^{-3}$	$9.844\cdot10^{-3}$	$9.84\cdot10^{-3}$	$9.805\cdot10^{-3}$	$9.413\cdot10^{-3}$
150	$9.292\cdot10^{-3}$	$9.291\cdot10^{-3}$	$9.287\cdot10^{-3}$	$9.16\cdot10^{-3}$	$8.794\cdot10^{-3}$
160	$8.719\cdot10^{-3}$	$8.718\cdot10^{-3}$	$8.714\cdot10^{-3}$	$8.595\cdot10^{-3}$	$8.251\cdot10^{-3}$
170	$8.213\cdot10^{-3}$	$8.212\cdot10^{-3}$	$8.208\cdot10^{-3}$	$8.098\cdot10^{-3}$	$7.771\cdot10^{-3}$
180	$7.762\cdot10^{-3}$	$7.761\cdot10^{-3}$	$7.757\cdot10^{-3}$	$7.651\cdot10^{-3}$	$7.343\cdot10^{-3}$
190	$7.358\cdot10^{-3}$	$7.357\cdot10^{-3}$	$7.354\cdot10^{-3}$	$7.253\cdot10^{-3}$	$6.961\cdot10^{-3}$
200	$6.994\cdot10^{-3}$	$6.993\cdot10^{-3}$	$6.99\cdot10^{-3}$	$6.894\cdot10^{-3}$	$6.616\cdot10^{-3}$
210	$6.664\cdot10^{-3}$	$6.663\cdot10^{-3}$	$6.661\cdot10^{-3}$	$6.569\cdot10^{-3}$	$6.304\cdot10^{-3}$
220	$6.364\cdot10^{-3}$	$6.363\cdot10^{-3}$	$6.361\cdot10^{-3}$	$6.273\cdot10^{-3}$	$6.02\cdot10^{-3}$
230	$6.09\cdot10^{-3}$	$6.089\cdot10^{-3}$	$6.087\cdot10^{-3}$	$6.003\cdot10^{-3}$	$5.76\cdot10^{-3}$
240	$5.839\cdot10^{-3}$	$5.838\cdot10^{-3}$	$5.835\cdot10^{-3}$	$5.755\cdot10^{-3}$	$5.522\cdot10^{-3}$
250	$5.607\cdot10^{-3}$	$5.606\cdot10^{-3}$	$5.604\cdot10^{-3}$	$5.526\cdot10^{-3}$	$5.303\cdot10^{-3}$
260	$5.393\cdot10^{-3}$	$5.393\cdot10^{-3}$	$5.39\cdot10^{-3}$	$5.316\cdot10^{-3}$	$5.1\cdot10^{-3}$
270	$5.195\cdot10^{-3}$	$5.194\cdot10^{-3}$	$5.192\cdot10^{-3}$	$5.12\cdot10^{-3}$	$4.913\cdot10^{-3}$
280	$5.011\cdot10^{-3}$	$5.01\cdot10^{-3}$	$5.008\cdot10^{-3}$	$4.939\cdot10^{-3}$	$4.738\cdot10^{-3}$
290	$4.839\cdot10^{-3}$	$4.839\cdot10^{-3}$	$4.837\cdot10^{-3}$	$4.77\cdot10^{-3}$	$4.576\cdot10^{-3}$
300	$4.679\cdot10^{-3}$	$4.679\cdot10^{-3}$	$4.677\cdot10^{-3}$	$4.612\cdot10^{-3}$	$4.424\cdot10^{-3}$
310	$4.529\cdot10^{-3}$	$4.529\cdot10^{-3}$	$4.527\cdot10^{-3}$	$4.464\cdot10^{-3}$	$4.283\cdot10^{-3}$
320	$4.389\cdot10^{-3}$	$4.388\cdot10^{-3}$	$4.386\cdot10^{-3}$	$4.325\cdot10^{-3}$	$4.15\cdot10^{-3}$
330	$4.257\cdot10^{-3}$	$4.256\cdot10^{-3}$	$4.254\cdot10^{-3}$	$4.195\cdot10^{-3}$	$4.024\cdot10^{-3}$
340	$4.132\cdot10^{-3}$	$4.132\cdot10^{-3}$	$4.13\cdot10^{-3}$	$4.072\cdot10^{-3}$	$3.907\cdot10^{-3}$
350	$4.015\cdot10^{-3}$	$4.014\cdot10^{-3}$	$4.013\cdot10^{-3}$	$3.957\cdot10^{-3}$	$3.796\cdot10^{-3}$
360	$3.904\cdot10^{-3}$	$3.903\cdot10^{-3}$	$3.902\cdot10^{-3}$	$3.848\cdot10^{-3}$	$3.691\cdot10^{-3}$
370	$3.799\cdot10^{-3}$	$3.799\cdot10^{-3}$	$3.797\cdot10^{-3}$	$3.744\cdot10^{-3}$	$3.592\cdot10^{-3}$
380	$3.7\cdot10^{-3}$	$3.699\cdot10^{-3}$	$3.698\cdot10^{-3}$	$3.646\cdot10^{-3}$	$3.498\cdot10^{-3}$
390	$3.605\cdot10^{-3}$	$3.605\cdot10^{-3}$	$3.603\cdot10^{-3}$	$3.553\cdot10^{-3}$	$3.408\cdot10^{-3}$
400	$3.516\cdot10^{-3}$	$3.515\cdot10^{-3}$	$3.514\cdot10^{-3}$	$3.465\cdot10^{-3}$	$3.324\cdot10^{-3}$

Table C.18: The sensitivity values of $\hat{x}_c(\omega_{k\alpha},\omega_{k\beta},0.707)$ with respect to Q_i in bandpass filter for different values of $\omega_{k\alpha}$ and $\omega_{k\beta}$

$\omega_{k\beta}$	$S_{Q_i}^{\hat{x}_c}(200,\omega_{k\beta},0.707)$	$S_{Q_i}^{\hat{x}_c}(100,\omega_{k\beta},0.707)$	$S_{Q_i}^{\hat{x}_c}(50,\omega_{k\beta},0.707)$	$S_{Q_i}^{\hat{x}_c}(10,\omega_{k\beta},0.707)$	$S_{Q_i}^{\hat{x}_c}(5,\omega_{k\beta},0.707)$
10	0.77	0.77	0.77	0.772	0.777
20	0.873	0.873	0.873	0.874	0.878
30	0.912	0.912	0.912	0.913	0.916
40	0.933	0.933	0.933	0.934	0.936
50	0.946	0.946	0.946	0.947	0.948
60	0.955	0.955	0.955	0.955	0.957
70	0.961	0.961	0.961	0.961	0.963
80	0.966	0.966	0.966	0.966	0.968
90	0.969	0.969	0.969	0.97	0.971
100	0.972	0.972	0.972	0.973	0.974
110	0.975	0.975	0.975	0.975	0.977
120	0.977	0.977	0.977	0.977	0.979
130	0.979	0.979	0.979	0.979	0.98
140	0.98	0.98	0.98	0.981	0.982
150	0.982	0.982	0.982	0.982	0.983
160	0.983	0.983	0.983	0.983	0.984
170	0.984	0.984	0.984	0.984	0.985
180	0.985	0.985	0.985	0.985	0.986
190	0.985	0.985	0.985	0.986	0.987
200	0.986	0.986	0.986	0.986	0.987
210	0.987	0.987	0.987	0.987	0.988
220	0.987	0.987	0.987	0.988	0.989
230	0.988	0.988	0.988	0.988	0.989
240	0.988	0.988	0.988	0.989	0.99
250	0.989	0.989	0.989	0.989	0.99
260	0.989	0.989	0.989	0.99	0.991
270	0.99	0.99	0.99	0.99	0.991
280	0.99	0.99	0.99	0.99	0.991
290	0.99	0.99	0.99	0.991	0.992
300	0.991	0.991	0.991	0.991	0.992
310	0.991	0.991	0.991	0.991	0.992
320	0.991	0.991	0.991	0.992	0.992
330	0.992	0.992	0.992	0.992	0.993
340	0.992	0.992	0.992	0.992	0.993
350	0.992	0.992	0.992	0.992	0.993
360	0.992	0.992	0.992	0.992	0.993
370	0.993	0.993	0.993	0.993	0.994
380	0.993	0.993	0.993	0.993	0.994
390	0.993	0.993	0.993	0.993	0.994
400	0.993	0.993	0.993	0.993	0.994

Table C.19: The sensitivity values of $d_n(\omega_{k\alpha}, \omega_{k\beta}, 0.707)$ with respect to $\omega_{k\alpha}$ in bandpass filter for different values of $\omega_{k\alpha}$ and $\omega_{k\beta}$

$\omega_{k\beta}$	$S^{dn}_{\omega_{k\alpha}}(200, \omega_{k\beta}, 0.707)$	$S^{dn}_{\omega_{k\alpha}}(100, \omega_{k\beta}, 0.707)$	$S^{dn}_{\omega_{k\alpha}}(50, \omega_{k\beta}, 0.707)$	$S^{dn}_{\omega_{k\alpha}}(10, \omega_{k\beta}, 0.707)$	$S^{dn}_{\omega_{k\alpha}}(5, \omega_{k\beta}, 0.707)$
10	$-3.038 \cdot 10^{-4}$	$-5.777 \cdot 10^{-4}$	$-1.04 \cdot 10^{-3}$	$-1.477 \cdot 10^{-3}$	$1.838 \cdot 10^{-3}$
20	$-1.792 \cdot 10^{-4}$	$-3.212 \cdot 10^{-4}$	$-4.98 \cdot 10^{-4}$	$2.099 \cdot 10^{-3}$	$9.725 \cdot 10^{-3}$
30	$-1.223 \cdot 10^{-4}$	$-2.04 \cdot 10^{-4}$	$-2.513 \cdot 10^{-4}$	$3.696 \cdot 10^{-3}$	0.013
40	$-9.012 \cdot 10^{-5}$	$-1.38 \cdot 10^{-4}$	$-1.124 \cdot 10^{-4}$	$4.59 \cdot 10^{-3}$	0.015
50	$-6.954 \cdot 10^{-5}$	$-9.568 \cdot 10^{-5}$	$-2.349 \cdot 10^{-5}$	$5.159 \cdot 10^{-3}$	0.016
60	$-5.524 \cdot 10^{-5}$	$-6.632 \cdot 10^{-5}$	$3.821 \cdot 10^{-5}$	$5.554 \cdot 10^{-3}$	0.017
70	$-4.475 \cdot 10^{-5}$	$-4.476 \cdot 10^{-5}$	$8.351 \cdot 10^{-5}$	$5.843 \cdot 10^{-3}$	0.018
80	$-3.671 \cdot 10^{-5}$	$-2.825 \cdot 10^{-5}$	$1.182 \cdot 10^{-4}$	$6.064 \cdot 10^{-3}$	0.018
90	$-3.036 \cdot 10^{-5}$	$-1.521 \cdot 10^{-5}$	$1.456 \cdot 10^{-4}$	$6.239 \cdot 10^{-3}$	0.019
100	$-2.522 \cdot 10^{-5}$	$-4.654 \cdot 10^{-6}$	$1.677 \cdot 10^{-4}$	$6.38 \cdot 10^{-3}$	0.019
110	$-2.097 \cdot 10^{-5}$	$4.07 \cdot 10^{-6}$	$1.881 \cdot 10^{-4}$	$6.496 \cdot 10^{-3}$	0.019
120	$-1.74 \cdot 10^{-5}$	$1.14 \cdot 10^{-5}$	$2.015 \cdot 10^{-4}$	$6.594 \cdot 10^{-3}$	0.019
130	$-1.436 \cdot 10^{-5}$	$1.765 \cdot 10^{-5}$	$2.146 \cdot 10^{-4}$	$6.677 \cdot 10^{-3}$	0.02
140	$-1.174 \cdot 10^{-5}$	$2.303 \cdot 10^{-5}$	$2.259 \cdot 10^{-4}$	$6.749 \cdot 10^{-3}$	0.02
150	$-9.457 \cdot 10^{-6}$	$2.772 \cdot 10^{-5}$	$2.357 \cdot 10^{-4}$	$6.812 \cdot 10^{-3}$	0.02
160	$-7.45 \cdot 10^{-6}$	$3.184 \cdot 10^{-5}$	$2.444 \cdot 10^{-4}$	$6.867 \cdot 10^{-3}$	0.02
170	$-5.673 \cdot 10^{-6}$	$3.549 \cdot 10^{-5}$	$2.52 \cdot 10^{-4}$	$6.915 \cdot 10^{-3}$	0.02
180	$-4.087 \cdot 10^{-6}$	$3.875 \cdot 10^{-5}$	$2.589 \cdot 10^{-4}$	$6.959 \cdot 10^{-3}$	0.02
190	$-2.663 \cdot 10^{-6}$	$4.167 \cdot 10^{-5}$	$2.65 \cdot 10^{-4}$	$6.998 \cdot 10^{-3}$	0.02
200	$-1.38 \cdot 10^{-6}$	$4.431 \cdot 10^{-5}$	$2.705 \cdot 10^{-4}$	$7.033 \cdot 10^{-3}$	0.02
210	$-2.141 \cdot 10^{-7}$	$4.67 \cdot 10^{-5}$	$2.756 \cdot 10^{-4}$	$7.065 \cdot 10^{-3}$	0.02
220	$8.471 \cdot 10^{-7}$	$4.888 \cdot 10^{-5}$	$2.801 \cdot 10^{-4}$	$7.094 \cdot 10^{-3}$	0.02
230	$1.818 \cdot 10^{-6}$	$5.087 \cdot 10^{-5}$	$2.843 \cdot 10^{-4}$	$7.12 \cdot 10^{-3}$	0.02
240	$2.709 \cdot 10^{-6}$	$5.27 \cdot 10^{-5}$	$2.882 \cdot 10^{-4}$	$7.145 \cdot 10^{-3}$	0.021
250	$3.532 \cdot 10^{-6}$	$5.439 \cdot 10^{-5}$	$2.917 \cdot 10^{-4}$	$7.167 \cdot 10^{-3}$	0.021
260	$4.291 \cdot 10^{-6}$	$5.595 \cdot 10^{-5}$	$2.95 \cdot 10^{-4}$	$7.188 \cdot 10^{-3}$	0.021
270	$4.998 \cdot 10^{-6}$	$5.74 \cdot 10^{-5}$	$2.98 \cdot 10^{-4}$	$7.207 \cdot 10^{-3}$	0.021
280	$5.652 \cdot 10^{-6}$	$5.874 \cdot 10^{-5}$	$3.008 \cdot 10^{-4}$	$7.225 \cdot 10^{-3}$	0.021
290	$6.262 \cdot 10^{-6}$	$5.999 \cdot 10^{-5}$	$3.035 \cdot 10^{-4}$	$7.242 \cdot 10^{-3}$	0.021
300	$6.833 \cdot 10^{-6}$	$6.117 \cdot 10^{-5}$	$3.059 \cdot 10^{-4}$	$7.257 \cdot 10^{-3}$	0.021
310	$7.367 \cdot 10^{-6}$	$6.226 \cdot 10^{-5}$	$3.082 \cdot 10^{-4}$	$7.272 \cdot 10^{-3}$	0.021
320	$7.869 \cdot 10^{-6}$	$6.329 \cdot 10^{-5}$	$3.104 \cdot 10^{-4}$	$7.286 \cdot 10^{-3}$	0.021
330	$8.34 \cdot 10^{-6}$	$6.426 \cdot 10^{-5}$	$3.124 \cdot 10^{-4}$	$7.299 \cdot 10^{-3}$	0.021
340	$8.785 \cdot 10^{-6}$	$6.517 \cdot 10^{-5}$	$3.143 \cdot 10^{-4}$	$7.311 \cdot 10^{-3}$	0.021
350	$9.204 \cdot 10^{-6}$	$6.603 \cdot 10^{-5}$	$3.161 \cdot 10^{-4}$	$7.322 \cdot 10^{-3}$	0.021
360	$9.6 \cdot 10^{-6}$	$6.685 \cdot 10^{-5}$	$3.179 \cdot 10^{-4}$	$7.333 \cdot 10^{-3}$	0.021
370	$9.975 \cdot 10^{-6}$	$6.762 \cdot 10^{-5}$	$3.195 \cdot 10^{-4}$	$7.343 \cdot 10^{-3}$	0.021
380	$1.033 \cdot 10^{-5}$	$6.835 \cdot 10^{-5}$	$3.21 \cdot 10^{-4}$	$7.353 \cdot 10^{-3}$	0.021
390	$1.067 \cdot 10^{-5}$	$6.904 \cdot 10^{-5}$	$3.225 \cdot 10^{-4}$	$7.362 \cdot 10^{-3}$	0.021
400	$1.099 \cdot 10^{-5}$	$6.97 \cdot 10^{-5}$	$3.238 \cdot 10^{-4}$	$7.371 \cdot 10^{-3}$	0.021

Table C.20: The sensitivity values of $d_n(\omega_{k\alpha},\omega_{k\beta},0.707)$ with respect to $\omega_{k\beta}$ in bandpass filter for different values of $\omega_{k\alpha}$ and $\omega_{k\beta}$

$\omega_{k\beta}$	$S^{dn}_{\omega_{k\beta}}(200,\omega_{k\beta},0.707)$	$S^{dn}_{\omega_{k\beta}}(100,\omega_{k\beta},0.707)$	$S^{dn}_{\omega_{k\beta}}(50,\omega_{k\beta},0.707)$	$S^{dn}_{\omega_{k\beta}}(10,\omega_{k\beta},0.707)$	$S^{dn}_{\omega_{k\beta}}(5,\omega_{k\beta},0.707)$
10	0.085	0.085	0.085	0.081	0.075
20	0.055	0.055	0.054	0.051	0.047
30	0.04	0.04	0.039	0.037	0.033
40	0.031	0.031	0.031	0.029	0.026
50	0.026	0.025	0.025	0.024	0.021
60	0.022	0.022	0.021	0.02	0.018
70	0.019	0.019	0.019	0.017	0.015
80	0.017	0.016	0.016	0.015	0.014
90	0.015	0.015	0.015	0.014	0.012
100	0.013	0.013	0.013	0.012	0.011
110	0.012	0.012	0.012	0.011	0.01
120	0.011	0.011	0.011	0.01	$9.228\cdot10^{-3}$
130	0.01	0.01	0.01	$9.589\cdot10^{-3}$	$8.54\cdot10^{-3}$
140	$9.712\cdot10^{-3}$	$9.677\cdot10^{-3}$	$9.605\cdot10^{-3}$	$8.927\cdot10^{-3}$	$7.948\cdot10^{-3}$
150	$9.086\cdot10^{-3}$	$9.053\cdot10^{-3}$	$8.986\cdot10^{-3}$	$8.349\cdot10^{-3}$	$7.432\cdot10^{-3}$
160	$8.536\cdot10^{-3}$	$8.505\cdot10^{-3}$	$8.442\cdot10^{-3}$	$7.842\cdot10^{-3}$	$6.98\cdot10^{-3}$
170	$8.048\cdot10^{-3}$	$8.019\cdot10^{-3}$	$7.959\cdot10^{-3}$	$7.393\cdot10^{-3}$	$6.579\cdot10^{-3}$
180	$7.613\cdot10^{-3}$	$7.586\cdot10^{-3}$	$7.529\cdot10^{-3}$	$6.993\cdot10^{-3}$	$6.221\cdot10^{-3}$
190	$7.223\cdot10^{-3}$	$7.197\cdot10^{-3}$	$7.143\cdot10^{-3}$	$6.634\cdot10^{-3}$	$5.901\cdot10^{-3}$
200	$6.871\cdot10^{-3}$	$6.846\cdot10^{-3}$	$6.795\cdot10^{-3}$	$6.31\cdot10^{-3}$	$5.612\cdot10^{-3}$
210	$6.551\cdot10^{-3}$	$6.528\cdot10^{-3}$	$6.479\cdot10^{-3}$	$6.016\cdot10^{-3}$	$5.35\cdot10^{-3}$
220	$6.26\cdot10^{-3}$	$6.238\cdot10^{-3}$	$6.191\cdot10^{-3}$	$5.748\cdot10^{-3}$	$5.111\cdot10^{-3}$
230	$5.994\cdot10^{-3}$	$5.972\cdot10^{-3}$	$5.927\cdot10^{-3}$	$5.503\cdot10^{-3}$	$4.893\cdot10^{-3}$
240	$5.749\cdot10^{-3}$	$5.729\cdot10^{-3}$	$5.685\cdot10^{-3}$	$5.278\cdot10^{-3}$	$4.692\cdot10^{-3}$
250	$5.524\cdot10^{-3}$	$5.504\cdot10^{-3}$	$5.462\cdot10^{-3}$	$5.071\cdot10^{-3}$	$4.508\cdot10^{-3}$
260	$5.315\cdot10^{-3}$	$5.296\cdot10^{-3}$	$5.256\cdot10^{-3}$	$4.879\cdot10^{-3}$	$4.337\cdot10^{-3}$
270	$5.122\cdot10^{-3}$	$5.104\cdot10^{-3}$	$5.065\cdot10^{-3}$	$4.701\cdot10^{-3}$	$4.179\cdot10^{-3}$
280	$4.942\cdot10^{-3}$	$4.925\cdot10^{-3}$	$4.887\cdot10^{-3}$	$4.536\cdot10^{-3}$	$4.032\cdot10^{-3}$
290	$4.775\cdot10^{-3}$	$4.758\cdot10^{-3}$	$4.722\cdot10^{-3}$	$4.382\cdot10^{-3}$	$3.894\cdot10^{-3}$
300	$4.618\cdot10^{-3}$	$4.602\cdot10^{-3}$	$4.567\cdot10^{-3}$	$4.238\cdot10^{-3}$	$3.766\cdot10^{-3}$
310	$4.472\cdot10^{-3}$	$4.456\cdot10^{-3}$	$4.422\cdot10^{-3}$	$4.104\cdot10^{-3}$	$3.646\cdot10^{-3}$
320	$4.334\cdot10^{-3}$	$4.318\cdot10^{-3}$	$4.286\cdot10^{-3}$	$3.977\cdot10^{-3}$	$3.534\cdot10^{-3}$
330	$4.205\cdot10^{-3}$	$4.19\cdot10^{-3}$	$4.158\cdot10^{-3}$	$3.858\cdot10^{-3}$	$3.428\cdot10^{-3}$
340	$4.083\cdot10^{-3}$	$4.068\cdot10^{-3}$	$4.037\cdot10^{-3}$	$3.746\cdot10^{-3}$	$3.328\cdot10^{-3}$
350	$3.968\cdot10^{-3}$	$3.954\cdot10^{-3}$	$3.924\cdot10^{-3}$	$3.641\cdot10^{-3}$	$3.234\cdot10^{-3}$
360	$3.859\cdot10^{-3}$	$3.845\cdot10^{-3}$	$3.816\cdot10^{-3}$	$3.541\cdot10^{-3}$	$3.146\cdot10^{-3}$
370	$3.756\cdot10^{-3}$	$3.743\cdot10^{-3}$	$3.714\cdot10^{-3}$	$3.446\cdot10^{-3}$	$3.062\cdot10^{-3}$
380	$3.659\cdot10^{-3}$	$3.645\cdot10^{-3}$	$3.618\cdot10^{-3}$	$3.357\cdot10^{-3}$	$2.982\cdot10^{-3}$
390	$3.566\cdot10^{-3}$	$3.553\cdot10^{-3}$	$3.526\cdot10^{-3}$	$3.272\cdot10^{-3}$	$2.906\cdot10^{-3}$
400	$3.478\cdot10^{-3}$	$3.465\cdot10^{-3}$	$3.439\cdot10^{-3}$	$3.191\cdot10^{-3}$	$2.834\cdot10^{-3}$

Table C.21: The sensitivity values of $d_n(\omega_{k\alpha}, \omega_{k\beta}, 0.707)$ with respect to Q_i in bandpass filter for different values of $\omega_{k\alpha}$ and $\omega_{k\beta}$

$\omega_{k\beta}$	$S_{Q_i}^{dn}(200, \omega_{k\beta}, 0.707)$	$S_{Q_i}^{dn}(100, \omega_{k\beta}, 0.707)$	$S_{Q_i}^{dn}(50, \omega_{k\beta}, 0.707)$	$S_{Q_i}^{dn}(10, \omega_{k\beta}, 0.707)$	$S_{Q_i}^{dn}(5, \omega_{k\beta}, 0.707)$
10	-0.302	-0.306	-0.315	-0.382	-0.455
20	-0.182	-0.187	-0.198	-0.282	-0.376
30	-0.131	-0.137	-0.148	-0.24	-0.343
40	-0.103	-0.109	-0.121	-0.217	-0.325
50	-0.085	-0.091	-0.104	-0.203	-0.314
60	-0.073	-0.079	-0.092	-0.193	-0.306
70	-0.064	-0.07	-0.083	-0.185	-0.3
80	-0.057	-0.064	-0.077	-0.18	-0.296
90	-0.052	-0.058	-0.072	-0.175	-0.293
100	-0.047	-0.054	-0.067	-0.172	-0.29
110	-0.044	-0.051	-0.064	-0.169	-0.288
120	-0.041	-0.048	-0.061	-0.167	-0.286
130	-0.038	-0.045	-0.059	-0.165	-0.284
140	-0.036	-0.043	-0.056	-0.163	-0.283
150	-0.034	-0.041	-0.055	-0.161	-0.282
160	-0.033	-0.039	-0.053	-0.16	-0.281
170	-0.031	-0.038	-0.052	-0.159	-0.28
180	-0.03	-0.037	-0.05	-0.158	-0.279
190	-0.029	-0.035	-0.049	-0.157	-0.278
200	-0.028	-0.034	-0.048	-0.156	-0.278
210	-0.027	-0.033	-0.047	-0.155	-0.277
220	-0.026	-0.033	-0.046	-0.154	-0.276
230	-0.025	-0.032	-0.046	-0.154	-0.276
240	-0.024	-0.031	-0.045	-0.153	-0.275
250	-0.023	-0.03	-0.044	-0.152	-0.275
260	-0.023	-0.03	-0.044	-0.152	-0.275
270	-0.022	-0.029	-0.043	-0.151	-0.274
280	-0.022	-0.029	-0.042	-0.151	-0.274
290	-0.021	-0.028	-0.042	-0.151	-0.274
300	-0.021	-0.028	-0.042	-0.15	-0.273
310	-0.02	-0.027	-0.041	-0.15	-0.273
320	-0.02	-0.027	-0.041	-0.15	-0.273
330	-0.019	-0.026	-0.04	-0.149	-0.273
340	-0.019	-0.026	-0.04	-0.149	-0.272
350	-0.019	-0.026	-0.04	-0.149	-0.272
360	-0.018	-0.025	-0.039	-0.148	-0.272
370	-0.018	-0.025	-0.039	-0.148	-0.272
380	-0.018	-0.025	-0.039	-0.148	-0.272
390	-0.018	-0.025	-0.038	-0.148	-0.271
400	-0.017	-0.024	-0.038	-0.147	-0.271

BIOGRAPHY

Shahram Minaei was born in Tehran, Iran, on August 16, 1970. He received his B.Sc degree in Electrical and Electronics Engineering from Iran University of Science and Technology in 1993. He received his M.Sc degree in Electronics and Communication Engineering from Istanbul Technical University in 1997. He has ten journal or conference papers in scientific review. He served as the scientific committee member of the 8th IEEE conference on Electronics, Circuits and Systems (*ICECS 2001*). His research interest includes current-mode circuits and analog signal processing.